Functional characterization of the homeodomain transcription factor Hdp1 in *Ustilago maydis*

Dissertation

zur
Erlangung des Doktorgrades
der Naturwissenschaften
(Dr. rer. nat.)

dem Fachbereich Biologie
der Philipps-Universität Marburg
vorgelegt von

Chetsada Pothiratana
aus Bangkok, Thailand

Marburg/Lahn 2007

Vom Fachbereich Biologie
der Philipps-Universität Marburg als Dissertation
angenommen am: 07.02.2008

Erstgutachter: Herr Prof. Dr. Michael Bölker
Zweitgutachter: Herr Prof. Dr. Jörg Kämper

Tag der mündlichen Prüfung am: 03.03.2008

The research pertaining this thesis was carried out at the Department of Organismic interactions of the Max-Planck-Institute for Terrestrial Microbiology, Marburg, from April 2004 to December 2007 under the supervision of Prof. Dr. Jörg Kämper.

Declaration

I hereby declare that the dissertation entitled “Functional characterization of the homeodomain transcription factor Hdp1 in *Ustilago maydis*” submitted to the Department of Biology, Philipps-Universität Marburg is the original and independent work carried out by me under the guidance of the PhD committee, and the dissertation is not formed previously on the basis of any award of Degree, Diploma or other similar titles.

_____ _____

(Date and Place) (Chetsada Pothiratana)

Abstract

Ustilago maydis is a phytopathogenic basidiomycete infecting corn plants. Pathogenic development is initiated via a pheromone/receptor-based system encoded by the *a*-mating type locus. Upon pheromone stimulation, two compatible haploid sporidia form conjugation hyphae that are cell cycle arrested in the G2 phase. Upon fusion of the conjugation tubes, a dikaryotic hyphae is formed in which the G2 cell cycle arrested is maintained until plant penetration. The processes subsequent to the *a*-mediated fusion are triggered by the *b*-mating type locus which encodes a pair of homeodomain proteins, termed bE and bW that can form a heterodimeric complex functioning as a transcriptional regulator.

hdp1 encodes an *a*- and *b*-dependently induced homeodomain transcription factor. Deletion of *hdp1* impairs filament formation and G2 cell cycle arrest. Upon fusion of compatible *Δhdp1* cells, the resulting filaments are reduced in length, and an increased number of hyphae with more than two nuclei is observed. Similarly, deletion of *hdp1* leads to a higher frequency of nuclei with single chromosomal content (1C) in pheromone induced conjugation hyphae, implying that *hdp1* is involved in the *a*-mediated G2 cell cycle arrest. In addition, induced *hdp1* expression is sufficient to trigger G2 cell cycle arrest and filament formation.

Both Prf1, the main transcriptional regulator within the a-mediated signaling cascade, and Rop1, a factor required for *prf1* expression in the saprophytic stage, are induced by Hdp1. Although not required for the pheromone dependent induction of both genes, *hdp1* modulates their expression, by that integrating a positive feedback loop from the b-regulatory cascade to the pheromone signaling pathway.

Microarray analysis revealed that two genes associated with cell cycle control are regulated by Hdp1. *pcl12*, encoding a Pho85-type cyclin, is induced, while *clb1* encoding a B-type cyclin, is repressed upon *hdp1* induction. Deletion of *pcl12* abolishes filament formation in axenic culture. The gene appears to be essential for the Hdp1-induced filamentation and G2 cell cycle arrest; however, its effect on cell cycle arrest is most likely also influenced by environmental cues. *clb1*, on the other hand, does not play a major role in Hdp1-mediated cell cycle arrest. The current model suggests that Hdp1 is used for fine-tuning the a- and b- mediated cell cycle regulation and integrating additional environmental cues.

Zusammenfassung

Der Beginn der pathogenen Entwicklung des Maisbrandpilzes *Ustilago maydis* wird durch ein vom *a*-Paarungstyp Locus kodiertes Pheromon/Rezeptor-System kontrolliert. Durch Perzeption des kompatiblen Pheromons werden Konjugationshyphen gebildet, die in der G2-Zellzyklusphase arretiert sind. Durch Fusion der Konjugationshyphen entsteht das dikaryotische Filament, in dem der G2-Zellzyklusarrest bis zur Penetration der Wirtspflanze aufrechterhalten wird. Im Dikaryon wird die weitere Entwicklung durch den *b*-Paarungstyp Locus vermittelt, der für die Homeodomänen-Transkriptionsfaktoren bE und bW kodiert.

hdp1 kodiert für einen *a*- und *b*-abhängig induzierten Homedomänen-Transkriptionsfaktor. Deletion von *hdp1* beeinflusst die Filamentbildung und den G2 Zellzyklusarrest. Fusion kompatibler *Δhdp1* Zellen führt zu Filamenten mit reduzierter Länge, und die Anzahl von Hyphen mit mehr als einem Zellkern ist erhöht. Konjugationshyphen von Pheromon-induzierten *Δhdp1* Zellen zeigen eine höhere Anzahl an Kernen mit nur einfachem Chromosomengehalt (1C) auf, was auf eine Funktion von Hdp1 während des *a*-induzierten G2-Arrestes hinweist. Weiterhin ist eine induzierte *hdp1*-Expression ausreichend, um die Filamentbildung und den G2-Arrest auszulösen.

Hdp1 induziert die Expression von Prf1, dem zentralen transkriptionellen Regulator in der *a*-Regulationskaskade, sowie von Rop1, einem Transkriptionsfaktor, der für die Prf1-Expression in der saprophytischen Phase benötigt wird. Obwohl nicht für die Pheromon-induzierte Expression notwendig, moduliert Hdp1 die Expression von Prf1 und Rop1 und etabliert so eine positive Rückkopplungsschleife zwischen der b-abhängigen Regulationskaskade und dem Pheromon-Signalweg.

Microarray-Analysen zeigten, dass zwei Regulatoren des Zellzyklus durch Hdp1 reguliert werden. Pcl12, ein Pho85-ähnliches Zyklin, wird durch Hdp1 induziert, wohingegen Clb1, ein B-Typ Zyklin, reprimiert wird. Pcl12 scheint für die Hdp1-induzierte Filamentbildung und den Hdp1-induzierten G2-Zellzyklus notwendig zu sein, zusätzlich scheint der Zellzyklusarrest jedoch noch von weiteren Umweltsignalen abhängig zu sein. Clb1 ist für die Hdp1-abhängige Zellzykluskontrolle nicht notwendig. Die in dieser Arbeit gewonnen Daten lassen auf eine Funktion von Hdp1 in der Feinabstimmung der *a*- und *b*-abhängigen Zellzykluskontrolle und der Integration von Umweltsignalen schließen.

Glossary

AA	two alanine residues
Amp	ampicillin
bbs	b-binding site
bp	base pair
ºC	degree Celcius
Cbx^R	carboxin-resistance
CM	complete medium
C-terminal	Carboxy-terminal
DAPI	4',6-diamidino-2-phenylindole
dCTP	deoxycytidine triphosphate
DIC	Differential Interference Contrast
DMSO	Dimethylsulfoxide
DNA	deoxyribonucleic acid
dNTP	deoxyribonucleotide
dpi	days post infection
EDTA	Ethylendiamintetraacetic acid
eGFP	enhanced green fluorescent protein
f.c.	final concentration
g	gravity
GFP	green fluorescent protein
hph	hygromycin phosphotransferase gene
Hyg^R	hygromycin-resistance
kb	kilobase
ip	iron sulphur subunit of the succinate dehydrogenase locus
M	molar
MAPK	Mitogen-activated protein kinase
MAPKK	MAPK-Kinase
MAPKKK	MAPKK-Kinase
Mfa1	(a1) mating factor encoded by the *a1* allele of *Ustilago maydis*
Mfa2	(a2) mating factor encoded by the *a2* allele of *Ustilago maydis*
min	minute
MOPS	3-[N-Morpholino] propanesulfonic acid
mM	millimolar
Nat^R	clonnat-resistance
N-terminal	amino-terminal
OD_{600}	optical density at 600 nm
ORF	open reading frame
PCR	Polymerase Chain Reaction
PD	potato-dextrose
PIPES	Piperazine-N-N'-bis-(2-ethane-sulfonatic acid)
$Phleo^R$	phleomycin-resistance
Pra1	pheromone receptor encoded by the *a1* allele of *Ustilago maydis*
Pra2	pheromone receptor encoded by the *a2* allele of *Ustilago maydis*
PKA	Protein kinase A
PRE	Pheromone response element
RNA	ribonucleic acid
RRS	Rop1 recognition site
RT	Reverse Transcription
SDS	Sodium lauryl sulfate
rpm	rotation per minute
T_m	melting temperature
Tris	Trishydroxymethylaminomethane
U	unit (enzymatic activity)
UTR	untranslated region
v/v	volume per volume
wt	wildtype
w/v	weight per volum
YFP	yellow fluorescent protein

Table of Content

1 Introduction..... 1
1.1 The corn smut fungus, *Ustilago maydis*..... 1
1.2 Life cycle of *Ustilago maydis*. 1
1.3 Mating type loci of *U. maydis* 3
1.3.1 *a*-mating type locus..... 4
1.3.2 *b*-mating type locus..... 4
1.4 Signalling cascades mediating developmental processes. 6
1.5 b-regulatory cascade in *U. maydis*..... 7
1.6 Cell cycle and cell shape controls in *Ustilago maydis*..... 8
1.6.1 G1/S transition in *Ustilago maydis* 9
1.6.2 G2/M transition in *Ustilago maydis*..... 10
1.7 Pho85-cyclins and its Pho85/Cdk5 cyclin dependent kinase..... 10
1.8 Aim of this study 12
2 Results 13
2.1 *hdp1* expression is dependent on the bE/bW-heterodimer and on pheromone stimulation 13
2.2 *hdp1* encodes a homeodomain transcription factor 15
2.3 *hdp1* deletion impairs filament formation and the cell cycle arrest 18
2.4 Hdp1 function is sufficient for filament formation and G2 cell cycle arrest. 21
2.5 Hdp1 is involved in the regulation of *b*-independent genes..... 26
2.6 Hdp1 potentially regulates the *prf1* expression via Rop1. 29
2.7 *hdp1* overexpression affects the expression of cell cycle related genes. 31
2.8 *pcl12* expression is bE/bW-heterodimer and pheromone dependent 32
2.9 *pcl12* is required for b- and Hdp1-mediated filamentation. 33
2.10 The role of *pcl12* in Hdp1-mediated G2 cell cycle arrest depends on nutrients. 35
2.11 Clb1 repression is not required for Hdp1-mediated G2 cell cycle arrest and filamentation. 36
2.12 *hdp1* deletion affects the pheromone response in minimal media..... 38
3 Discussion..... 40

3.1 Hdp1 is a homeodomain transcription factor. 40
3.2 Regulation of *hdp1* expression 41
3.3 Hdp1-dependent gene regulation 42
3.4 Hdp1 modulates G2 cell cycle arrest and filamentation. 45
3.5 Mechanism of Hdp1-mediated cell cycle arrest and filamentation 46
3.6 Hdp1 is required for fine-tuning the cell cycle regulation during pathogenic development of *U. maydis* 49
4 Materials and methods 52
4.1 Materials and source of supplies 52
4.1.1 Chemicals, buffers and solutions, media, enzymes, and kits 52
4.1.2 Oligonucleotide list 55
4.1.3 Strains 56
4.1.4 Plasmids and Plasmid constructs 57
4.1.5 Plasmids and Plasmid constructions during this work 58
4.2 Genetic, microbiology and cell biology methods 58
4.2.1 *Escherichia coli* 58
4.2.2 *Ustilago maydis* 60
4.3 Molecular biology standard methods 64
4.3.1 Isolation of nucleic acids 64
4.3.2 Nucleic acid blotting and hybridization 66
4.3.3 Sequence and structure analysis 68
4.3.4 PCR techniques 69
4.4 DNA microarray analyses 72
5 References 76
6 Appendixes 83

1 Introduction

1.1 The corn smut fungus, *Ustilago maydis*.

Ustilago maydis is a phytopathogenic basidiomycete infecting corn (*Zea mays*) and teosinte (*Zea mexicana*), an ancestor of cultivated corn. *U. maydis* is the causal agent of the so called corn smut disease and causes severe economical losses in agriculture. However, in Mexico smut infected sweet corn ("huitlacoche") is considered a delicacy (Ruiz-Herrera and Martinez-Espinoza, 1998). *U. maydis* is taxonomically classified in the class of Heterobasidiomycetes, in the order *Ustilaginales* and the family *Ustilaginaceae*. Due to the ease of genetic manipulation and the availability of its genome sequence, *U. maydis* is considered a model organism to study sexual development and pathogenicity of fungi (Bölker, 2001).

1.2 Life cycle of *Ustilago maydis*.

The life cycle of *U. maydis* can be divided into a saprophytic and a biotrophic phase. In the saprophytic phase, the haploid cells, called sporidia, divide yeast-like and live saprophytically. In this stage, the cells are not able to infect the host plant. The biotrophic phase is initiated after fusion of two compatible sporidia. The fusion is mediated via a pheromone/receptor-based system encoded by the *a*-mating type locus. Upon pheromone recognition, two compatible sporidia form conjugation tubes that are cell cycle arrested in the G2 phase (Garcia-Muse *et al.*, 2003). The conjugation tubes of compatible cells grow towards each other, resulting in a cell fusion. The processes subsequent to the *a*-mediated fusion are controlled by the *b*-mating type locus that encodes a pair of homeodomain proteins, termed bE and bW. Upon fusion of the conjugation tubes, the infective dikaryotic hypha is formed. In this stage, both nuclei are still in a G2 cell cycle arrest (Snetselaar and Mims, 1992), and during filamentous growth, only the tip portion of the hypha is filled with cytoplasm. The remaining part consists of empty sections originating from the regular insertion of septa at the distal end of the tip-cell (Banuett and Herskowitz, 1994b). To complete the sexual cycle, the host plant is strictly required. Only upon penetration of the plant, the cell cycle arrest of the dikaryotic hyphae is released (Snetselaar and Mims, 1993). Plant penetration is associated with the formation of appressoria that appear as a swelling of the hyphal tip. The penetration mechanism is probably mediated by lytic enzymes. (Kahmann and Kämper, 2004; Snetselaar and Mims, 1993). After

penetration, fungal hyphae grow intra- and intercellular without branching and the plasma membrane of the invaded host cells remains intact. Plant defense reactions such as necrosis, cannot be observed (Banuett and Herskowitz, 1996; Snetselaar and Mims, 1992). Between three and four days after infecion, the hyphae start to branch extensively, and chlorosis and anthocyanin streaks can be observed. Already 5 days after infection tumor formation becomes obvious. At later stages, hyphal branching increases profoundly, indicating the onset of spore formation. Hyphae twist around each other and are surrounded by mucilaginous material. The fungal hyphae fragment into segments that contain single nuclei. Karyogamy presumably takes place at this stage and is followed by the development of rounded cells to mature teliospores (Banuett and Herskowitz, 1996). Teliospores can be spread by wind, rain and insects and germinate under suitable conditions (Christensen, 1963). Germinating teliospores form the promycelium, which, after meiosis, gives rise to haploid sporidia (Christensen, 1963).

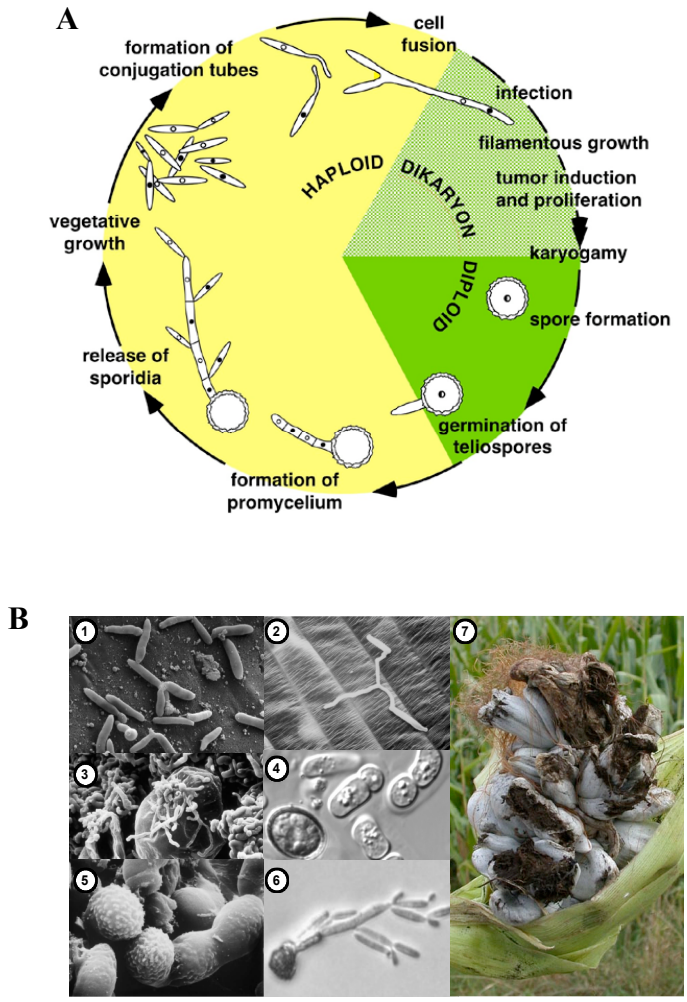

Figure 1 The life cycle of *Ustilago maydis*.
A) Schematic diagram of life cycle of *U. maydis* (see details in text). B) Different developmental of stages *U. maydis* are shown: (1) haploid sporidia dividing by budding (G. Wanner). (2) Fusion of two haploid sporidia and formation of dikaryotic hyphae on the leaf surface (Snetselaar and Mims, 1993). (3) Proliferation of the mycelium in tumor (K. Snetselaar). (4) Pre-sporulation stage consisting of round cells derived from fragmented hyphae (S. Huber) (5) Formation of the teliospores (Snetselaar and Mims, 1994). (6) Germinations of the diploid teliospore and release of haploid sporidia (S. Huber) (7) Tumor formation on a cob of corn (J. Kämper).

1.3 Mating type loci of *U. maydis*

Mating is a crucial step in the life cycle of sexually reproducing organisms. The mating-type genes in fungi function as a barrier to prevent self-fertilization, maintaining the genetic variability within the population (Casselton and Olesnicky, 1998). The mating system of *U. maydis* is tetrapolar. The term "tetrapolar" refers to the four distinct interactions between haploid cells that are attributed to the presence of two genetically unlinked loci working independently to determine mating-type

specificity (Kothe, 1996). The *a*-mating type locus in *U. maydis* consists of two alleles, while the *b*-mating type locus is multiallelic.

1.3.1 *a*-mating type locus

Fusion between haploid cells that harbor compatible mating-types is mediated via a pheromone/receptor-based system encoded by the *a*-mating type locus (Bölker *et al*., 1992; Urban *et al.*, 1996b). The two *a* alleles in *U. maydis* are defined by nonhomologous DNA sequences consisting of 4.5 kb for *a1* and 8 kb for *a2*, flanked by identical sequences. Each allele encodes a precursor of a lipopeptide pheromone (Mfa1 or Mfa2) and for a pheromone receptor (Pra1 or Pra2). The pheromone receptor of one allele can recognize the pheromone of the other allele and mediates the subsequent fusion process. Within the *a2* locus two additional genes are present, termed *lga2* and *rga2*. Recently, Lga2 has been proposed to be involved in prevention of mitochondrial fusion (Bortfeld *et al.*, 2004). The genomic organization of the *a1* and *a2* locus is depicted in Figure 2.

1.3.2 *b*-mating type locus

The *b*-mating type locus of *U. maydis* has at least 19 different alleles (J. Kämper, unpublished data). Each *b*-mating type allele encodes for a pair of unrelated homeodomain proteins, termed bEast (bE), 473 amino acids long, and bWest (bW), 645 amino acids long (Figure 3A). Both proteins harbor a variable domain at the N-terminus, whereas the C-terminal regions display a high degree of sequence conservation, including the homeodomain motif (Gillissen *et al.*, 1992; Kämper *et al.*, 1995). bE and bW are able to dimerize when they are derived from different alleles (Figure 3B). The bE/bW heterodimeric complex acts as a transcription factor that binds to a conserved DNA motif (bbs, b-binding site) in the promoter region of directly b-regulated genes, such as *lga2* and *frb52* (Brachmann *et al.*, 2001; Romeis *et al.*, 2000).

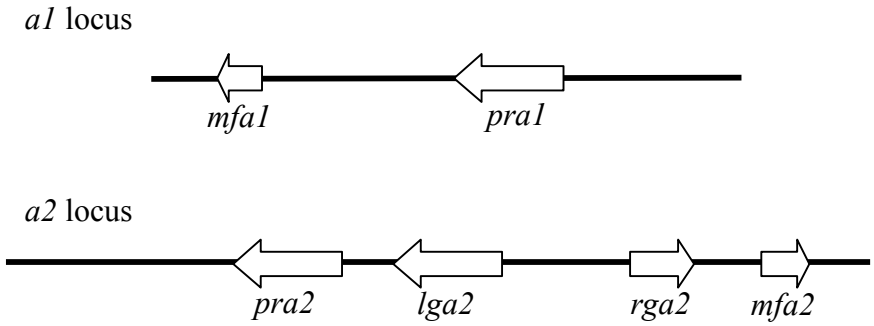

Figure 2 Genomic organization of the *a*-mating type loci of *Ustilago maydis*.
(for details see text). The directions of arrow indicate the direction of transcripion; this diagram does not represent a scaled distance.

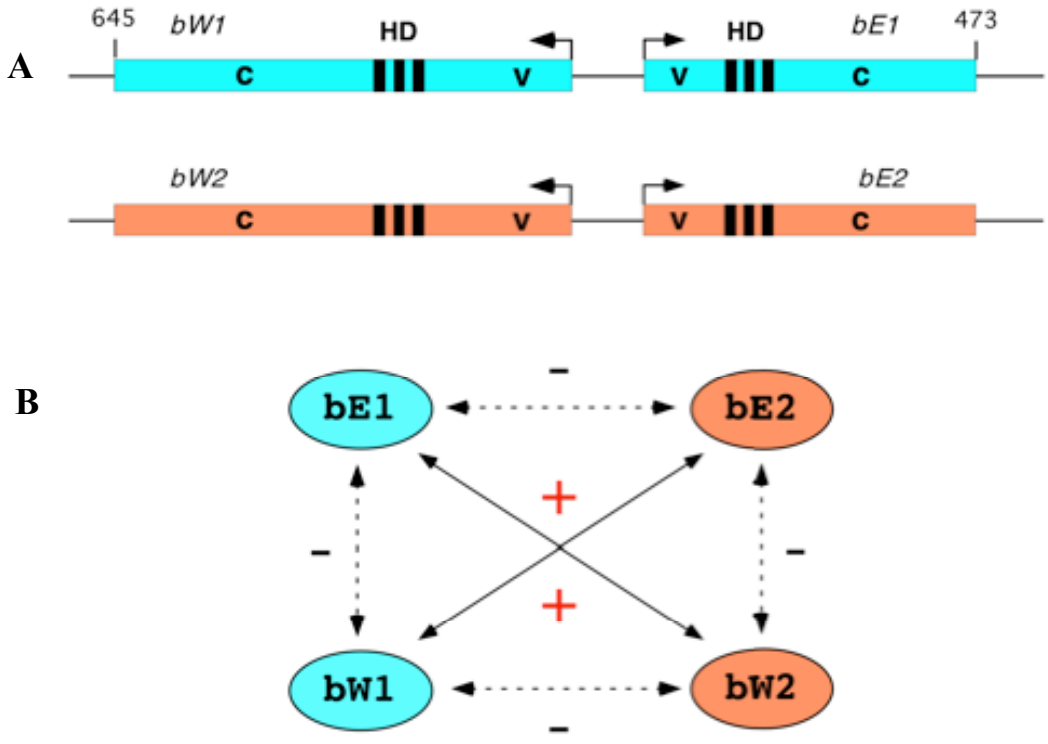

Figure 3 The *b*-mating type locus of *Ustilago maydis*.
A) Schematic diagram of the *b*-mating type locus of *U. maydis* encoding two distinct homeodomain containing proteins, bW and bE. HD = Homeodomain, V=variable domain, C= constant domain.
B) Allele-specific dimerization of the b proteins. bW and bE proteins will dimerize with each other only when originated from a different allele.

1.4 Signalling cascades mediating developmental processes.

During mating and subsequent developmental processes, pheromone signalling, as well as environmental and plant host cues are integrated. Pheromone signalling is triggered by the recognition of the pheromone by its cognate receptor. The main regulatory factor within this cascade is Prf1, a HMG-domain transcription factor that recognizes conserved pheromone responsive elements (PRE) within the *a*- and *b*-mating type loci. Regulation of Prf1 occurs at both transcriptional and post-transcriptional levels. The regulatory region of the *prf1* gene harbors an upstream activating sequence (UAS), two PRE and three Rop1 Recognition sites (RRS). The PRE motif is likely to be used for Prf1 autoregulation, the RRS motif is recognized by Rop1 (Regulator of Prf1) that is required for the expression of *prf1* in axenic culture. The UAS (upstream activating sequence) elements are required for the integration of environmental signals, as different carbon sources (Brefort *et al.*, 2005; Hartmann *et al.*, 1996; Hartmann *et al.*, 1999).

On the posttranscriptional level, Prf1 is regulated by a MAPK (**M**itogen **A**ctivated **P**rotein **K**inase) cascade, and by cAMP signalling via the PKA (**P**rotein **k**inase **A**) Adr1. In addition to mating, both cAMP signalling and the MAPK cascade are also involved in environmental response, for example, in modulating the pH-induced dimorphic transition from yeast-like to filamentous growth (Martinez-Espinoza *et al.*, 2004).

The cAMP signalling cascade is composed of the α and β subunits of a heterotrimeric G protein, Gpa3 and Bpp1, the adenylate cyclase Uac1 and the cAMP-dependent protein kinase with its catalytic and regulatory subunits, Adr1 and Ubc1. From the 4 Gα-subunits identified, only Gpa3 is required for pheromone signalling and pathogenicity. High levels of intracellular cAMP lead to a dissociation of Adr1 and Ubc1 that allows Adr1 to phosphorylate its downstream targets (Dürrenberger *et al.*, 1998; Gold *et al.*, 1994; Gold *et al.*, 1997; Regenfelder *et al.*, 1997). The MAPK cascade module is composed of the MAPKKK Kpp4/Ubc4 (Andrews *et al.*, 2000; Müller *et al.*, 2003), the MAPKK Fuz7/Ubc5 (Andrews *et al.*, 2000; Banuett and Herskowitz, 1994a), and the MAPK Kpp2/Ubc3 (Mayorga and Gold, 1999; Müller *et al.*, 1999). Crk1 encodes a new family of MAP kinases. Together with Fuz7/Ubc5, Crk1 is required for the transcription of *prf1* (Garrido *et al.*, 2004). Kpp6 encodes an unusual MAP kinase that is necessary for effective plant penetration (Brachmann *et al.*, 2003). Additionally an adaptor protein, Ubc2, is proposed to act directly upstream

of the MAP kinase module (Mayorga and Gold, 2001). A cross-talk between cAMP signalling and MAPK cascade module has been described, as the cAMP pathway can suppress the Crk1 transcription (Garrido and Perez-Martin, 2003).

1.5 b-regulatory cascade in *U. maydis*

The active heterodimeric complex functions as a transcription factor binding to a conserved motif (bbs) in the regulatory regions of directly b-regulated genes. Due to the requirement of an active b-heterodimer for pathogenic development, the target genes were assumed to include pathogenicity factors. 20 b-regulated genes have been identified by differential techniques and candidate gene approaches. However, the bbs motif was identified only in a minority of these genes, indicating that the majority of b-regulated genes are indirectly regulated. It has been proposed that the active b-heterodimer triggers a downstream transcriptional cascade with one or more regulatory genes as direct targets. Examples of direct b-targets are *lga2*, *polX*, a gene which encodes for a putative DNA-Polymerase X (Brachmann *et al.*, 2001), and *dik6*, a gene which encodes a membrane protein (Brachmann *et al.*, 2001; Kahmann and Kämper, 2004; Romeis *et al.*, 2000; Weinzierl, 2001). Among 11 b-regulated genes analyzed in more detail, only the MAP kinase kpp6 is required for pathogenicity (Brachmann *et al.*, 2003).

With the availability of DNA-Microarrays that allow the expression analysis of up to 6200 *U. maydis* genes in parallel, it was possible to investigate the processes regulated by the b-heterodimer on a global level.

Expression analysis was performed with the AB31 and AB33 strains harboring compatible *b* genes under the control of the arabinose-inducible (*crg1*) or nitrate-inducible (*nar1*) promoter during a 12 h time course. The induced expression of incompatible *bE* and *bW*, by using AB32 and AB34, served as control (Brachmann *et al.*, 2001). A total of 347 genes that are induced or repressed by the *b*-mating type locus were identified using this approach (J. Kämper and M. Scherer, unpublished data).

Functional classification of the identified b-regulated genes showed that cellular processes such as the restructuring of the cell wall or alterations in lipid metabolism are controlled by the *b*-mating type locus. For example, the genes encoding putative chitin synthases, chitin deacetylases and endoglucanase were found to be up or down-regulated, indicating that the modification of cell wall structure is based on the

differential expression of each isoenzyme having different activities (J. Kämper and M. Scherer, unpublished data). In addition, a large number of differentially expressed genes is predicted to be involved in cell cycle regulation, mitosis and/or DNA replication, which is consistent with the observation that, after *b*-induction, the cell cycle is arrested (J. Kämper and M. Scherer, unpublished data). Moreover, a large part of genes encode for proteins that show no similarity to known proteins, suggesting functions specific for the biotrophic phase of *U. maydis* (J. Kämper and M. Scherer, unpublished data).

rbf1 (Regulator of b-filament 1) encodes a putative C_2H_2 zinc-finger transcription factor that is most likely directly b-regulated and that is required for both filamentous growth and pathogenic development. Rbf1 represents the major regulator downstream b, since it regulates about 90% of the *b*-dependent genes at transcriptional level (J. Kämper and M. Scherer, unpublished data).

Another presumably direct b-target is *clp1* that encodes a protein with sequence similarity to Clp1 from *Coprinopsis cinerea* that is required for clamp formation. *clp1*-mutant strains are able to penetrate the plant surface, however, cell proliferation cannot be observed *in planta*. Thus, Clp1 is proposed to be involved in the regulation of the cell division and clamp formation of the dikaryon *in planta* (Scherer *et al.*, 2006).

biz1 (b-induced zinc-finger 1) encodes a C_2H_2 zinc-finger transcription factor which is required for the expression of a large number of secreted proteins and is essential for pathogenicity (Vranes, 2006). Moreover, it has been demonstrated that Biz1 down-regulates the expression of the mitotic cyclin *clb1* (Flor-Parra *et al.*, 2006).

1.6 Cell cycle and cell shape controls in *Ustilago maydis*

Developmental decisions often involve differentiation processes that need the reset of the cell cycle and the induction of a morphogenetic program. Therefore, the ability of the fungus to modify its cell cycle is thought to be an important determinant for a successful infection (Perez-Martin *et al.*, 2006). *U. maydis* haploid cells are cigar-shaped and normally produce one polar bud per cell cycle (Jacobs *et al.*, 1994) after completion of DNA synthesis in the G2 phase (Snetselaar and McCann, 1997). The growth of the bud relies almost entirely on polar growth (Steinberg *et al.*, 2001). Rapidly growing cells have a very brief G1 phase, and the S phase starts shortly after cytokinesis because of a similar mass of daughter cells to mother cells (Perez-Martin

et al., 2006). However, *U. maydis* cells can adjust their cell cycle depending on environmental conditions. Under starvation conditions, a prolongation of the doubling time is observed. This delay of the cell cycle is caused by increasing the length of the G1 phase, until the cell reaches a minimum size to enter a new S phase; however, the G2 phase is also prolonged, allowing the bud to reach a correct size (Garrido and Perez-Martin, 2003; Snetselaar and McCann, 1997). *U. maydis* has three cyclins dedicated to cell cycle regulation that are able to associate with the Cdk1(cyclin dependent kinase1): Cln1, a G1-cyclin, and two B-type cyclins, Clb1 and Clb2. In general, cyclin levels are strictly regulated both at transcriptional and post-transcriptional levels. For example, high levels of Clb1 can affect viability, provoking defects in chromosomal segregation (Garcia-Muse *et al.*, 2004).

1.6.1 G1/S transition in *Ustilago maydis*

The Clb1 cyclin associated to Cdk1 is required for both the G1/S and G2/M transitions. Therefore, conditional *clb1* mutants arrest at restrictive conditions in both the G1 and G2 phase (Garcia-Muse *et al.*, 2004). Clb1 is specifically required for the G1/S transition and cannot be bypassed by the other cyclins (i.e. Cln1 or Clb2). During the G1 phase, the complex of the Cru1-associated APC/C controls the Clb1 level. In *cru1* mutant strains, Clb1 accumulates faster than in wildtype, leading to a premature entry into the S phase (Castillo-Lluva *et al.*, 2004). The ability to delay the G1/S transition is possibly required for small cells that have to prolong the G1 phase until they achieve the minimum cell size sufficient to start DNA replication (Perez-Martin *et al.*, 2006). Additionally, the *cru1* mRNA level is dependent on nutritional conditions; therefore, it can be used to link nutrient availability to cell cycle control (Castillo-Lluva *et al.*, 2004). Cln1 is a protein with high sequence similarities to G1 cyclins from other fungi (Castillo-Lluva and Perez-Martin, 2005) and interacts with Cdk1, similar to Clb1. *cln1* mutants display a delayed G1 phase when compared to wild-type (Castillo-Lluva and Perez-Martin, 2005). Despite the apparent minor role of Cln1 on the G1/S transition, it has a major role at the morphological level. The absence of Cln1 leads to cell aggregates that still remain attached after cytokinesis, and often lose their polarity. Consistently, high levels of Cln1 provoke a strong polar growth, resulting in multinucleated filaments with septations (Castillo-Lluva and Perez-Martin, 2005).

1.6.2 G2/M transition in *Ustilago maydis*

After DNA replication, formation of the bud indicates the beginning of the G2 phase. When the bud has a proper size, mitosis is induced, starting M phase. Both Clb1/Cdk1 and Clb2/Cdk1 complexes are required for G2/M transition. However, the Clb2 cyclin appears to be specific for G2/M transition. In *U. maydis*, Clb2 levels possibly determine the length of the G2 phase and the size of the bud. Probably a G2/M size control is operated through the Clb2/Cdk1 complex. Apparently, the B-cyclin/Cdk1 complex activity is controled via inhibitory phosphorylation of Cdk1 during the G2 phase (Sgarlata and Perez-Martin, 2005a; Sgarlata and Perez-Martin, 2005b).

In *U. maydis*, this tyrosine inhibitory phosphorylation depends on the Wee1 kinase that can function as a dose-dependent inhibitor of mitosis (Sgarlata and Perez-Martin, 2005a). The primary target of Wee1 is probably the Clb2/Cdk1 complex. The requirement of *wee1* indicates the importance of controlling the length of G2 phase in *U. maydis*. After DNA replication, *U. maydis* cells have to decide whether to bud or to enter the mating program, a decision that relies on external stimuli (Garcia-Muse *et al.*, 2003). Controlling the length of G2 phase seems to be primordial for *U. maydis* to make the correct decision (Perez-Martin *et al.*, 2006). In addition, the inhibitory phosphorylation is removed at the onset of mitosis by the activity of the Cdc25 phosphatase. Cdc25 is essential for the growth of *U. maydis*; cells lacking Cdc25 arrest their cell cycle at G2 phase (Sgarlata and Perez-Martin, 2005b). Summarily, the G2/M transition seems to be regulated by the balance between Wee1 and Cdc25 activities in *U. maydis*, thereby controlling the phosphorylation of Cdk1 associated to Clb2 (Perez-Martin *et al.*, 2006).

1.7 Pho85-cyclins and its Pho85/Cdk5 cyclin dependent kinase

The Pho85 cyclin-dependent kinase represents a homolog of mammalian Cdk5 which is involved in several signal transduction pathways through the association with cyclins of the Pho85 family (Pcls) in fungi. In mammals, Cdk5 belongs to a family of cyclin-dependent kinases that seem to be involved mainly in the control of cell differentiation and morphology rather than cell division (Dhavan and Tsai, 2001).

The Pho85 cyclin-dependent kinase was initially identified in *Saccharomyces cerevisiae* because of its involvement in the regulation of phosphate-scavenging enzymes; moreover, it has been implicated in many other cellular processes, including

stress adaptation, glycogen storage, cell cycle progression and morphogenesis (Carroll and O'Shea, 2002). The pleiotropic phenotype caused by *pho85* deletion supports its multiple function. Although these responses require the phosphorylation of different substrates and have different mechanistic consequences as a result of this phosphorylation, all are involved in responses to changes in environmental conditions (Carroll and O'Shea, 2002).

In the filamentous fungus *Aspergillus nidulans,* two highly related Cdk5-like proteins, PhoA and PhoB, have important roles in integrating environmental cues and developmental responses (Bussink and Osmani, 1998; Dou *et al.*, 2003).

In budding yeast, Pho85 was shown to have ten cyclin partners, so called Pcls (Pho85-cyclin). Pcls were identified primarily through sequence homology and two-hybrid screens. They have been grouped by sequence homology into two subfamilies, each with five members. Of these ten cyclins, four (PCL1, PCL2, PCL7 and PCL9) show cell-cycle-regulated expression patterns, suggesting that at least some functions of Pho85 are cell-cycle dependent or relevant. Transcriptional regulation could be important for those PCLs whose expression is not regulated by the cell cycle (For review, see (Carroll and O'Shea, 2002).

Recently, a Cdk5/Pho85 homolog in *U. maydis* has been identified. By using temperature-sensitive mutants, Cdk5 was shown to be required at all morphological stages of *U. maydis* – the yeast-like sporidia, the conjugation tubes and the dikaryotic hyphae – thereby affecting its pathogenicity (Castillo-Lluva *et al.*, 2007). From the seven Pcl-homologues identified in the *U. maydis* genome, only *U. maydis* Pcl12 has been studied in detail. Pcl12 interacts specifically with Cdk5 in *U. maydis*. *pcl12* expression is induced by pheromone stimulation and induced by an active b-heterodimer. Interestingly, *pcl12* overexpression is sufficient to induce hyperpolarized growth and G2 cell cycle arrest. The mutant phenotypes suggest a crucial role for Pcl12 during morphogenesis, the formation of the *b*-dependent filament, the induction of the conjugation hyphae, and the formation of a promycelium during spore germination. Nevertheless, *pcl12* mutant strains were still pathogenic (Flor-Parra *et al.*, 2007).

1.8 Aim of this study

In *U. maydis*, a G2 cell cycle arrest is observed after stimulation with mating pheromone as well as in the dikaryon prior to plant penetration. This cell cycle arrest is mediated via the *a*-mating type dependent signaling pathway, as well as via the bE/bW transcription factor encoded by the *b*-mating type. Currently, the knowledge about transcription factors involved in this processes is limited.

The aim of this study was the functional characterization of a novel transcription factor that is regulated via both mating types. Hdp1 (**H**omeo**d**omain **p**rotein**1**) affects the cell cycle regulation and has impact on filament formation. Further aims were to identify downstream targets of *hdp1* by means of microarray analysis, and to use reverse genetics to elucidate their specific roles in the context of the *hdp1* mediated phenotypes.

2 Results

2.1 *hdp1* expression is dependent on the bE/bW-heterodimer and on pheromone stimulation

To identify genes that are regulated by the bE/bW-heterodimer, a microarray analysis by means of custom Affymetrix arrays covering approximately 90 % of the predicted 7050 *U. maydis* genes was performed. Two haploid strains AB31 and AB33 that harbor compatible *bW2*/*bE1* genes under the control of the arabinose-inducible *crg1* promoter and the nitrate inducible *nar1* promoter, respectively (Brachmann *et al.*, 2001), were used for initiation of *b*-dependent development in axenic culture. The changes in the expression profiles upon *b*-induction were monitored independently in both strains during a 12-hours time course. As a control, strains AB32 and AB34, harboring the incompatible combinations *bE2* and *bW2*, were used. In total, more than 350 *b*-dependent genes were identified (M. Scherer and J. Kämper, unpublished data). One of the *b*-dependently regulated genes identified was *hdp1* (**H**omeo**d**omain **p**rotein**1**), annotated as um12024 at the **M**IPS ***U****stilago* ***m****aydis* **D**ata**B**ase (MUMDB; http://mips.gsf.de/genre/proj/ustilago). Deduced from the microarray experiment, expression of *hdp1* was induced early after formation of the bE1/bW2 heterodimer. By real-time RT-PCR, *hdp1* expression in the strain AB31 ($a1bW2^{crg1P}bE1^{crg1P}$) showed a peak at 5 hours after *b*-induction that could not be observed in the control strain AB32 ($a1bW2^{crg1P}bE2^{crg1P}$) (Figure 4A). In axenic culture, *hdp1* message was barely detectable in the haploid wildtype strains FB1 (*a1b1*) and FB2 (*a2b2*), but was induced when an active bE/bW heterodimer was formed upon mating of two compatible strains (FB1xFB2). A similar result was obtained in the diploid strain FBD11 (*a1a2b1b2*) and the solopathogenic haploid strain SG200 (*a1mfa2 bW2bE1*); both strains carry active bE/bW combinations. However, in a SG200 derivative deleted for the *rbf1* gene, *hdp1* expression was drastically reduced, indicating that the expression of *hdp1* also depends on *rbf1* (Figure 4B). Rbf1 is a *b*-dependently expressed transcription factor that is required for the regulation of the majority of *b*-dependent genes (M. Scherer and J. Kämper, unpublished). In addition, *rbf1* deletion also led to a decreased expression of the *bE* gene, suggesting a positive feedback regulation of Rbf1 on *b* genes (Figure 4B). *hdp1* is also expressed during pathogenic development in tumor tissue 2d, 5d, 7d, 9d and 13 days post infection (dpi) compared to FB1 in axenic culture (Figure 4C).

A

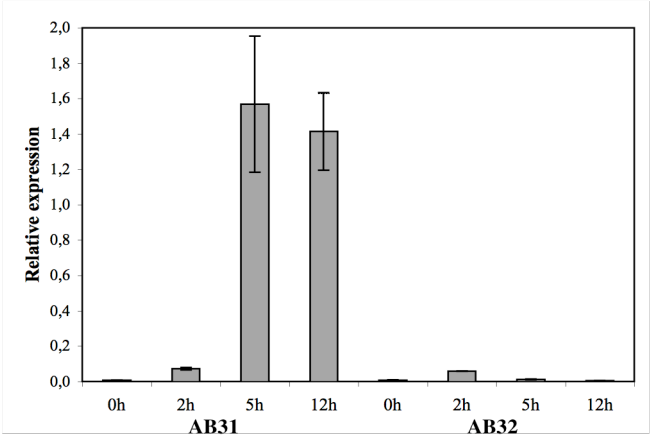

Figure 4. ***hdp1* expression is *b*-dependent.**

(A) Real-time quantitative RT-PCR analysis of *hdp1* expression after induction of compatible (AB31) and incompatible (AB32) combinations of bW and bE. A clear induction of *hdp1* is detectable after 5h.

B

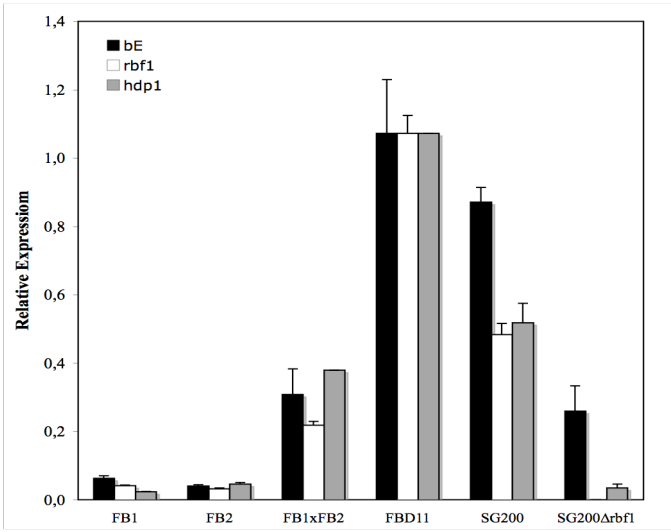

(B) Real-time quantitative RT-PCR analysis of *bE*, *rbf1 and hdp1* expression. Analyzed were the haploid strains FB1 (*a1b1*) and FB2 (*a2b2*), a crossing of FB1 and FB2, the solopathogenic strains FBD11 (*a1a2b1b2*) and SG200 (*a1mfa2bW2bE1*) and the SG200 derivative SG200*Δrbf1*, which carries a deletion for *rbf1*. All strains were grown on charcoal containing CM-glucose plates at 22 ºC for 48 hours.

C

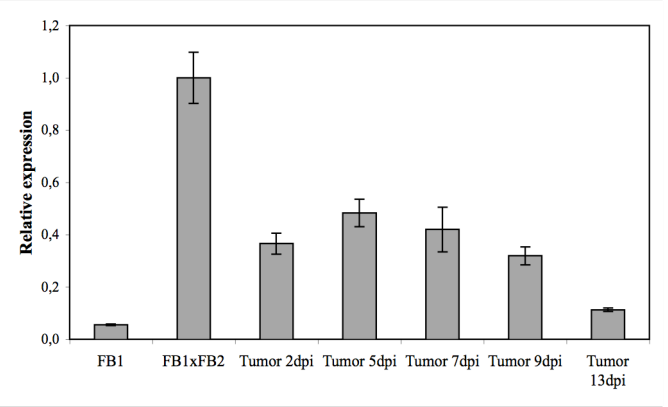

(C) Real-time quantitative RT-PCR analysis of *hdp1* during pathogenic development. Expression was measured in haploid FB1 (*a1b1*) cells, a crossing of FB1 and FB2, grown on charcoal containing CM-glucose plates at 22 ºC for 48 hours and tumor tissues 2d, 5d, 7d, 9d and 13 days post infection (dpi).

In all experiments, *bE*, *rbf1 and hdp1* expression was measured relatively to the constitutively expressed gene for the elongation factor 2B (*elf2B*: um04689). Bar graphs depict the mean value and standard deviation of two technical replicates.

In addition, when FB1 (*a1b1*) cells were incubated with the compatible pheromone Mfa2, *hdp1* expression was induced, and a similar result was obtained in strain FB1*Pcrg1:fuz7DD* (Müller *et al.*, 2003) (Figure 5A and 5B). In this strain, a gene encoding a constitutive active form of the MAPK kinase, Fuz7 is placed under the control of the arabinose inducible *crg1* promoter. Induction of the *fuz7DD* gene upon growth of FB1*Pcrg1:fuz7DD* in CM-arabinose medium leads to an activation of the pheromone pathway; as a response, the *hdp1* gene is induced. Taken together, the data show that *hdp1* is regulated both via the pheromone signalling pathway as well as via the b- regulatory cascade.

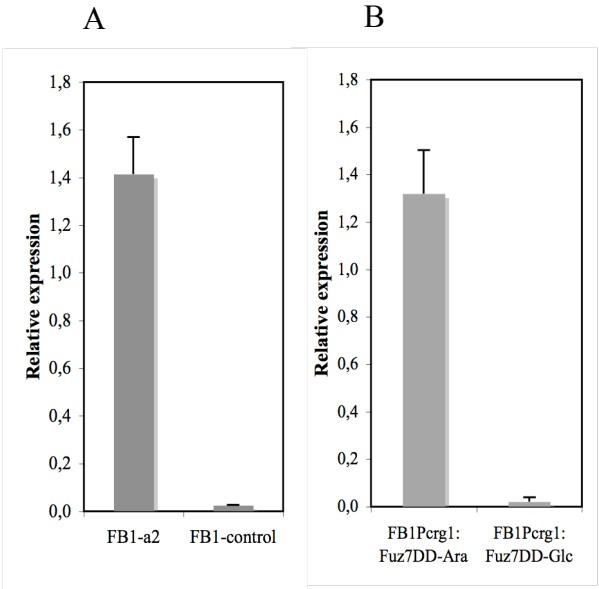

Figure 5. *hdp1* expression is pheromone dependent.

Real-time quantitative RT-PCR analysis of (A) *hdp1* expression in FB1 after treatment with compatible pheromone Mfa2 (FB1-a2). DMSO, the solvent for Mfa2, was used as a control (FB1-control). Expression was measured 6h after treatment. (B) *hdp1* expression in FB1*Pcrg1:fuz7DD*. Transcript levels were measured 6h after induction. Non-induced strain FB1*Pcrg1:fuz7DD* served as a control.

hdp1 expression was measured relatively to the constitutively expressed gene coding for the elongation factor 2B (*elf2B*: um04869). Bar graphs show the mean values and standard deviations of two technical replicates.

2.2 *hdp1* encodes a homeodomain transcription factor

The MUMDB gene prediction for *hdp1* was verified by cDNA fragments generated by means of 5´- and 3´-RACE (**R**apid **A**mplification of **c**DNA **E**nds). Sequence analysis revealed the presence of two introns positioned 612 bp and 684 bp within the predicted *hdp1* ORF. The length of the 5'- and 3'-untranslated regions (5' and 3' UTRs) were 648 and 69 nucleotides, respectively. The ORF encodes for a predicted protein of 856 amino acids. The predicted protein contains a putative homeodomain, a conserved DNA-binding domain, from amino acid position 184 to 240 (Pfam 22.0 at http://pfam.janelia.org, with an E-value 1.3e -11). With the exception of the homeodomain region no significant similarities to known proteins are present (Appendix 6.1 and Figure. 6). The PSORT algorithm predicted for Hdp1 a high probability for nuclear localization (P = 94.1). To verify the subcellular location, a

hdp1–green fluorescent protein (GFP) fusion gene was used to replace the native *hdp1* locus in the haploid strain AB31 (UECP98). Fluorescence microscopy revealed bright signals in the nucleus (Figure 7) upon induction of the compatible b-heterodimer. Three putative b-binding sites (TGA N_9 TGA) (Brachmann *et al.*, 2001; Romeis *et al.*, 2000) in the promoter regions of *hdp1* at position -490, -578 and -2255 bp (Figure. 8) suggest that *hdp1* is a direct *b*-target gene.

homeodomain

hdp1: 856 amino acids

```
Homeobox          *->RrkRTtFtpeQleeLEkeFqknpYPsreeReeLAkkLgLterqVkvWFQNRRaKwKk<-*
                      r+R   + eQ ++L k   k++ Ps + Re  A +Lg ++r V+vWFQNRR+  Kk
Hdp1        184   GRSRRLLSLEQSKVLYKILDKTHFPSTQSREAAASQLGVSPRKVQVWFQNRRQVGKK    240
```

Figure 6. Schematic diagram of Hdp1. *hdp1* encodes a protein with 856 amino acids containing one putative homeodomain from amino acid position 184 to 240. The alignment of the homeodomain consensus sequence (Pfam 22.0) with the homeodomain of Hdp1 is outlined.

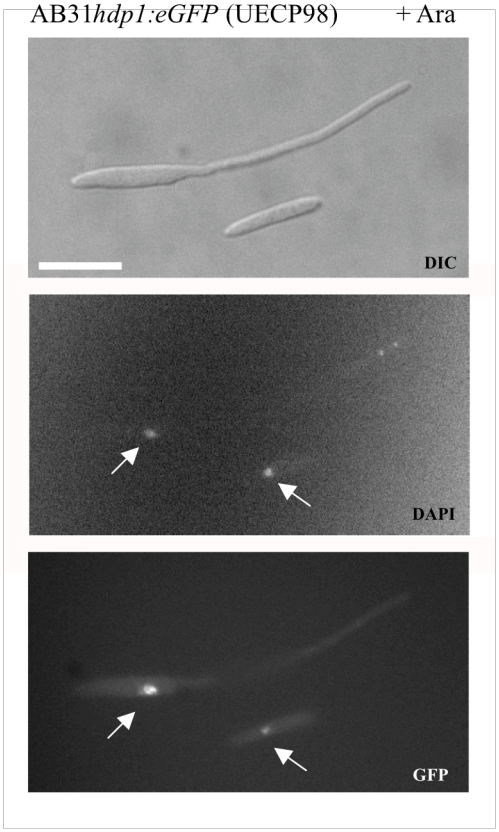

Figure 7. Hdp1:eGFP C-terminal in-frame fusion protein localizes in the nucleus.

Hdp1:eGFP was induced by induction of the b-heterodimer in strain UECP98. Microscopic observations were performed 6h after induction in liquid CM-arabinose medium. The upper picture shows the cell morphology (DIC). Filament formation can be observed. The middle and lower panel depict stained nuclei (DAPI) and GFP-fluorescent signals (GFP), respectively. DAPI and GFP signals in the middle and lower pictures are indicated by arrows. Scale bar = 10 µm

```
frb52-233   GAATGATCAGCAGAATGACACGCTTG
lga2 -155   TCATGATGAGAAGTGTGACAGACTGT
hdp1 -490   CGGTGAGGTGCGCGATGAGGATGTGG
hdp1 -578   AGATGAAATGGCAGATGAAATGAAGA
hdp1 -2255  ACTTGAATCAAGTCGTGAGTGCAGCT
            TGANNNNNNNNNTGA
```

Figure 8. Putative b-binding sites in the *hdp1* promoter. Shown is the comparison of the putative b-binding sequences (TGA N_9 TGA) at positions -490, -578 and -2255 upstream of the predicted transcription start site of *hdp1* with the published b-binding sites of *frb52* (Brachmann *et al*., 2001) and *lga2* (Romeis *et al*., 2000).

To address whether the homeodomain is required for the function of Hdp1, two highly conserved amino acids in the homeodomain of Hdp1, $W_{230}F_{231}$, (Schlesinger *et al.*, 1997) were replaced with two alanines. The altered gene was placed under the control of the *crg1* promoter and integrated into the *ip* locus of FB1, generating strain FB1*Pcrg1:hdp1*$_{AA}$ (UECP106). Induced *hdp1* expression in FB1*Pcrg1:hdp1*$_{wt}$ (UECP19) led to filament formation (see 2.4). However, induction of the *hdp1* variant with the altered homeodomain did not lead to morphological alterations (Figure 9A), although expression of the *hdp1* variant is clearly detectable (Figure 9B). The nuclear localization and the requirement of the homeodomain for function strongly suggest that Hdp1 functions as a homeodomain transcription factor.

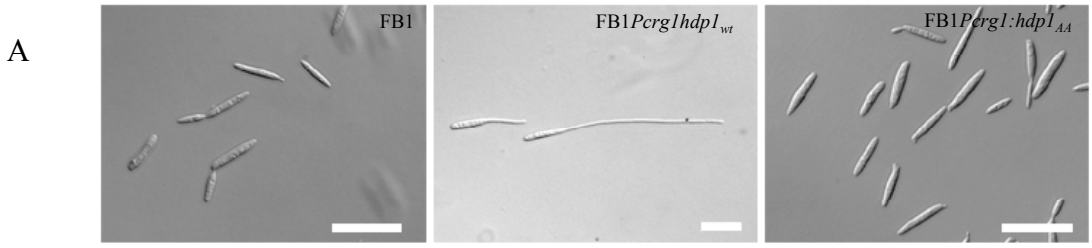

Figure 9. The homeodomain is required for function of Hdp1.

(A) Cell morphology (DIC) of FB1, FB1*Pcrg1:hdp1*$_{wt}$ (UECP19) and FB1*Pcrg1:hdp1*$_{AA}$ (UECP106) after growth in liquid CM-arabinose medium for 6 hours. Only FB1*Pcrg1:hdp1*$_{wt}$ (UECP19) grows filamentously (middle picture). Scale bar = 10 μm.

(B) Northern blot analysis; 10 μg of total RNA were loaded per lane. As a loading control, the membrane was stained with methylene blue to visualize the rRNA. A 300 bp-fragment at the 3'end of the *hdp1* ORF was used as a probe. *hdp1* expression is detectable in both FB1*Pcrg1:hdp1*$_{wt}$ (UECP19) and FB1*Pcrg1:hdp1*$_{AA}$ (UECP106).

2.3 *hdp1* deletion impairs filament formation and the cell cycle arrest

The open reading frame of the *hdp1* gene was deleted by replacement with a hygromycin resistance cassette in the wildtype strains FB1 (*a1b1*), FB2 (*a2b2*), and in a haploid solopathogenic strain SG200 (*a1mfa2 bW2bE1*). The deletion caused neither obvious morphological alterations, nor was the growth rate affected in $YEPS_{Light}$ or CM complete medium (data not shown). Both SG200*Δhdp1* as well as a mixture of the compatible strains FB1*Δhdp1* and FB2*Δhdp1* caused symptoms in plant infection experiments that were indistinguishable from those of infections with the respective progenitor strains (Figure 10A). In CM medium, FB1*Δhdp1* and FB2*Δhdp1* formed conjugation hyphae after treatment with compatible pheromone that were indistinguishable from those of wildtype strains (Figure 10B).

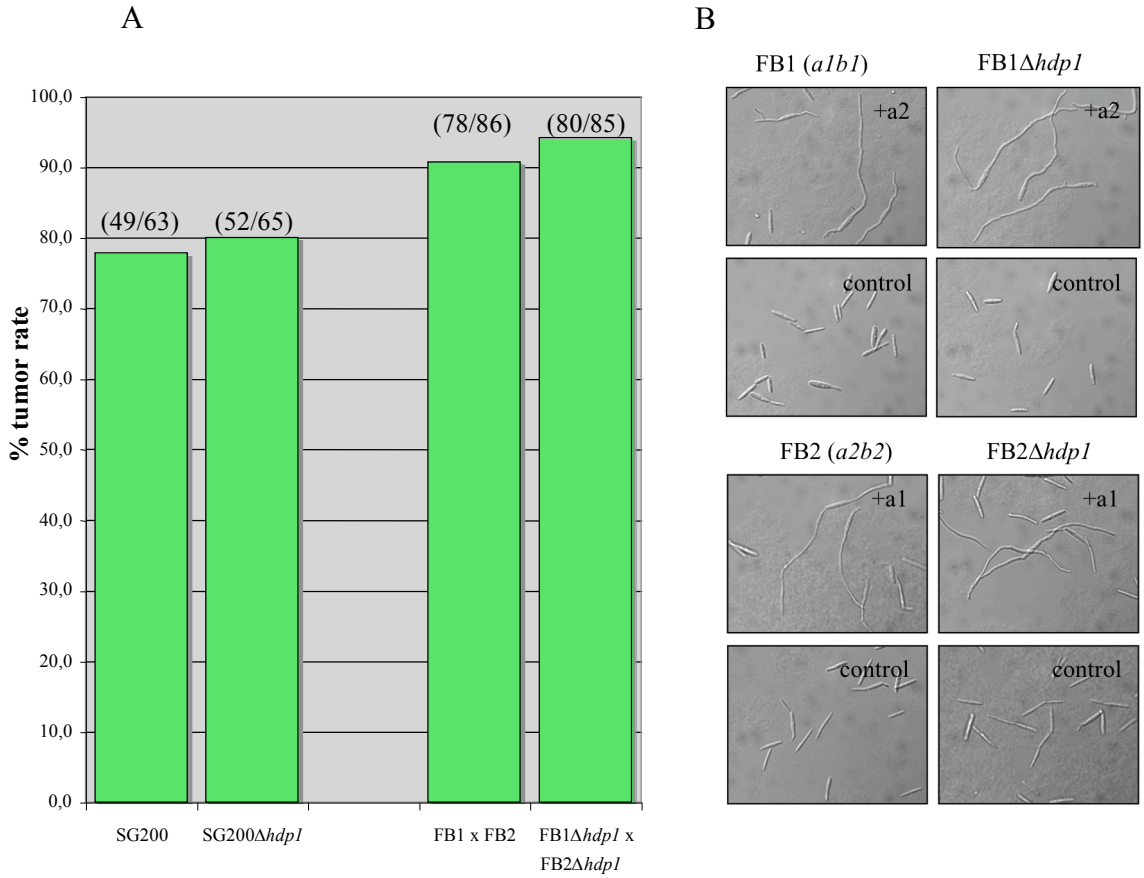

Figure 10 Deletion of *hdp1* does not affect pathogenicity and conjugation hyphae formation. (A) **Pathogenicitiy of Δ*hdp1* strains**; bar graphs show the tumor rates of solopathogenic strains SG200 and SG200Δ*hdp1*, and of a mixture of compatible wildtype (FB1xFB2) and Δ*hdp1* cells (FB1Δ*hdp1* x FB2Δ*hdp1*). Numbers in brackets represent the number of plants with tumors divided by the number of infected plants. (B) **Conjugation hyphae formation of Δ*hdp1* strains;** shown is the conjugation hyphae formation of wildtype and Δ*hdp1* strains after treatment with the synthetic compatible pheromone for 6 hours. DMSO, the solvent for the pheromone, was used as control.

However, when a mixture of FB1*Δhdp1* and FB2*Δhdp1* was spotted onto solid CM-glucose medium containing charcoal, the developing filaments of the *Δhdp1 strains* were shorter than that of the wildtype strains. Similar results were observed for the hyphae of the solopathogenic haploid strain SG200*Δhdp1* (Figure 11A). In order to quantify the effect of the *hdp1* deletion on hyphal length, the diameter of colonies obtained from single SG200 and SG200*Δhdp1* cells was measured after 72 hours of incubation on solid CM-glucose medium containing charcoal. Under these conditions, the average diameter of SG200*Δhdp1* colonies was 1.16 ± 0.15 mm, whereas that of wildtype SG200 colonies was 2.20 ± 0.18 mm (Figure 11B).

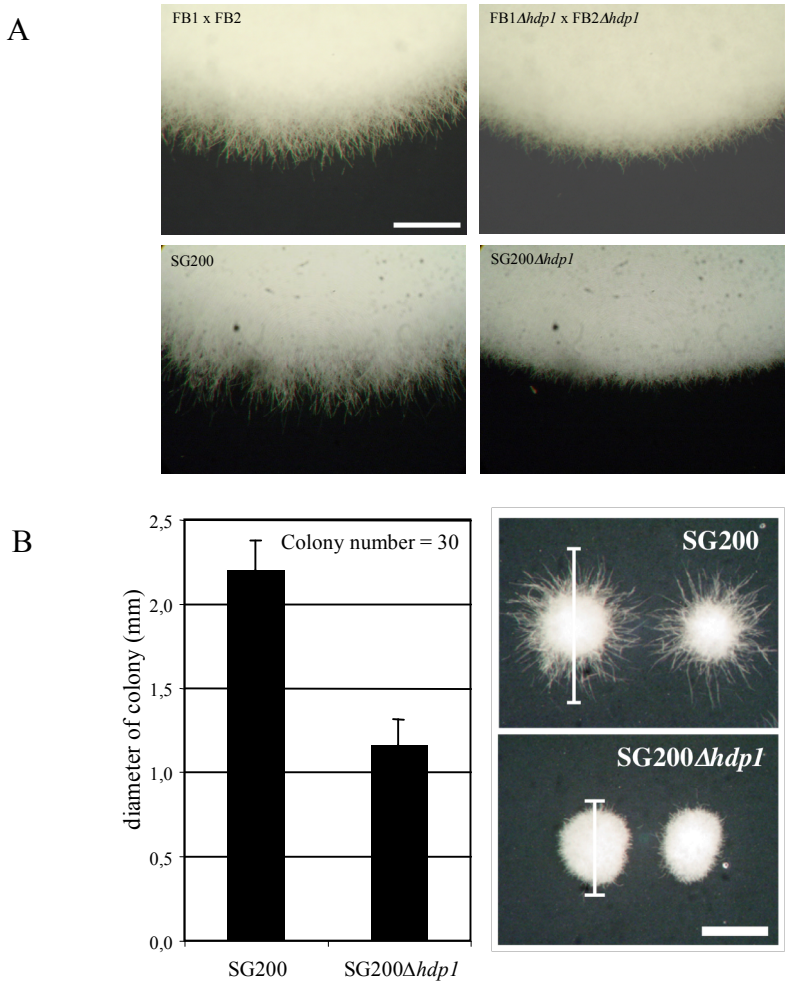

Figure 11. *hdp1* deletion impairs filament formation.
(A) Colony edges of spotted cultures grown for 48 hours at 22ºC on solid CM-glucose medium containing charcoal. The upper panel depicts a mating reaction of the wildtype crossing FB1xFB2 and of the *hdp1* deletion derivatives FB1*Δhdp1*xFB2*Δhdp1*. The lower panel shows the solopathogenic strains SG200 and SG200*Δhdp1*. Scale bar = 0.5 mm
(B) Graph shows the average diameters of SG200 and SG200*Δhdp1* single colonies grown for 72 hours at 22ºC on solid CM-glucose medium containing charcoal. The colony diameter was measured as indicated in the figures on the right-hand side of the graph (for additional information, see text). The bar- and error bars indicate mean values and SD, respectively. Colony number measured per strain = 30. Scale bar = 1 mm

Despite the shorter overall length, the dikaryotic filaments of *hdp1* deletion strains grown on solid CM-glucose medium containing charcoal did not show an altered morphology when compared to that of wildtype strains. However, when nuclei were visualized by DAPI staining, filaments containing more than two nuclei were found more frequently in crossings of Δ*hdp1* strains than in crossings of wildtype strains (Figure 12A and 12B).

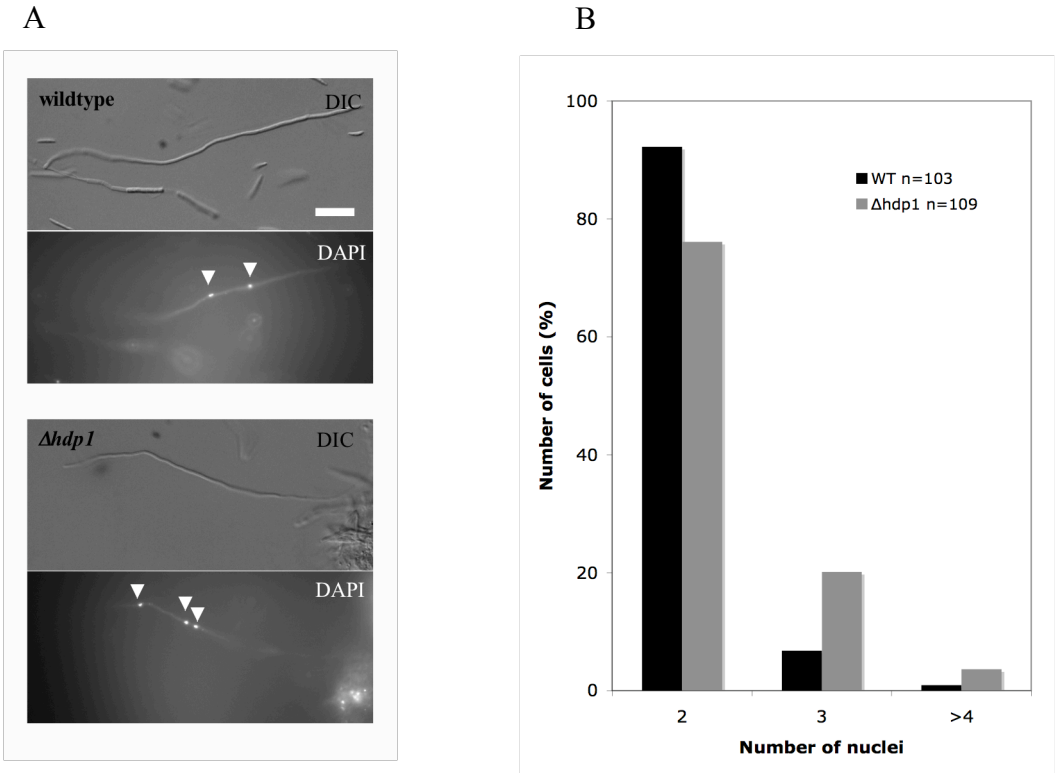

Figure 12. *hdp1* deletion affects the number of nuclei in dikaryotic filaments

(A) Microscopic pictures of wildtype and *Δhdp1* dikaryotic filaments grown on solid CM-glucose medium containing charcoal at 22°C for 24 hours. Both types of filaments have an identical appearance (upper pictures, DIC). Nuclei in the filaments are visualized by DAPI staining and indicated with arrows (lower pictures, DAPI). Scale bar = 10 μm

(B) Bar graphs compare the percentage of the diakaryotic filaments containing the number of nuclei indicated per filament in wildtype and *Δhdp1* strains. In *Δhdp1* filaments, the frequency of cells with more than two nuclei is increased.

In *U. maydis*, the cell cycle of dikaryotic hyphae is arrested in the G2 phase after formation of an active bE/bW heterodimer, and this block is only released after infection of the host plant (Snetselaar and Mims, 1993). The increased number of nuclei in the *Δhdp1* dikaryotic hyphae indicates that Hdp1 is possibly involved in the maintenance of the bE/bW-mediated cell cycle arrest.

2.4 Hdp1 function is sufficient for filament formation and G2 cell cycle arrest.

To study the function of *hdp1* independently from the b-mediated regulation, *hdp1* was fused to the arabinose-inducible *crg1* promoter and integrated into the *ip* locus of FB1, resulting in the strain FB1*Pcrg1:hdp1* (UECP19). Induced expression of *hdp1* in FB1*Pcrg1:hdp1* in CM-arabinose medium led to the formation of filaments; the filamentation was neither observed under non-inducing conditions, nor in the wildtype strain FB1 that was used as a control (Figure 13A). Staining with DAPI revealed that the elongated cells contained single nuclei. Filament formation has been associated with *U. maydis* cells that are arrested in the G2 phase (Banuett and Herskowitz, 2002; Steinberg *et al.*, 2001). Consistently, FACS analysis revealed that after *hdp1* induction cells had a 2C DNA content (Figure 13B). Additionally, cells overexpressing Hdp1 had a drastically reduced growth rate, while under non-inducing conditions the doubling times of strains FB1 and FB1*Pcrg1:hdp1* were similar (130 and 149 minutes, respectively). The induced overexpression of *hdp1* led to a drastically longer doubling time when compared to wildtype cells (357 and 167 minutes, respectively). Taken together, these results clearly demonstrate that *hdp1* induction leads to the formation of filaments that are arrested in the G2 phase of the cell cycle.

A

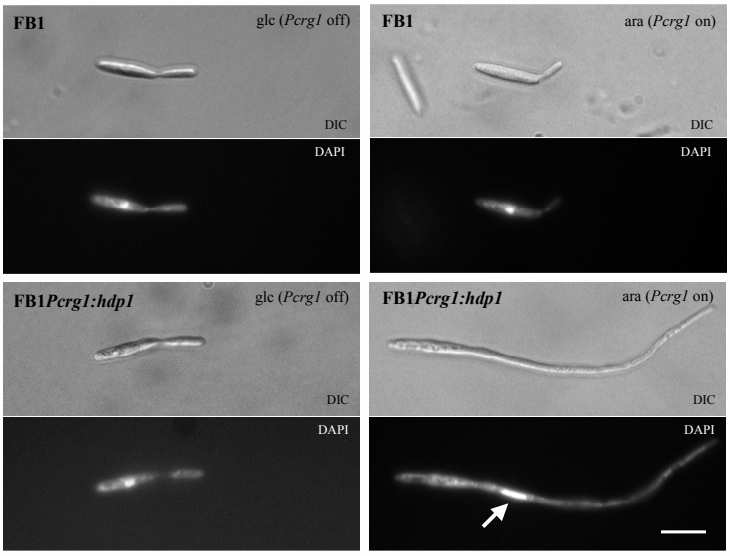

B

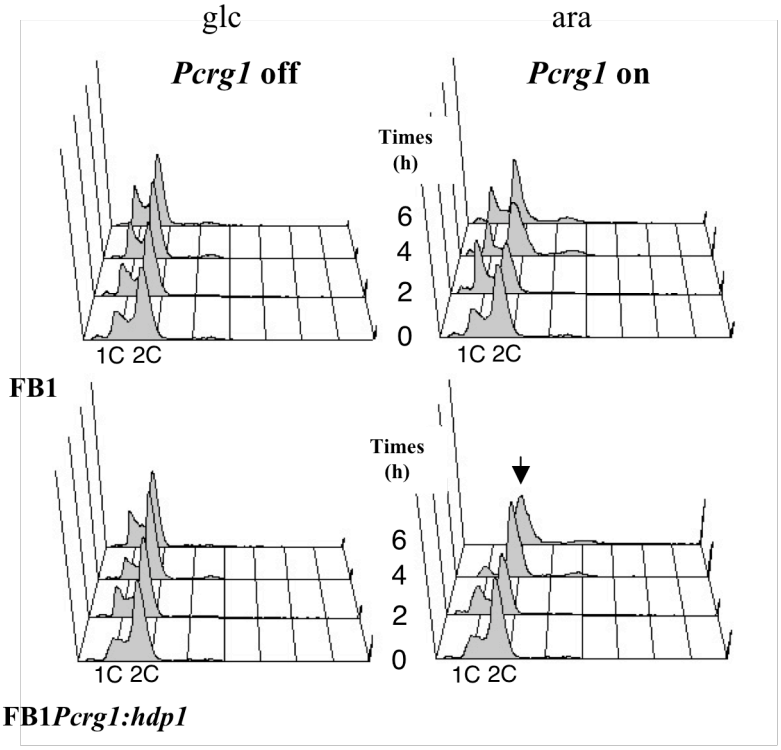

Figure13. *hdp1* induction induces filamentous growth and a G2-cell cycle arrest.
(A) Cell morphology of FB1 wildtype and FB1*Pcrg1:hdp1* (UECP19) cells. Cell morphology was analyzed microscopically with a DIC filter, and nuclei were visualized by DAPI staining. Only FB1*Pcrg1:hdp1* cells under induced conditions (ara) grow filamentously and contain a single nucleus (indicated by arrow). Cells were induced for 6h. Scale bar = 5 μm.
(B) FACS analysis of FB1 and FB1*Pcrg1:hdp1* (UECP19). Samples were taken at 0h, 2h, 4h and 6h after induction. After 6 hours of *hdp1* induction, FB1*Pcrg1:hdp1* shows an accumulation of 2C DNA containing cells (indicated by arrows), demonstrating that the cell cycle is arrested in the G2 phase. The shift to DNA content higher than 2C was due to mitochondrial DNA staining (Experiment was done in cooperation with Ignacio Flor-Parra, Spain).

Induction of filaments was also observed when FB1*Pcrg1:hdp1* cells were grown on solid CM-arabinose medium containing charcoal. However, the aerial hyphae formed by FB1*Pcrg1:hdp1* stuck together and formed bundles, by that differing substantially from the single filaments formed in SG200. In addition, no aerial hyphae were formed at the edge of FB1*Pcrg1:hdp1* colonies (Figure 14A and 14B). To compare the surface hydrophobicity of the SG200 and FB1*Pcrg1:hdp1* colonies grown on solid CM-arabinose medium containing charcoal, droplets of dye were carefully applied to the colony surface. The contact angle was calculated from the diameter of the dye droplet with respect to the hydrophobicity of the colony surface. While the surface of FB1 colonies did not allow to apply the dye droplet, the contact angle of FB1*Pcrg1:hdp1* was found to be only slightly lower than of SG200 (107.3°±6.1° compared to 129.0°±4.0°) (Figure 14C). The expression of *rep1*, which encodes a hydrophobic surface protein that accounts for surface hydrophobicity of *U. maydis* hyphae (Teertstra *et al.*, 2006; Wösten *et al.*, 1996), was similar in cells from FB1*Pcrg1:hdp1* and from SG200 (Figure 14D). In addition, the *hum2* gene, encoding a hydrophobin 2, was found to be the most up-regularated gene after *hdp1* induction, as assessed by microarray analysis (see Table 1). To test whether Hum2 is accountable for the observed bundling of the hyphae, the gene was deleted in FB1*Pcrg1:hdp1*. However, in the resulting FB1*Pcrg1:hdp1*Δ*hum2* strain, the bundling of hyphae was observed similar as found in its progenitor strain (Figure 15).
Similar to *hdp1*, induced expression of *biz1*, a bE/bW-responsive gene encoding a C_2H_2-zinc-finger transcription factor, leads to a G2 cell cycle arrest; *U. maydis* strains deleted for *biz1* are drastically impaired in appressoria formation and are not pathogenic, and their ability to form filaments is not impaired (Flor-Parra *et al.*, 2006). Since in both *Δhdp1* as well as in *Δbiz1* strains induction of the bE/bW heterodimer led to a G2 cell cycle arrest, the two transcription factors could have a redundant function with respect to cell cycle regulation. To test this assumption, both *hdp1 and biz1* were deleted simultaneously in strain AB31. Upon *b*-induction, AB31*Δhdp1Δbiz1* cells grew filamentously, and hyphae contained a single nucleus, comparable to AB31, AB31*Δhdp1* and AB31*Δbiz1* (Figure16 A-D). In contrast, AB31*Δrbf1* cells did not form filaments upon *b*-induction, and had a doubling time comparable to AB32 cells (Figure 16E, J Kämper and M Scherer, unpublished data), implying that Rbf1 is required for b-mediated filamentation and cell cycle arrest.

Additional factors regulating filamentous growth and cell cycle arrest downstream of Rbf1 could be postulated; however, a direct involvement of Rbf1 in these processes cannot be excluded either.

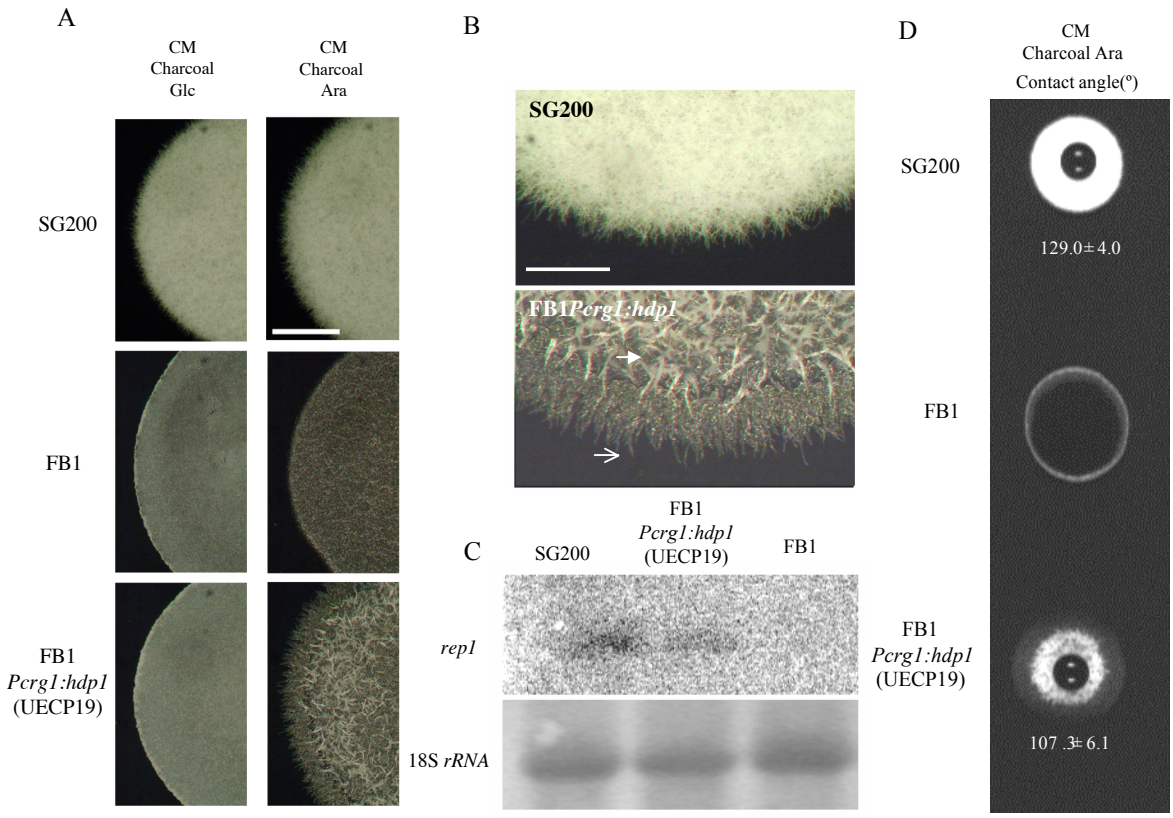

Figure 14. Induced expression of *hdp1* leads to hyphal bundling on solid charcoal-containing media.
(A) Edges of 1 day-old colonies of SG200, FB1 and FB1*Pcrg1:hdp1* (UECP19) grown on CM-glucose (non-inducing condition, left panel) and CM-arabinose (inducing condition, right panel) at 22ºC. Scale bar = 1 mm
(B) Enlargements of colony edges of SG200 and FB1:*Pcrg:hdp1* (UECP19) grown on CM-arabinose media shown in (A). FB1:*Pcrg:hdp1*(UECP19) displays the bundling of aerial hyphae (indicated by ➔ filled arrow), in contrast to SG200. In addition, hyphal bundles growing on the medium surface were only observed at the edge of UECP19 colonies (➔ skeleton arrow). Scale bar = 0.5 mm
(C) Northern Blot analysis; 10 µg of total RNA of SG200, FB1*Pcrg1:hdp1* (UECP19) and FB1 wildtype cells grown under induced condition were loaded per each lane. As a loading control, the membrane was stained with methylene blue to visualize 18S rRNA. A 500 bp-fragment of *rep1* was used as a probe. *rep1* expression was detected only in SG200 and FB1*Pcrg1:hdp1* (UECP19).
(D) Surface hydrophobicity assay. A 5µl-droplet of 0.4% Evan blue solution was placed on the colony surface of strains indicated, grown for 72 hours on CM-arabinose (inducing condition) at 22ºC. Droplets were dispersed on the surface of FB1 colonies, but remain on the colony surface of SG200 and FB1:*Pcrg:hdp1* (UECP19). Droplets were air-dried over night and then the diameter of the dye on the surface of colonies was measured. The obtained values (n =3) were used to calculate contact angles as described in (Doehlemann *et al.*, 2006). Increasing contact angles are indicative for higher hydrophobicity.

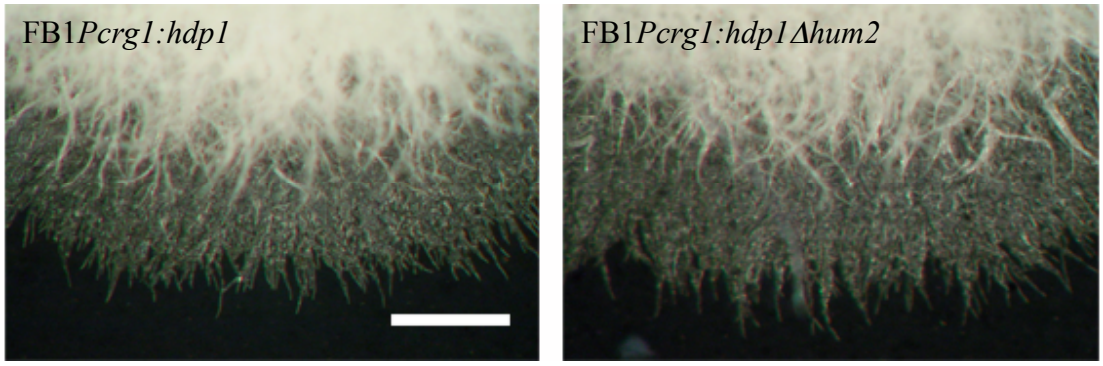

Figure 15. *hum2* does not account for bundling of hyphae.
Shown are the edges of 2 day-old colonies of FB1*Pcrg1:hdp1* and FB1*Pcrg1:hdp1Δhum2* grown for 48 hours on solid CM-arabinose media containing charcoal, at 22ºC. FB1*Pcrg1:hdp1Δhum2* displays the bundling of aerial hyphae similar to its progenitor. Scale bar = 0.5 mm.

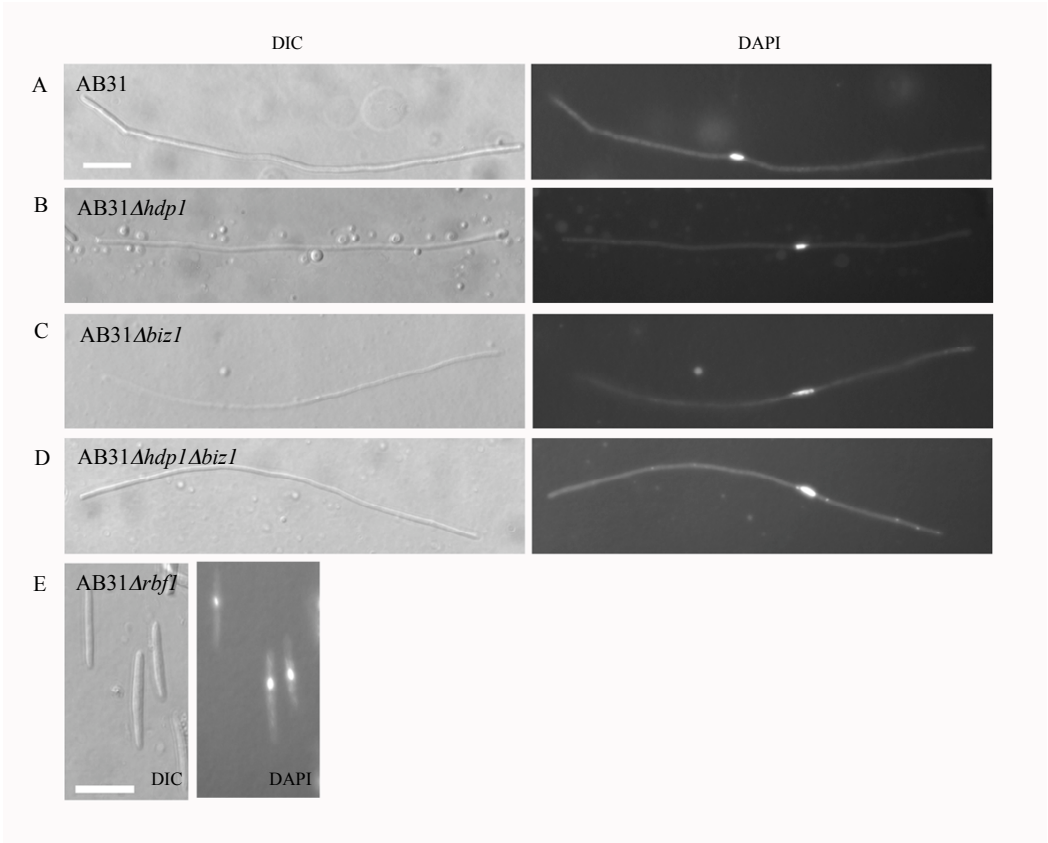

Figure 16. Double deletion of *hdp1* and *biz1* does not affect b-heterodimer mediated filamentation and cell cycle arrest.
Cell morphology (DIC, left) and DAPI nuclear staining (right) of strains AB31(A), AB31*Δhdp1*(B), AB31*Δbiz1*(C), AB31*Δhdp1Δbiz1*(D) and AB31*Δrbf1* (E) after b-heterodimer induction for 15 hours. All strains, except AB31*Δrbf1*, grow filamentously and contain single nuclei. Scale bar = 10 μm

2.5 Hdp1 is involved in the regulation of *b*-independent genes.

Induced expression of *hdp1* was performed to identify genes regulated by *hdp1* independent from the b-regulatory cascade. To this end, the *hdp1* gene under control of the arabinose-inducible *crg1* promoter was integrated into the *ip* locus of strain AB32 (*a2bW2*^{crg1P},*bE1*^{crg1P}), resulting in AB32*Pcrg1:hdp1* (UECP32). The expression profiles of AB32*Pcrg1:hdp1* and AB32 were compared after 5 and 12 hours of induction by means of microarray analysis. Genes showing a differential regulation of more than two fold ($P < 0.01$) were considered as *hdp1*-regulated genes. After 5 hours after of induction, 43 genes were identified as up-, and 72 genes as down-regulated. After 12 hours of induction, these numbers decreased to 16 and 22, respectively. At this time point, 7 induced and 9 down-regulated genes were identified additionally. The 20 most up- and down-regulated genes are shown in Table 1 (For a complete list, see Appendix 6.2).

Interestingly, two groups of genes are arranged in clusters. Five *hdp1* down-regulated genes (um05783, um11585, um05785, um05786 and um05787) are located in a cluster that has been previously identified as the *cab* locus. Genes within the *cab* locus show both *a*- and *b*-dependent repression (Brachmann, 2001 and Figure 17) Deduced from the potential function of the gene products, the *cab* locus is possibly involved in cell wall/ cell membrane structure modification of *U. maydis*. Possibly, Hdp1 is involved in the modification of cell wall and/or cell membrane structure via the repression of these genes.

In the second cluster, 4 out of 5 genes that are required for the synthesis of the secondary metabolite mannosylerythritol lipid (MEL) are *hdp1*-dependently repressed (Figure 18). The MEL gene cluster is induced under nitrogen limitation conditions (Hewald *et al.*, 2006); however, the *emt1* gene, encoding a glycosyltransferase (um03117), that shows the highest induction under nitrogen starvation (Hewald *et al.*, 2006), is not regulated via Hdp1.

Table 1. List of 20 the most up- and down-regulated genes after 5 and 12 hours of *hdp1*- induction. (AB32*Pcrg1:hdp1*/AB32).

* 4 *hdp1* down-regulated genes belonging to the MEL cluster are marked in grey.

probe set	MUMDB	Annotation	Fold change	
			5 hours	12 hours
up-regulated				
W70um170	um11562	hydrophobin 2	71,37	22,69
W40um030	um10528	related to STE6 - ABC transporter	12,17	
W15um049	um00082	putative protein		9,48
W40um261	um11935	conserved hypothetical Ustilago-specific protein		9,20
C112um175	um02713	pheromone response factor Prf1	8,21	6,05
W175um086	um06158	probable glutaminase A		7,31
C85um097	um11514	probable High-affinity glucose transporter	7,03	5,94
W40um248	um03034	conserved hypothetical protein	6,09	4,47
C158um132	um10189	ferrichrome siderophore peptide synthetase	5,08	
W5um075	um11596	related to CSR1 - phosphatidylinositol transfer protein	3,88	2,29
W75um036	um02763	conserved hypothetical protein	3,76	
W75um145	um04385	hypothetical protein	3,64	
C105um075	um06063	related to GAD1 - glutamate decarboxylase	3,59	
W20um109	um04347	probable isp4 - oligopeptide transporter	3,58	3,58
W30um135	um01663	conserved hypothetical protein	3,30	
UG16-16l20-80e12	um10992	conserved hypothetical Ustilago-specific protein, pseudogene	3,30	3,90
C155um019	um06422	conserved hypothetical protein	3,26	
C135um025	um04114	probable PHO8 - repressible alkaline phosphatase vacuolar	3,20	
C140um075	um06071	related to Para-nitrobenzyl esterase	3,12	
W20um280	um11605	related to THG1 - protein required for tRNA-His guanylylation at 5 prime end	3,06	
down-regulated				
W105um021	um03114	conserved hypothetical protein (*mat1*)	-4,64	-6,21
W65um175	um02721	conserved hypothetical protein	-4,71	
W4um060	um02137	conserved hypothetical Ustilago-specific protein	-4,93	
C25um256	um05783	related to UDP-galactose transporter	-4,99	
C117um228	um01902.2	conserved hypothetical protein	-5,30	
C11um184	um05520	conserved hypothetical protein		-5,38
W40um273	um06266	putative protein	-5,87	
W50um095	um01070	related to cyclopropane-fatty-acyl-phospholipid synthase	-6,01	-3,06
W7um082	um15095	HobS polyprotein, pseudogene	-6,24	
C110um127	um12007	related to cellulase	-6,99	-4,43
W60um250	um10365	related to YBT1 - Vacuolar, ABC protein transporting bile acids	-7,44	
C25um042	um05690	conserved hypothetical Ustilago-specific protein	-8,85	
W10um164	um10120	chitin synthase 3	-8,92	
C75um047	um03585	conserved hypothetical protein	-10,19	
W35um258	um04410	probable siderophore iron transporter mirC	-13,50	
C110um021	um03115	related to Sge1 - drug resistance protein (*mmf1*)	-14,19	-9,84
W15um008	um04364	probable EXG1 - Exo-1,3-beta-glucanase precursor	-14,57	-6,90
C115um021	um03116	conserved hypothetical protein (*mac1*)	-14,65	-10,22
W130um021	um10636	conserved hypothetical protein (*mac2*)	-16,45	-10,50
ncp1	um04000	DNA binding protein Ncp1	-40,83	-3,82

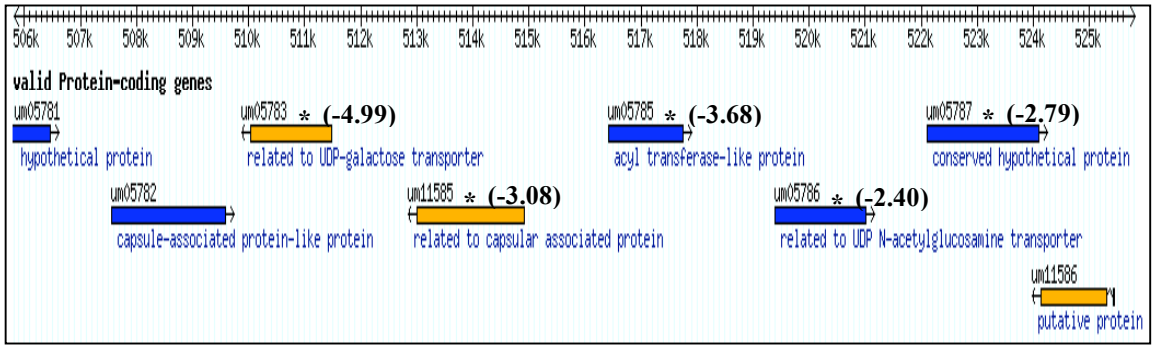

Figure 17. Organization of 5 *hdp1*-repressed genes (*) within the *cab* locus (Brachmann, 2001) The numbers in blankets represent the fold changes of genes indicated. Graphic was modified from http://mips.gsf.de/genre/proj/ustilago/.

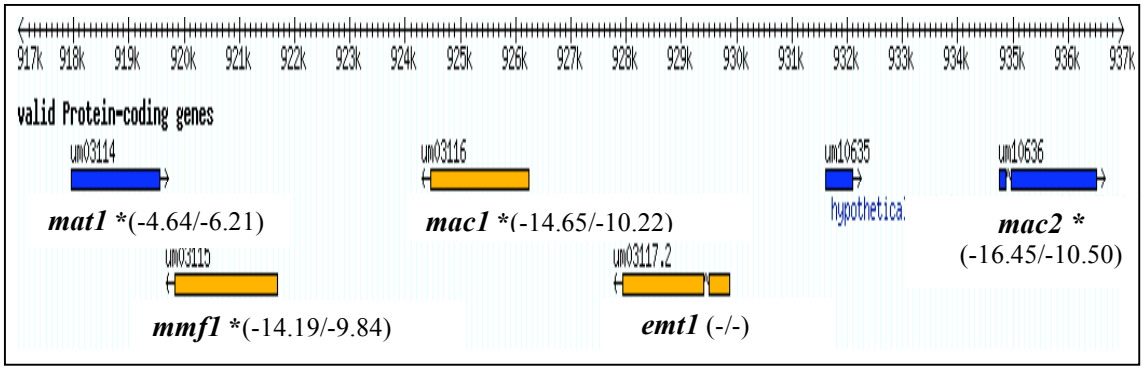

Figure 18. Organization of 4 genes (*) repressed by Hdp1 and located in the MEL biosynthesis gene cluster (Hewald *et al.*, 2006) Numbers in blankets represent the fold changes 5 hours and 12 hours after *hdp1* induction, respectively. Modified from http://mips.gsf.de/genre/proj/ustilago/.

Functional classification of *hdp1*-regulated genes using the MIPS functional categories (FunCat) revealed that 37 out of 131 (28.2%) genes are classified in the category "metabolism": 25 out of 37 genes are in the category "C-compound and carbohydrate", or "lipid, fatty acid and isoprenoid metabolism". In addition, two chitin synthases [um10718: chitin synthase 1, Chs1 (type III) and um10120: chitin synthase 3, Chs3 (type I)] were found to be regulated by Hdp1. Moreover, two genes involved in the cAMP signal transduction cascade, *gpa2* and *adr1,* were approximately two-fold up and down regulated upon *hdp1* induction, respectively.

Comparisons between microarray data of *hdp1* induction and those of pheromone and b-heterodimer inductions revealed that 38 out of 131 (29.0%) *hdp1*-regulated genes were pheromone dependent (Zarnack, 2006), and that 38 out of 131 (29.0%) *hdp1*-

regulated genes were regulated via the b-heterodimer (M Scherer and J Kämper, unpublished data). 15 genes of these genes are regulated by both, the pheromone pathway and the b-heterodimer. Therefore, *hdp1* potentially plays a role in the regulation within both pheromone signalling pathway and b-regulatory cascade (For details see Appendix 6.3).

2.6 Hdp1 potentially regulates the *prf1* expression via Rop1.

Six *hdp1*-regulated genes were identified to contain pheromone response elements (PREs), (ACAAAGGGA motif), which is required for binding of the Pheromone response factor (Prf1). Prf1 is a high-mobility-group (HMG) transcription factor required for mating and pathogenicity (Hartmann *et al.*, 1996). In accordance, five of these six genes have been described to be induced by pheromone treatment (for details, see Appendix 6.3), indicating that the regulation of these genes by Hdp1 might function indirectly via Prf1. In accordance with this assumption, *prf1* was found to be up-regulated upon *hdp1* induction (7.03 and 5.94 fold after 5 and 12 hour induction, respectively). In addition, the *rop1* gene encoding a transcription factor required for *prf1* expression during axenic growth (Brefort *et al.*, 2005) was found to be induced 2.51 fold after 5 hours of induction.

To investigate whether *hdp1* is required for the expression of *rop1* and *prf1*, their gene expression after pheromone treatment (Figure 19A) and after activation of the MAPK cascade by induction of Fuz7DD, a constitutive active form of the MAPK Fuz7, was examined by real-time RT-PCR (Figure 19B). In wildtype and the *hdp1*-deletion derivatives, *rop1* and *prf1* were induced in both cases to a comparable level (Figure 19A and 19B), indicating that Hdp1 is not the main regulator for the two genes in the pheromone signalling cascade. However, an approximately 3-fold reduction of the *rop1* basal expression in *hdp1* deletion derivatives was observed (Figure 19A)

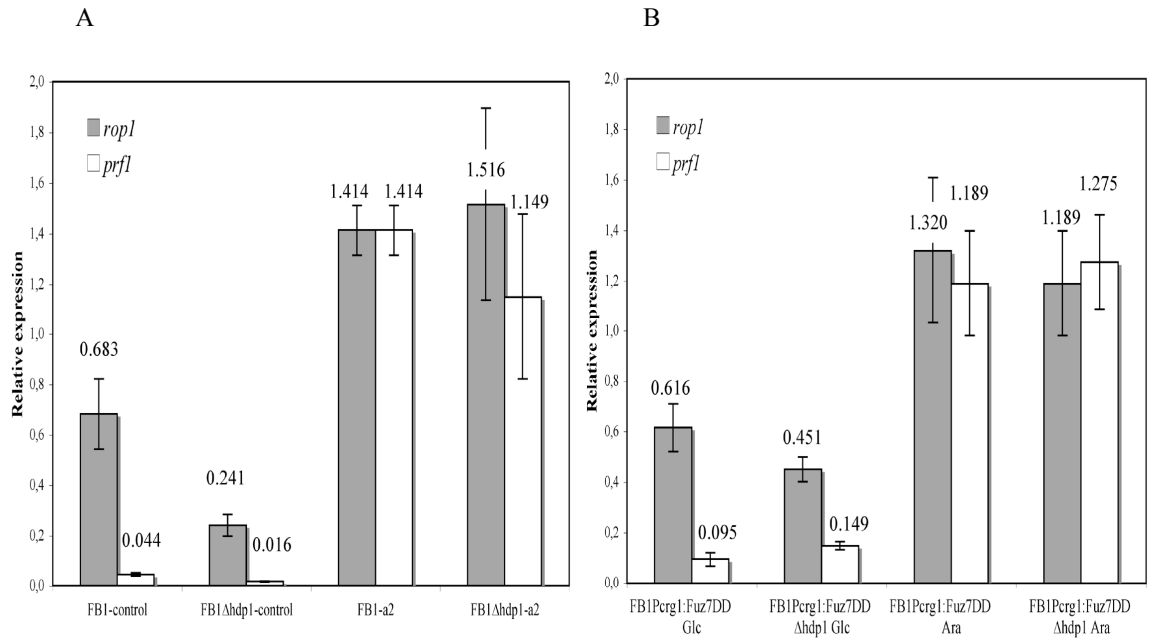

Figure 19. *hdp1* deletion only affects the basal *rop1* expression.
To investigate the effect of the *hdp1* deletion on *rop1* and *prf1* expression, the relative expression of *rop1* and *prf1* after (A) pheromone treatment and (B) induction of constitutively active MAPK kinase *Fuz7DD* were monitored by using real-time quantitative RT-PCR,
(A) Expression in wildtype FB1 and FB1*Δhdp1* grown in CM-glucose after treatment with DMSO (FB1-control, FB1Δhdp1-control) and Mfa2 pheromone in DMSO (FB1-a2, FB1Δhdp1-a2) for 6 hours. (B) Expression of wildtype FB1*Pcrg1:Fuz7DD* and the respective *Δhdp1* derivative under non-inducing conditions (CM-glucose; FB1Pcrg:Fuz7DD-Glc, FB1Pcrg:Fuz7DDΔhdp1-Glc) and induction conditions (CM-arabinose; FB1Pcrg::Fuz7DD-Ara, FB1Pcrg::Fuz7DDΔhdp1-Ara) for 6 hours.
rop1 and *prf1* expression was measured relatively to the constitutively expressed gene for the elongation factor 2B (*elf2B*: um04869). Bar graphs show the mean value and standard deviation of two technical replicates.

To investigate whether the *hdp1*-mediated *prf1* induction is dependent on Rop1, the gene was deleted in FB1*Pcrg1:hdp1* (UECP19), and expression of *hdp1*, *rop1* and *prf1* was monitored by real-time RT-PCR (Figure 20). Rop1 is absolutely required for *prf1* expression in axenic culture (Brefort *et al.*, 2005), and, consistently, the deletion of *rop1* led to a complete loss of *prf1* expression when *hdp1* was not induced (Figure 20). Induction of *hdp1* led to an induction of *rop1* and *prf1* similarly as observed in the microarray experiment; however, the Rop1 dependency on *prf1* expression could not be overcome (Figure 20).

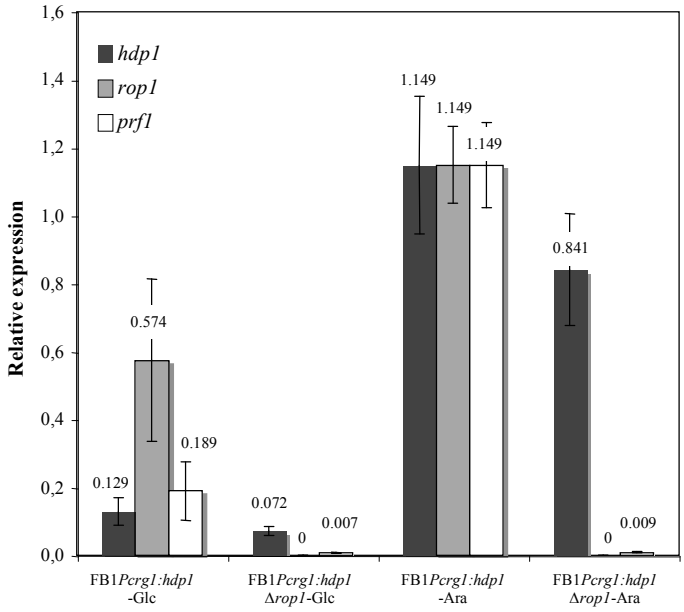

Figure 20. *rop1* is required for Hdp1-induced *prf1* expression
Real-time quantitative RT-PCR was used to investigate the dependency of Rop1 on *prf1* expression. Expression of *hdp1*, *rop1* and *prf11* were monitored in FB1*Pcrg1:hdp1* and the respective *Δrop1* derivative before (Glc) and after (Ara) *hdp1* induction for 6 h in CM medium. Gene expression was measured in relation to the constitutively expressed gene for elongation factor 2B (*elf2B*: um04869). Bar graphs indicate mean values and standard deviations of two technical replicates.

2.7 *hdp1* overexpression affects the expression of cell cycle related genes.

Hdp1 was shown to be sufficient for the induction of a G2 cell cycle arrest (see 2.4). To identify possible target genes responsible for this phenotype, the set of *hdp1*-regulated genes identified by microarray analysis was screened for genes potentially involved in cell cycle regulation or progression (i.e. DNA replication, chromosome condensation). A total of 8 cell cycle related genes were found to be down-regulated at least two fold (Table 2).

Table 2. List of 8 cell cycle related genes down-regulated by Hdp1

probe set	MUMDB	Annotation	Yeast homolog (E-value)	Fold change 5 hours
C35um164	um00469	probable histone H2A F/Z family member HTZ1	YOL012c HTZ1 Evolutionarily conserved member of the histone... (9e-42)	-2,02
W20um136	um02579	related to RFA2 - DNA replication factor A, 36 kDa subunit	YNL312w RFA2 DNA replication factor A, 36 kDa subunit (5e-29)	-2,07
W80um175	um02718	related to PIF1 - DNA helicase involved in mitochondrial DNA repair and telomere length control	YHR031c RRM3 DNA helicase involved in rDNA replication and Tyl1 transposition (2e-97)	-2,12
W10um154	um02557	related to DNA polymerase alpha 70 kDa subunit	YBL035c POL12 DNA-directed DNA polymerase alpha, 70 KD sub... (5e-40)	-2,14
C10um226	um11750	probable RNR1 - ribonucleoside-diphosphate reductase large subunit	YER070w RNR1 Ribonucleoside-diphosphate reductase, large su... (0.0)	-2,18
C10um081	um03234	related to CDC5 - Serine/threonine-protein kinase	YMR001c CDC5 Protein kinase, involved in regulation of DNA ... (8e-83)	-2,51
W85um164	um00459	related to Condensin complex subunit 3	YDR325w YCG1 Yeast Condensin G (4e-89)	-2,52
C85um054	um00657	related to RAD7 - nucleotide excision repair protein	YJR052w RAD7 Nucleotide excision repair protein (1e-41)	-2,98

In addition, *clb1*, encoding a B-type cyclin accounting for the *biz1*-induced G2 cell cycle arrest (Flor-Parra *et al.*, 2006) was found to be repressed by Hdp1 (- 1.67 fold). Furthermore, *pcl12* (um10529) encoding a cyclin domain containing protein involved in polarized growth (Flor-Parra *et al.*, 2007) was found to be induced more than two fold. (2.14 fold, P = 0.017 at 5 hours post induction; 2.71 fold, P = 0.023 at 12 hours post induction). Expression of both genes after *hdp1* induction was confirmed by real-time PCR analysis. *pcl12* expression was found to be induced 18.5-fold (1.035/0.056), whereas *clb1* expression was down-regulated 2.2-fold (0.451/1.000) 6 hours after *hdp1* induction (Figure 21).

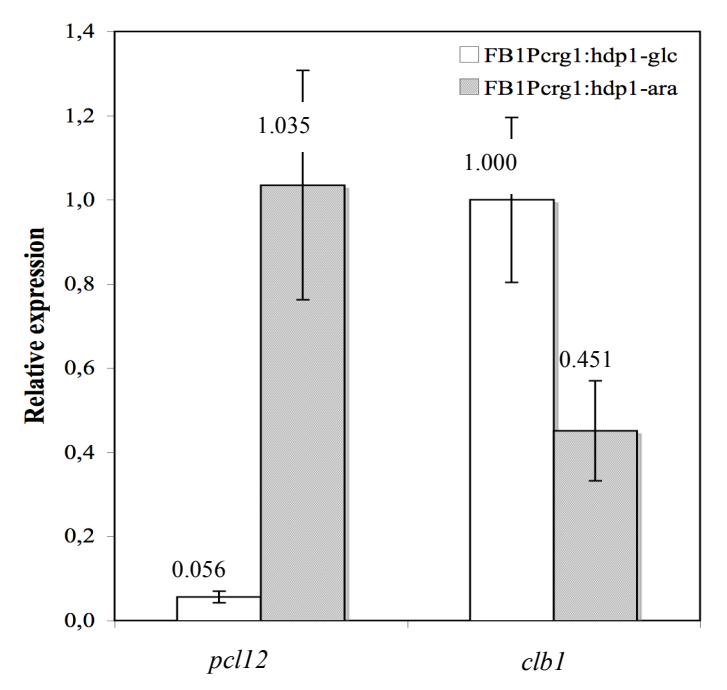

Figure 21. **Two genes encoding cell cycle regulators are regulated by Hdp1.**
Real-time quantitative PCR analysis of *pcl12* and *clb1* expression. Strain FB1*Pcrg1:hdp1* was grown in CM-glucose (FB1Pcrg1:hdp1-glc) and, to induce *hdp1* expression, in CM-arabinose (FB1Pcrg1:hdp1-ara) for 6 hours. Gene expression was measured in relation to the constitutively expressed gene for elongation factor 2B (*elf2B*: um04869). Bar graphs indicate the mean values and standard deviation of two technical replicates.

2.8 *pcl12* expression is bE/bW-heterodimer and pheromone dependent

pcl12 has been described first as the b-induced gene *frb63* (Brachmann *et al.*, 2001). The *b*-dependent expression was confirmed after induction of the b-heterodimer in strain AB31 (Figure 22A). In addition, induction of *pcl12* expression was observed after pheromone induction (Figure 22B), similar to the induction described by Flor-Parra *et al.*, 2007.

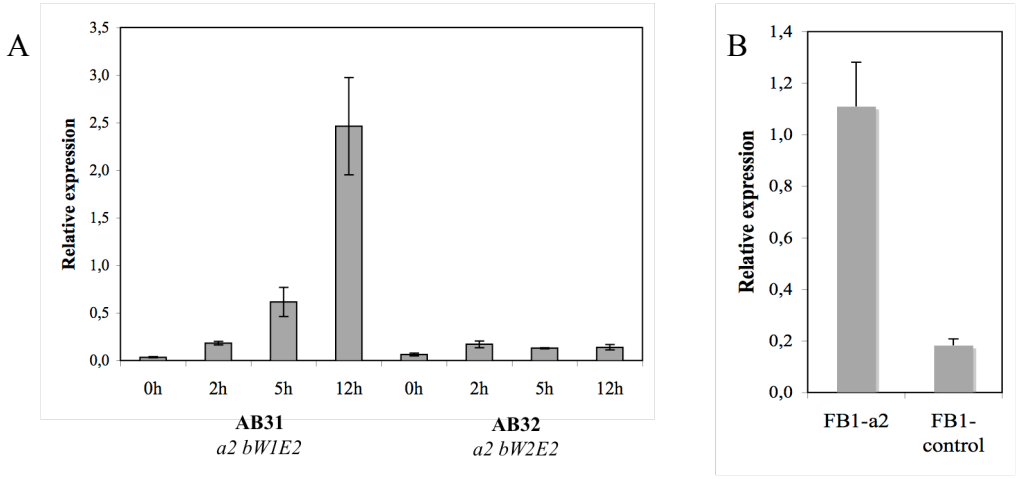

Figure 22. *pcl12* is induced by the b-heterodimer and by pheromone treatment
Real-time quantitative PCR analysis of *pcl12* expression. (A) Induction of compatible (AB31) and incompatible (AB32) combinations of bE and bW. Samples were taken before and 2, 5 and 12 hours after induction. (B) Pheromone induction of FB1 6 h after treatment with compatible pheromone Mfa2 (FB1-a2) or DMSO, the solvent for Mfa2, (FB1-control). Gene expression was measured relatively to the constitutively expressed gene encoding for the elongation factor 2B (*elf2B*: um04869). Bar graphs show mean values and standard deviations of two technical replicates.

2.9 *pcl12* is required for b- and Hdp1-mediated filamentation.

To investigate the impact of *pcl12* on the mating ability of compatible sporidia and the pathogenic development of *U. maydis*, *pcl12* was deleted in the haploid strains FB1, FB2 and in the solopathogenic strain SG200. The deletion caused no obvious morphological alteration. Both SG200*Δpcl12,* and a mixture of the compatible strains FB1*Δpcl12* and FB2*Δpcl12* caused symptoms in plant infection experiments that were indistinguishable from those of infections with the respective progenitor strains (Figure 23A). After treatment with compatible pheromone FB1*Δpcl12* formed conjugation hyphae indistinguishable from those of wildtype strains with respect to morphology and length (Figure 23B). However, filamentation of SG200*Δpcl12* was drastically reduced when compared to that of SG200 (Figure 24A). To investigate the effect of *pcl12* on Hdp1-mediated filamentation, *pcl12* was deleted in strain UECP19 that harbors an inducible *hdp1* gene, resulting in FB1*Pcrg1:hdp1Δpcl12* (UECP77). Similar to the observed filamentation defect in SG200*Δpcl12*, the *pcl12* deletion led to short filaments upon Hdp1 induction (Figure 24B and 24C). Taken together, the result indicates that *pcl12* is required for both b- and Hdp1-mediated filamentation.

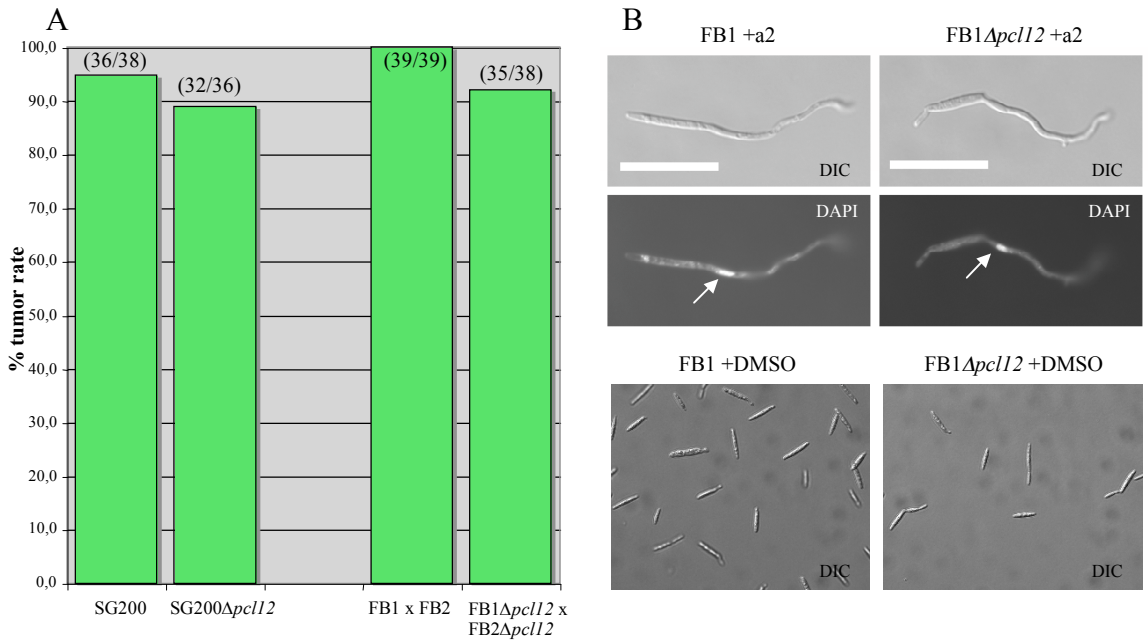

Figure 23 Deletion of *pcl12* does not affect pathogenicity and conjugation hyphae formation.
(A) **Pathogenicity of Δ*pcl12* strains**; depicted bar graphs show the tumor rates of solopathogenic strains (SG200, SG200Δ*pcl12*), and of a mixture of compatible sporidia (FB1xFB2, FB1Δ*pcl12*xFB2Δ*pcl12*). Numbers in blankets represent the fraction of plants with tumors per infected plants. (B) **Conjugation hyphae formation of FB1Δ*pcl12*.** Conjugation hyphae formation of wildtype FB1and FB1Δ*pcl12* strains was investigated after treatment with Mfa2 pheromone. Top and middle panels show the cell morphology (DIC) and nuclear staining with DAPI, respectively. In conjugation hyphae of both FB1 wildtype and FB1*Δpcl12* cells, single nuclei were observed (indicated by arrow). The bottom panel shows cells treated with DMSO, the solvent for Mfa2, as a control. Scale bar = 10 μm

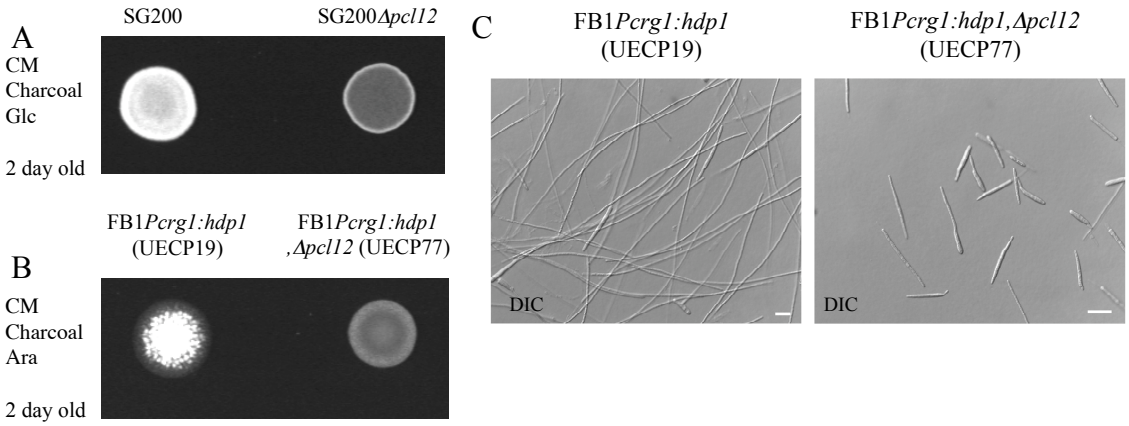

Figure 24. *pcl12* deletion affects b- and Hdp1-mediated filamentation.
(A) and (B) show the filament formation of wildtype and Δ*pcl12* strains either expressing an active b-heterodimer (A) or Hdp1 (B). Strains were spotted on charcoal containing CM media with the sugar indicated and incubated at 22°C for 48 hours. The white colony morphology indicates filament formation. (C) Microscopic analysis of FB1*Pcrg1:hdp1* (UECP19) and its *pcl12*-deletion derivative UECP77 grown in liquid CM-arabinose medium for 15 hours to induce *hdp1* expression. Filament formation is only observed in UECP19, but not in UECP77. Scale bar = 10 μm

2.10 The role of *pcl12* in Hdp1-mediated G2 cell cycle arrest depends on nutrients.

Similar to filaments formed by wildtype cells, the stunted filaments formed by UECP77 always contained single nuclei (Figure 25A). FACS analysis revealed that Hdp1-induced filaments in both wildtype cells and in a *Δpcl12* background have a 2C content, when the cells were induced in CM-arabinose medium (Figure 25B). The growth rate of UECP77 cells under *hdp1*-induced conditions was as slow as of the progenitor strain UECP19 (370 minutes and 357 minutes doubling time, respectively). Therefore, in CM-media the deletion of *pcl12* apparently had no influence the Hdp1-mediated G2 cell cycle arrest (see details in 2.4). When *hdp1* was induced in strains grown in NO_3/arabinose minimal media, stunted filamentation was still observed (Figure 26A and 26C). However, the FACS analysis revealed that under these conditions UECP77 cells displayed a delayed or incomplete G2 cell cycle arrest (Figure 26B and 26C), arguing for a nutrient-dependent function of *pcl12* in cell cycle regulation.

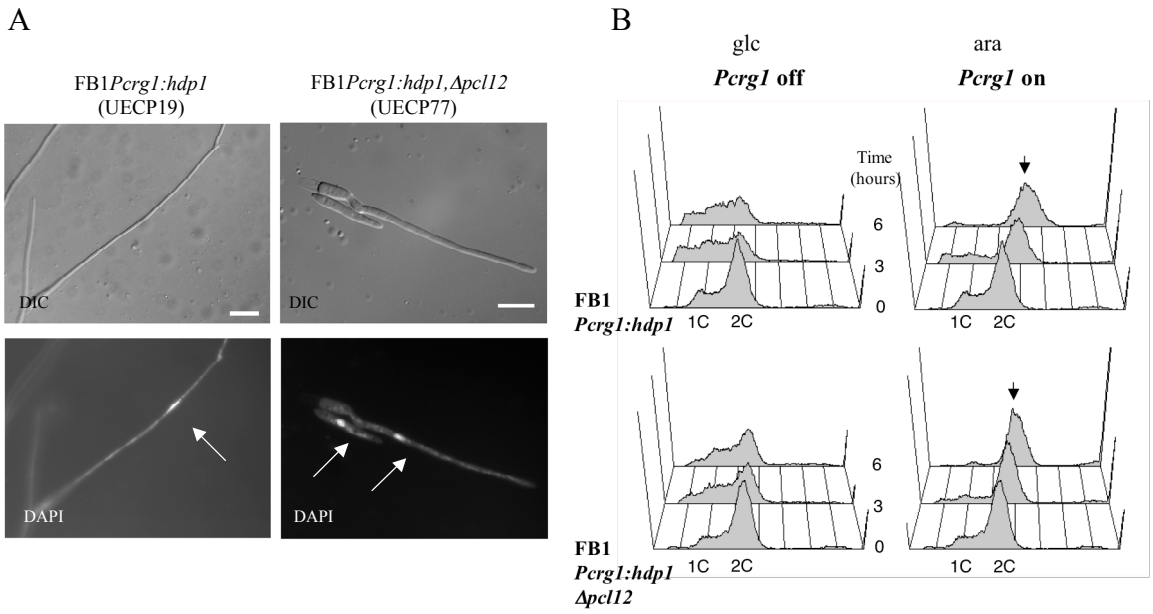

Figure 25. *pcl12* deletion does not affect Hdp1-mediated G2 cell cycle arrest in CM-media.
(A) Microscopic analysis of filaments (top panel: DIC; bottom panel: DAPI staining) from strains FB1*Pcrg1:hdp1* (UECP19) and FB1*Pcrg1:hdp1,Δpcl12* (UECP77). Cells were grown in CM-arabinose media for 15 hours to induce *hdp1* expression. Only single nuclei were observed both in filaments of UECP19 and UECP77 (indicated by arrow). Scale bar = 10 μm
(B) FACS analysis of UECP19 and UECP77 non-induction (CM-glucose; glc) and induction of *hdp1* (CM- arabinose; ara). Samples were taken before, and 3 and 6 hours after induction. After 6 hours, both UECP19 and UECP77 show an accumulation of 2C DNA containing cells (indicated by arrows). (Experiments was done in cooperation with Ignacio Flor-Parra, Spain)

2.11 Clb1 repression is not required for Hdp1-mediated G2 cell cycle arrest and filamentation.

Repression of *clb1* has been shown to be responsible for the *biz1*-induced G2 cell cycle arrest (Flor-Parra *et al.*, 2006). Since the *clb1* gene was found to be 2.2 fold down-regulated by Hdp1, its function in Hdp1-mediated cell cycle regulation was investigated. The *hdp1* gene under control of the *crg1* promoter was integrated into the *ip* locus of TAU41(FB1*clb1*^{nar1}) (Garcia-Muse *et al.*, 2004), generating FB1*Pcrg1:hdp1,clb1*^{nar1P} (UECP101). When cells were grown under conditions where both *hdp1* and *clb1* were induced (arabinose/NO_3), UECP101 was still able to form filaments; however, the percentage of filamentous cells decreased to 48.5%, compared to 93.1% in wildtype UECP19 (Figure 26A and 26C). FACS analysis revealed that UECP101 cells, similar to UECP19 cells, were arrested in the G2 phase of the cell cycle under these conditions (Figure 26B). To address a possible dominant effect of *pcl12* over *clb1*, *pcl12* was deleted in strain UECP101, resulting in FB1*Pcrg1:hdp1,clb1*^{nar1P}*,Δpcl12* (UECP113). The additive effect (i.e. the complete loss of G2 cell cycle arrest) cannot be observed in UECP113; it showed a phenotype comparable to FB1*Pcrg1:hdp1,Δpcl12* (UECP77) in terms of filamentation and G2 cell cycle arrest, indicating that the *clb1* down-regulation is not involved in Hdp1-mediated G2 cell cycle arrest and filamentation.

Figure 26. Effect of *pcl12* deletion and *clb1* overexpression on Hdp1-mediated filamentation and cell cycle arrest in NO_3/ arabinose-MM media. (see the next page)

(A) Cell morphology of strains indicated grown under inducing conditions in NO_3/arabinose -MM media for 24 hours. Scale Bar = 10 μm (B) FACS analysis of strains indicated grown in NO_3/ arabinose-MM media (B1) FACS diagram of UECP19. The fraction of cells with 2C-DNA contents increased with the induction time. 24 hours after induction, only cells with a 2C-DNA content were observed. (B2) FACS diagram of UECP77. DNA content of cells did not change during the induction period. 24 hours after induction the majority of cells had a 2C-DNA content, but still cells with 1C-DNA content were present. (B3) FACS diagram of UECP101. The observed FACS result is similar to (B1). (B4) FACS diagram of UECP101. The observed FACS result is similar to (B2). The shift to DNA content higher than 2C was due to mitochondrial DNA staining. (C) The stack columns show a quantitative analysis of (A); percentages and standard deviations of budding and filamentous cells are indicated (Cell number > 80, two independent experiments). The table shows the capability to arrest the cell cycle in the G2 phase characterized in (B). The middle part of the table shows the genotypes of the investigated strains. The lower part of the table shows the expression status of the investigated genes. For *hdp1* and *pcl12*, symbol (+) means "induced" and symbol (-) means "non-induced" or "absent" (Confirmed by real-time quantitative RT-PCR, data not shown). For *clb1*, *Pnative* means controlled by its native promoter and *Pnar1* means controlled by the nitrate inducible (*nar1*) promoter (Garcia-Muse *et al.*, 2004)

A

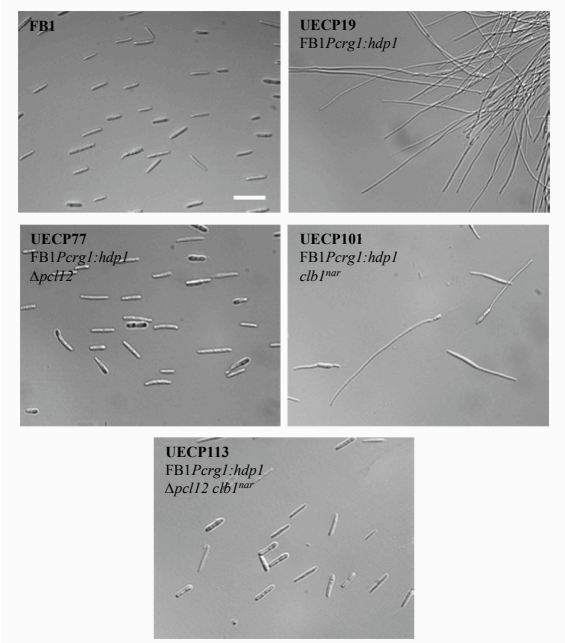

C

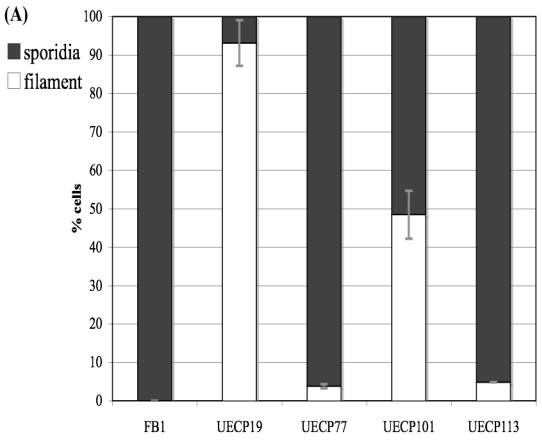

G2 cell cycle arrest (B)	no (García-Muse et al., 2003)	yes	no	yes	no
Genotype	FB1(*a1b1*)	FB1(*a1b1*) *Pcrg1:hdp1*	FB1(*a1b1*) *Pcrg1:hdp1* *Δpcl12*	FB1(*a1b1*) *Pcrg1:hdp1* *clb*^{nar}	FB1(*a1b1*) *Pcrg1:hdp1* *Δpcl12, clb*^{nar}
hdp1	-	+	+	+	+
pcl12	-	+	-	+	-
clb1	*Pnative*	*Pnative*	*Pnative*	*Pnar*	*Pnar*

B

B1

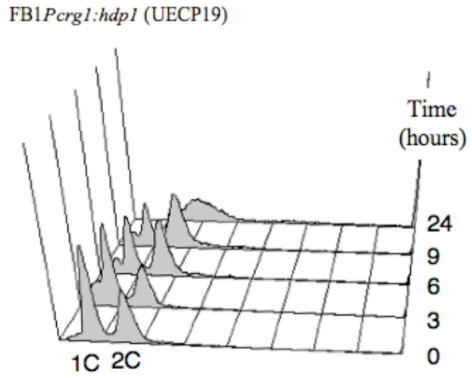

B2

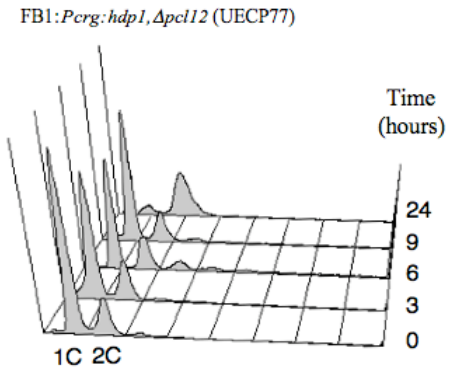

B3

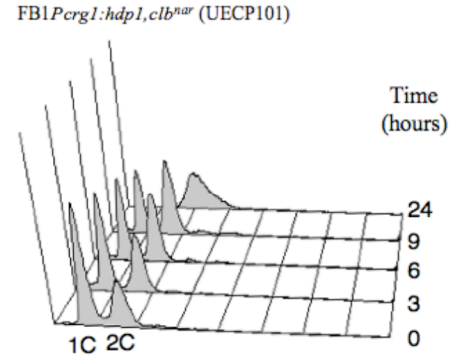

B4

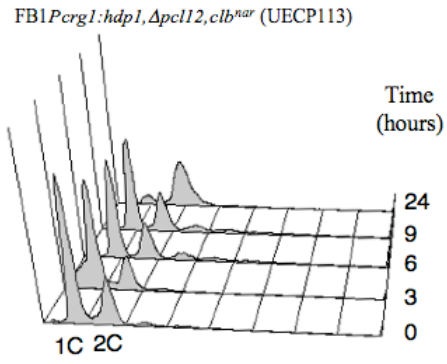

2.12 *hdp1* deletion affects the pheromone response in minimal media

The effect of *hdp1* and *pcl12* deletions on conjugation hyphae formation of FB1 was further investigated by treatment with the Mfa2 pheromone in NO_3-minimal medium. The percentage of FB1*Δhdp1*- and FB1*Δpcl12*-cells developing conjugation hyphae was reduced, when compared to the FB1 wildtype strain (Figure 27). Similar observations were made in the study of Flor-Parra et al., 2007; however, no growth differences on NO_3-minimal media were observed by thee authors (Figure 28). The reason for the reduced conjugation hyphae formation of FB1*Δhdp1* might be the partial loss of *pcl12* regulation.

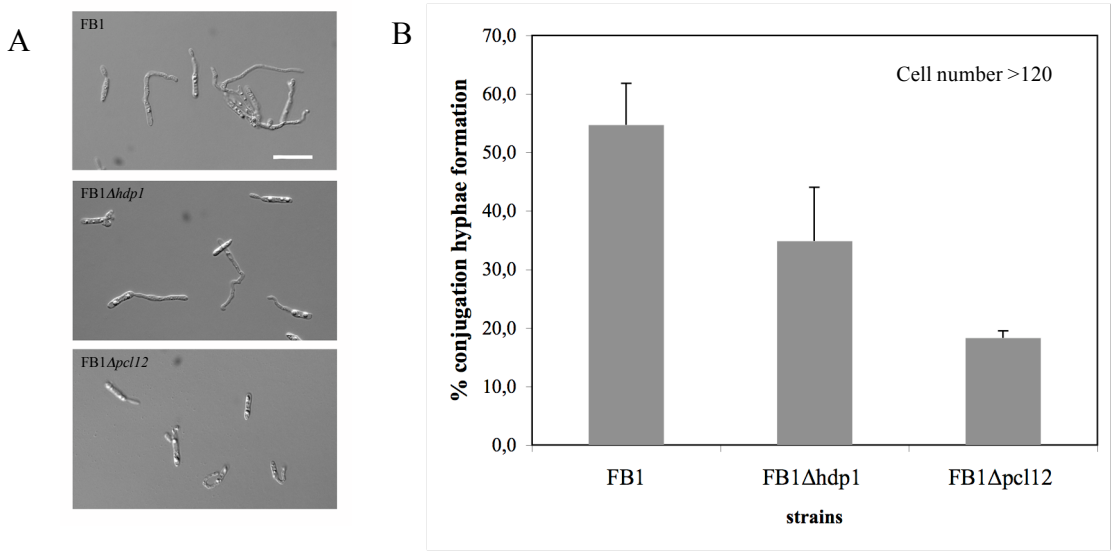

Figure 27. Pheromone response of FB1, FB1*Δhdp1* and FB1*Δpcl12* in glucose/NO_3 MM media
(A) Microscopic analysis of FB1, FB1*Δhdp1* and FB1*Δpcl12* after treatment with Mfa2 pheromone for 8 hours in glucose/NO_3 MM media. Scale bar = 15 µm
(B) Percentage of cells forming conjugation hyphae in FB1, FB1*Δhdp1* and FB1*Δpcl12* cultures. Experiments were performed two times.

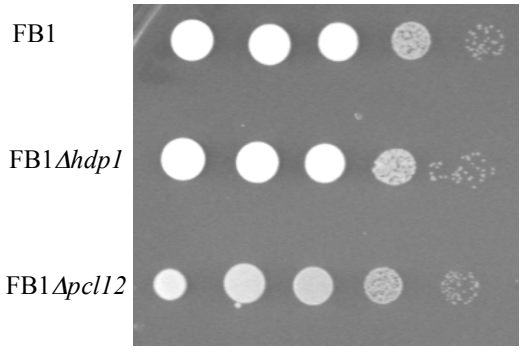

Figure 28. Growth of of FB1, FB1*Δhdp1* and FB1*Δpcl12* in glucose/NO_3 MM media.
Serial ten-fold dilutions of FB1, FB1*Δhdp1* and FB1*Δpcl12* grown in liquid glucose/NO_3 MM media were spotted on solid glucose/NO_3 MM and incubated for 2 days (48 hours) at 28°C.

A partial defect in maintaining the G2 cell cycle arrest after pheromone treatment of FB1Δ*hdp1* can be observed in glucose/NO_3 MM-media; however, screening of more than 150 cells revealed no cells with more than one nucleus. When the nuclear DNA content was calculated by means of microdensitometry (See Materials and Methods, 4.2.2 and Appendix 6.4), the fraction of conjugation hyphae with a 1C-DNA content was higher in FB1Δ*hdp1* populations than in wildtype populations, even though the majorities of both had 2C DNA contents (Figure 29). Thus, we have to assume that *hdp1* has only a minor function (i.e. fine-tuning) in maintaining the cell cycle arrest after pheromone induction.

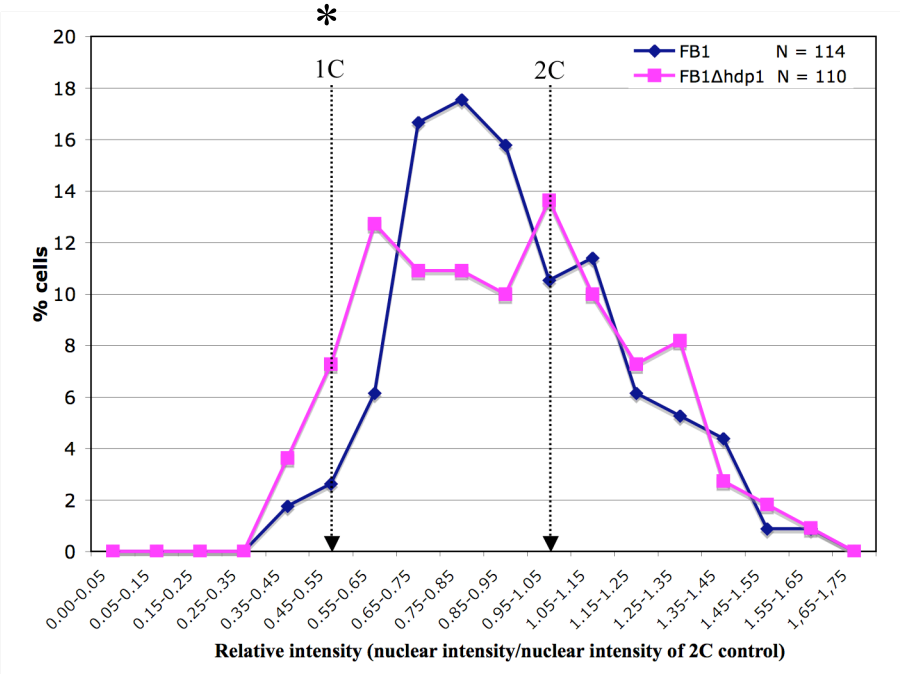

Figure 29. *hdp1* deletion affects the G2 cell cycle arrest after pheromone treatment in glucose/NO_3 MM-media
Curves show the DNA content of hyphal nuclei relative to the nuclei of FB1 sporidia with small buds that have been described to have a 2C DNA content (Snetselaar and McCann, 1997). Theoretically expected 1C-DNA and 2C-DNA contents are indicated by arrows. The number of cells with 1C-DNA content is higher in a FB1*Δhdp1* population than in FB1 (indicated by *). Mean±SD value of FB1 = 0.9191 ± 0.247 and Mean±SD value of FB1*Δhdp1* = 0.9000 ± 0.281, indicate that the majorities of cells in both have a 2C DNA content.

3 Discussion

In *Ustilago maydis*, crucial steps for switching from saprophytic to biotrophic life style are the pheromone reception between compatible mating strains and the formation of the dikaryon by cell fusion, resulting in a G2 cell cycle arrest. Only after penetration of the host plant by the infectious dikaryon, the cell cycle is released. The homeodomain transcription factor Hdp1 is up-regulated both in response to pheromone signalling and after the fusion event. Although *hdp1* is not necessary for pathogenicity, it affects cell cycle arrest and filament formation in those two steps. The mechanism of Hdp1-mediated cell cycle regulation and filamentation as well as additional putative functions of Hdp1 are discussed.

3.1 Hdp1 is a homeodomain transcription factor.

Consistent with the predicted nuclear localization, the Hdp1:eGFP fusion protein was found to be localized within the nucleus (Figure 7). In addition, the replacement of two highly conserved amino acids, $W_{230}F_{231}$, with two alanine residues within the predicted homeodomain abolished the Hdp1-dependent induction of filamentous growth (Figure 9), demonstrating that the function of the homeodomain is required. Taken together, these data strongly support the function of Hdp1 as a homeodomain transcription factor.

The homeodomain of Hdp1 is more related to chordate homedomains than to the class of fungal mating type homeodomains; the closest relative is the homeodomain of the paired-like homeodomain transcription factor Shox (short stature homeobox) protein from *Branchiostoma floridae* (AF465939; E-value = 4e-06). Homeodomain transcription factors unrelated to the mating type homeodomain have been discovered in other fungi as well. Similar to Hdp1, these proteins are involved in the regulation of developmental processes. Examples are Hoy1 from *Yarrowia lipolytica*, which is involved in hyphal formation (Torres-Guzman and Dominguez, 1997), and Pah1 from *Podospora anserina*, which plays a role in hyphal morphology and micro-conidiogenesis (Arnaise *et al.*, 2001).

3.2 Regulation of *hdp1* expression

The expression of *hdp1* is controlled via both the b- and the pheromone signalling-cascade, as shown by DNA microarray analysis and real-time quantitative RT-PCR (Figure 4 and 5). A similar observation has been made for the expression of *hdp1* on the plant surface, comparing the gene expression in SG200 and SG200*Δb* cells (Vranes, 2006). The b-heterodimer binds to conserved promoter elements (b-binding sites, bbs) in the regulatory regions of b-regulated genes (Brachmann *et al.*, 2001; Romeis *et al.*, 2000). Since three putative bbs are present in the upstream region of *hdp1* (Figure 8), a direct regulation of *hdp1* by the bE/bW heterodimer is likely. Various pheromone responsive genes are directly regulated by the pheromone response factor1 (Prf1) that binds to pheromone response elements (PRE), ACAAAGGGA (Hartmann *et al.*, 1996; Urban *et al.*, 1996a) in the promoter regions of those genes. Within the *hdp1* promoter region, no sequences similar to PRE are present, suggesting that the *a*-dependent regulation occurs indirectly. The prime candidate for this suggested regulation is the zinc finger transcription factor Rbf1 (**R**egulator of **b f**ilament **1**). Since deletion of *rbf1* affects expression of the majority (up to 90%) of the *b*-dependent genes (Scherer *et al.*, 2006), it is thought to be the central regulator within the b-regulatory cascade. Rbf1 is induced by both the formation of a b-heterodimer as well as by pheromone treatment (Scherer *et al.*, 2006); M. Scherer and J. Kämper, unpublished data). The *rbf1* promoter harbors PRE elements as well as bbs sites, suggesting that the gene is directly regulated by both the-bE/bW-heterodimer and Prf1 (Finkernagel, 2007; Scherer *et al.*, 2006; Zarnack, 2006). *hdp1* is one of the genes that is induced upon ectopic overexpression of *rbf1*, independent from the presence of an active bE/bW heterodimer (M. Scherer and J. Kämper, unpublished data). Currently, the Rbf1-binding site is not known, but preliminary data indicate that it is not overlapping with the b-binding sites, so that two independent regulatory circuits have to be assumed. Thus, it is likely that the *b*-dependent regulation of *hdp1* functions directly via binding of the b-heterodimer and in addition by binding of Rbf1, while the *a*-dependent regulation of *hdp1* functions exclusively via Rbf1. A similar regulation was observed for other b-regulated genes. *lga2* and *frb52* are two of the earliest identified *b*-dependent genes; both harbor bbs elements in their upstream regulatory regions, and the physical interaction of the b-binding sites with the bE/bW heterodimer has been shown by means of electrophoretic mobility shift assays (EMSA) and DNaseI protection assays

(Brachmann *et al.*, 2001; Romeis *et al.*, 2000). However, in both cases the expression was found to be additionally controlled by Rbf1 (M. Scherer and J. Kämper unpublished data).

3.3 Hdp1-dependent gene regulation

Upon induction of the *hdp1* gene, 50 genes were found as up- and 81 as down-regulated. 38 of these genes have been previously described as pheromone dependently regulated (Zarnack, 2006), of which 5, mostly involved in pheromone processing and cell fusion, contain PRE elements (Appendix 6.3 and Table 3). Thus, regulation of these genes by Hdp1 might function indirectly via Prf1. Although not required for the pheromone dependent induction of *rop1* and *prf1*, it is conceivable that *hdp1* modulates the expression of both genes. Firstly, *hdp1* was shown to affect the basal expression level of *rop1* (Figure 19A), and, secondly, similar induction levels for *rop1* were found upon pheromone treatment, induction of Fuz7DD and after *hdp1* induction (Figures 19 and 20). Since the Hdp1-dependent induction of *prf1* depends on the presence of *rop1*, it is likely that Hdp1 regulates *prf1* indirectly via Rop1; this scenario would be similar to the regulation after pheromone treatment. In this model, Hdp1 would integrate a positive feedback loop from the b-regulatory cascade to the pheromone signalling pathway (see Figure 30).

Table 3 Hdp1-induced genes with a potential function in processing and export of mating pheromone and cell fusion processes.

probe set	MUMDB	description	fold change 5 hours	fold change 12 hours	Proposed functions	Presence in Pheromone induction array?	Presence of PRE*	References
W40um030	um10528	related to STE6 - ABC transporter	12,17		Pheromone export	Yes	Yes	(Ketchum *et al.*, 2001) (Huyer *et al.*, 2006)
C20um077	um12220	related to PRM1 - Pheromone-regulated multispanning membrane protein	2,47		Cell membrane fusion	Yes	Yes	(Heiman and Walter, 2000)
W115um227	um11672	related to Protein farnesyltransferase alpha subunit (putative Ram2p)	2,27		Pheromone processing	Yes	Yes	(Huyer *et al.*, 2006)
W55um007**	um05348	related to RAM1 - protein farnesyltransferase, beta subunit	2,23 (P=0,0143)		Pheromone processing	Yes	Yes	(Huyer *et al.*, 2006)
UG14-15c10-91c8	um11682	related to STE14 - farnesyl cysteine carboxyl-methyltransferase	2,14		Pheromone processing	Yes	Yes	(Huyer *et al.*, 2006)

* In 1 kb ustream region of the open reading frame
** Not included in 131 genes listed due to P value higher than 0.01

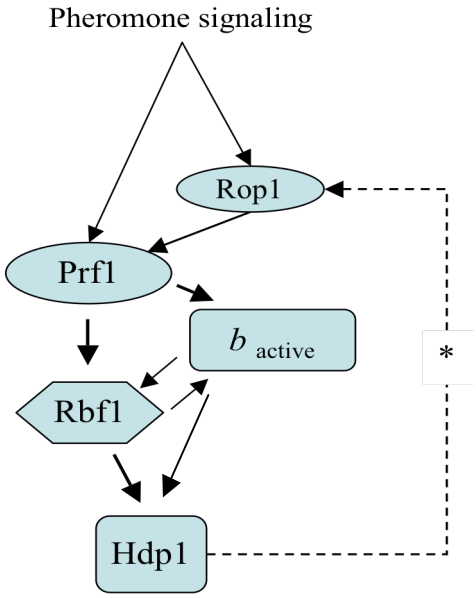

Figure 30. Hdp1 regulatory circuits
Detailed descriptions are given in the text.
Rop1: Regulator of Prf1, Prf1: Pheromone response factor, b_{active}: active b-heterodimer, Rbf1: regulator of b-filament 1, Hdp1: Homeodomain protein 1,
Oval shape: HMG transcription factor, Square shape: homeodomain transcription factor, Hexagon shape: zinc finger transcription factor.

The meanings of lines are as described:

→ Induce/Activate

——— Regulation is verified.

– – – Nature of regulation is unclear.

* The proposed positive feedback regulation of Hdp1 on *rop1* expression is marked.

Although the pheromone- and b-regulatory cascade differ in their two main transcriptional regulators, Prf1 and the bE/bW heterodimer, they share common components, as the regulators Rbf1 and Hdp1. *hdp1*-regulated genes that are either *a*- and/or *b*-dependent and that lack PRE elements are likely to be indirectly regulated via Rbf1. 38 genes of the *hdp1*-regulated genes are *b*-dependent, and out of these 15 genes are dependent on both pathways. For example, the genes of the *cab* locus, that have been shown to be repressed by both *a* and *b,* are also repressed upon *hdp1* induction.

Although a transcriptional regulation of Prf1 was observed in this study, the main regulation of Prf1 is mediated by posttranscriptional phosphorylation by the protein kinase A (PKA) and the MAP Kinase kpp2 (Kaffarnik *et al.*, 2003). These modifications are most probably not occurring after *hdp1* induction, which may explain the relatively small number of direct Prf1-target genes induced upon *hdp1* induction.

The *hdp1*-regulated genes that are not dependent on *a* or *b* give clues about the function of Hdp1 independent from the pheromone- and the b-regulatory cascade. For example, Hdp1 regulates the expression of genes encoding potential sugar transporters, oligopeptide transporters, ABC transporters and tetracycline resistance proteins (Table 4). Although some of them are also *a* and/or *b* dependent, Hdp1 seems to regulate genes involved in uptake or secretion as a response to environmental cues.

Table 4: *hdp1*-regulated genes coding for potential transporters.

probe set	MUMDB	Annotation	fold change		InterPro, (Number of transmembranes (TM))	Funcat: 20
			5 hours	12 hours		
W40um030	um10528	related to STE6 - ABC transporter	12,17		ABC transporter, (11 TM)	No
C85um097	um11514	probable High-affinity glucose transporter	7,03	5,94	Sugar transporter, (10 TM)	Yes
W40um248	um03034	conserved hypothetical protein	6,09	4,47	Sugar transporter, (11 TM)	Yes
W5um075	um11596	related to CSR1 - phosphatidylinositol transfer protein	3,88	2,29	Cellular retinaldehyde-binding)/triple function, (- TM)	Yes
W75um036	um02763	conserved hypothetical protein	3,76		Oligopeptide transporter OPT superfamily (13TM)	No
W20um109	um04347	probable isp4 - oligopeptide transporter		3,58	Tetrapeptide transporter, OPT1/isp4 (15 TM)	Yes
W85um258	um04399	probable succinate-fumarate transporter (mitochondrial)	3,04		Mitochondrial substrate carrier (- TM)	Yes
W10um134	um05114	related to multidrug resistance protein 4	2,54		ABC transporter (12 TM)	Yes
W50um103	um01986	probable sterol carrier protein	2,53		Thiolase (- TM)	Yes
C135um096	um03958	probable fatty acid elongase (FEN1)	2,09		GNS1/SUR4 membrane protein (5 TM)	Yes
C40um172	um02900	conserved hypothetical protein	2,06		General substrate transporter (12 TM)	No
W40um256	um05786	related to UDP N-acetylglucosamine transporter	-2,40		UDP-galactose transporter (5 TM)	Yes
UG23-1i5-133h4	um05421	related to Multidrug resistance protein	-2,51		General substrate transporter (13 TM)	Yes
W35um189	um00712	probable YOR1 - ABC transporter	-3,01		ABC transporter (8 TM)	Yes
C230um012	um02062	related to multidrug resistance proteins	-4,45		Tetracycline resistance protein TetB (14 TM)	Yes
W25um089	um10815	conserved hypothetical protein	-4,51		Major facilitator superfamily (12 TM)	Yes
C25um256	um05783	related to UDP-galactose transporter	-4,99		Nucleotide-sugar transporter (7 TM)	No
W60um250	um10365	related to YBT1 - Vacuolar, ABC protein transporting bile acids	-7,44		ABC transporter (14 TM)	No
W35um258	um04410	probable siderophore iron transporter mirC	-13,50		Major facilitator superfamily (14 TM)	No
C110um021	um03115	related to Sge1 - drug resistance protein	-14,19	-9,84	Tetracycline resistance protein TetB (13 TM)	Yes

Note: Genes are marked as follows: *a*-dependent: yellow; *a*-and *b*-dependent: grey; *b*-dependent: blue.

One of the *hdp1* up-regulated genes, um10189 (*sid2*), encodes a ferrichrome siderophore peptide synthetase, which is involved in siderophore synthesis, suggesting that Hdp1 is also involved in triggering a cellular response to iron limitation. (Yuan *et al.*, 2001).

The genes of the MEL cluster are repressed by both *a*- and *b*-cascades, but also induced under nitrogen limiting conditions (Hewald *et al.*, 2006). Therefore, Hdp1 may function as a repressor of the MEL cluster under nitrogen-rich conditions. Concomitantly, *ncp1*, encoding a transcription factor binding to the UAS motif within the *prf1* promoter in response to environmental signals (Hartmann *et al.*, 1999), is strongly repressed by Hdp1 (Table 1). It is conceivable that Ncp1 may function as a positive regulator of the MEL cluster genes; the down-regulation by Hdp1 would then lead to a repression of the MEL genes.

Interestingly, not all of the MEL cluster genes are down-regulated by Hdp1. The key genes for MEL biosynthesis, *mac1* and *mac2*, are both repressed, similar as *mmf1*, the putative exporter of MELs. The expression of the *emt1* gene, however, was not altered. Emt1 catalyzes the condensation of mannose and erythritol, the first step of MEL production (Hewald *et al.*, 2006). The down-regulation of MELs production observed probably still allows the production (or accumulation) of

mannosylerythritol, facilitating the production of MELs when *U. maydis* cells are shifted to nitrogen limiting conditions again.

Hdp1 regulates 25 genes involved in carbohydrate- and lipid-metabolism, for example a putative fatty acid elongase; the homologous gene in *S. cerevisiae*, *fen1*, is involved in fatty acid elongation and sphingolipid formation. The induction of these genes can be attributed as an indirect effect of the Hdp1-induced filament formation and the associated *de novo* synthesis of membranes (Oh *et al.*, 1997). In addition, the cell wall of filamentously growing cells may have an altered structure. Hdp1 regulates two chitin synthases, Chs1 and Chs3, which may be involved in this process.

The colonies of strains in which *hdp1* is overexpressed display aerial hyphae on charcoal containing plates that stick together and form bundles (Figure 14A and 14B). However, the surface hydrophobicity of such colonies is only insignificantly reduced when compared to colonies of the respective wildtype strains (Figure 14D). In accordance with this observation, the bundling of the hyphae is neither caused by the missing expression of the hydrophobic surface protein Rep1, nor due to the increased expression level of the hydrophobin Hum2 (Figure 14C and 15). Rep1 was found to be the most important protein contributing for the surface hydrophobicity of *U. maydis* hyphae (Wösten *et al.*, 1996). Thus, we have to assume that additional factors which are not induced by Hdp1 are required for aerial growth of single hyphae.

3.4 Hdp1 modulates G2 cell cycle arrest and filamentation.

In saprophytically growing haploid sporidia, the phenotype of a *hdp1* deletion is indistinguishable from that of wildtype sporidia, which is consistent with the observed low level of *hdp1* expression under these conditions. However, the deletion of *hdp1* leads to the formation of stunted hyphae in both solopathogenic as well as dikaryotic filaments. Furthermore, in hyphae resulting from the fusion of compatible *Δhdp1*-sporidia, more than two nuclei are found more frequently than in wildtype hyphae. In conjugation hyphae of Δ*hdp1* strains, the DNA content is shifted towards a 1C DNA content because less cells were arrested in the pheromone-mediated G2 cell cycle arrest. The overexpression of *hdp1* in turn induces a G2 cell cycle arrest. *U. maydis* cells are as well arrested in G2 after overexpression of *biz1*, a transcription factor that is also regulated by b and Rbf1 (Flor-Parra *et al.*, 2006; Vranes, 2006). However, the deletion of both genes, *hdp1* and *biz,* does not abolish the b-mediated cell cycle arrest and filament formation. Rbf1 appears to be the main regulator required for

filamentation and G2 cell cycle arrest. Thus, either Rbf1 itself, or a transcription factor regulated by Rbf1 seems to trigger a G2 cell cycle arrest in addition to Biz1 and Hdp1. Since *hdp1* expression is both *a*-and *b*-dependent, the Hdp1-dependent G2 cell cycle arrest can be observed before cell fusion by pheromone stimulation, as well as after the cell fusion event due to the formation of a b-heterodimer. Thus, Hdp1 could be required to fine-tune a G2 cell cycle arrest in both stages, or even in the transition stage after cell fusion when pheromone signalling is still active and the b-heterodimer is already formed.

In addition, Hdp1 is probably involved in fine-tuning the cell cycle, independent from *a* and *b*, due to environmental cues. In NO_3-containing minimal media strains deleted for *U. maydis pcl12*, a Pho85-like cyclin, show an incomplete G2 cell cycle arrest after *hdp1* induction, which was not observed in complete media (See 2.10). Under starvation conditions, as in minimal media or on the leaf surface, it might be advantageous for *U. maydis* cells to arrest the cell cycle and switch to filamentous growth to overcome this unfavourable situation. Pcl1, Pcl2 and Pcl9 the *U. maydis* Pcl12 homologues in *S. cerevisiae* are all cell cycle and pheromone regulated proteins. *pcl1* and *pcl2* expression peaks at the late G1 phase, while *pcl9* expression peaks at the late M and early G1 phase. *pcl2* is induced by pheromone stimulation, while *pcl1* and *pcl9* are down-regulated (Espinoza *et al.*, 1994; Measday *et al.*, 1994; Measday *et al.*, 1997). Similar to the regulation pattern of *pcl2*, *U. maydis pcl12* is induced by pheromone and leads to a G2 cell cycle arrest (Flor-Parra *et al.*, 2007 ; See 2.8). In yeast it was shown that the kinase Pho85 interacts with Pcl2 and forms a complex which has a G1 periodic activity (Measday *et al.*, 1994). In addition, Pho85 is involved in the regulation of the cell cycle in response to environmental signals such as phosphate starvation (Hirst *et al.*, 1994; Kaffman *et al.*, 1994; Schneider *et al.*, 1994; Toh-e *et al.*, 1988). These findings indicate that in *U. maydis* Hdp1 might regulate the cell cycle in a nutrition dependent manner via the induction of *U. maydis pcl12*, which triggers a G2 cell cycle arrest under starvation conditions.

3.5 Mechanism of Hdp1-mediated cell cycle arrest and filamentation

Two *hdp1*-regulated genes, *pcl12* and *clb1*, that could possibly account for the Hdp1-mediated cell cycle arrest and filamentation, were identified by means of microarray analysis. Both genes encode proteins that are involved in cell cycle control (Figure 31).

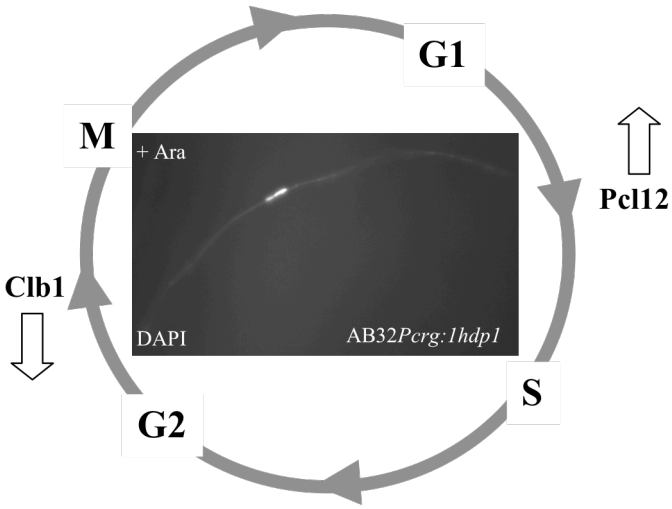

Figure 31 Model of cell cycle regulation via Hdp1.
The induction of *pcl12* and repression of *clb1* via Hdp1 could account for the observed G2 cell cycle arrest.
Pcl12 is a Pho85-cyclin that is able to induce a G2 cell cycle arrest. Clb1 is a B-cyclin required for the transition G1/S and G2/M. The repression of *clb1* should block the transition from G2 to M.
Microscopic picture: AB32P*crg1:hdp1* grown in CM-arabinose media (DAPI filter)

G1: G1 phase, S: Synthesis phase, G2: G2 phase, M: Mitotic phase

Real-time quantitative RT-PCR analysis after induced expression of *hdp1* in strain FB1*Pcrg1:hdp1* revealed a 18.5 fold induction of *pcl12* and a 2.2 fold down-regulation of *clb1*. Pcl12 is a Cdk5-interacting cyclin. Cdk5 is a cyclin dependent kinase with sequence similarity to the Cdk5/Pho85 protein family that is required for cell polarity and pathogenicity (Castillo-Lluva *et al.*, 2007). *pcl12* expression is dependent on *a* and *b*. The gene is required for b-induced filament formation, as well as for the formation of conjugation hyphae and proper promycelium morphogenesis. However, *Δpcl12* strains are still able to cause tumors and to produce teliospores (Flor-Parra *et al.*, 2007); Figures 22, 23, 24A). The overexpression of *pcl12* induces a G2 cell cycle arrest. Thus, the observed up-regulation of *pcl12* upon *hdp1* induction could account for the cell cycle arrest at G2 phase.

Clb1 is a B-cyclin, required for the transition of G1/S and G2/M. Thus, the down-regulation of *clb1* by *hdp1* overexpression could account for the inhibition of the transition from G2 to M phase, similar to the observations made after overexpression of the *biz1* gene (Flor-Parra *et al.*, 2006).

Our data show that *pcl12* is not only required for the formation of the b-induced filament, but also for Hdp1-mediated filamentation (Figure 24B and 24C), suggesting that Hdp1-induced filaments are mediated via a mechanism common with *b*-

dependent filament formation. Consequently, the pheromone dependent induction of *pcl12* might occur via Hdp1 as well.

However, *pcl12* expression upon formation of an active b-heterodimer in a strain deleted for *hdp1* was not significantly different from that of the respective wildtype, indicating that other regulator(s), such as Rbf1, must participate in *pcl12* regulation (see detail in Appendix 6.5). The function of *pcl12* in Hdp1-mediated cell cycle arrest seems to be affected by environmental cues (see 2.10). One possible explanation is that cells grown under limiting growth conditions (NO_3-MM medium) have a higher frequency of cells with 1C DNA content (Figure 26B) compared to cells grown in rich medium as CM medium (Figures 13B and 25B). Therefore, the G1 cyclin function of *U. maydis* Pcl12 could be required in NO_3-MM medium, where the majority of cells are in the G1 phase, to facilitate the transition from G1 to G2. In cells grown in CM medium, where the majority of cells are already in G2, the gene is not required.

The deletion of *pcl12* causes a delay of the conjugation tube formation (Flor-Parra *et al.*, 2007), similar to observations made in this study. When the pheromone treatment was performed in NO_3-MM media, both *Δhdp1* and *Δpcl12* strains produced less conjugation hyphae than wildtype strains (Figure 27). In budding yeast, there is no clear evidence for an alteration in the pheromone response in strains deleted for *pho85* or any other *pcl* gene (Measday *et al.*, 1997). However, in *Schizosaccharomyces pombe*, the Pcl-like cyclin Pas1p has been shown to control pheromone signalling. Cells lacking $pas1^+$ are highly sensitive to pheromone, responding with a G1 arrest and a premature commitment for conjugation. Additionally, Pas1p plays a role in nutrient-controlled repression of the pheromone signalling (Tanaka and Okayama, 2000). It is likely that Pas1p is involved in both pheromone signalling and nutrient control. Similarly to the observations in this study that Pcl12 is required for a wildtype-like conjugation hyphae formation in NO_3-MM. Whereas in fission yeast, cells lacking *pas1+* are highly sensitive to mating pheromone, in *U. maydis pcl12* deletion strains shows a delayed or reduced conjugation hyphae formation. These controversy results are possibly due to the difference stages of cell cycle arrest, G1 phase in both budding and fission yeasts (Herskowitz *et al.*, 1995; Imai and Yamamoto, 1994), and G2 in *U. maydis*, respectively (Garcia-Muse *et al.*, 2003). Since Hdp1 is able to induce *pcl12* expression, the defect in conjugation hyphae

formation observed in *Δhdp1* strains is probably due to the reduced expression of *pcl12*.

Clb1, a B-cyclin in *U. maydis*, is required for the transition of G1/S and G2/M. Clb1 depletion can cause a cell cycle arrest at G2 phase (Garcia-Muse *et al.*, 2004). Unlike as described for *biz1*, induced expression of *clb1* only interferes with Hdp1-mediated filament formation, but cannot counteract the Hdp1-mediated cell cycle arrest (Figure 26B3). One possible explanation is that *pcl12* induction acts dominant over the *clb1* down-regulation. However, since induction of both *clb1* and *hdp1* in a strain deleted for *pcl12* does not lead to an altered phenotype compared to a strain in which *clb1* is not induced (Figure 26A, 26B2 and 26B4), it can be excluded that Clb1 down-regulation is the major mechanism of Hdp1-mediated cell cycle arrest.

In *U. maydis*, at least 4 factors are involved in the regulation of G2/M transition: the Cdk1/Clb1 and Cdk1/Clb2 complexes, Wee1 and Cdc25 (Garcia-Muse *et al.*, 2004; Sgarlata and Perez-Martin, 2005a; Sgarlata and Perez-Martin, 2005b). Wee1 and Cdc25 are involved in the phosphorylation of Cdk1 (cyclin dependent kinase1) to regulate the activity of the Cdk1/Clb2 complex in G2/M phase transition. Thus, in addition to the transcriptional control of cell cycle regulators observed in this study, the regulation at the posttranscriptional or posttranslational level plays a major role.

3.6 Hdp1 is required for fine-tuning the cell cycle regulation during pathogenic development of *U. maydis*

In *U. maydis,* Hdp1 is involved in inducing a G2 cell cycle arrest that is triggered by both the pheromone-cascade and the b-regulatory cascade. Under both conditions the G2 cell cycle arrest is essential for further development of the fungus. The cell cycle arrest induced after pheromone recognition enables the fungus to form conjugation hyphae for the subsequent mating event, and the b-mediated cell cycle arrest is necessary to develop the filamentous hyphae, which are able to infect the host plant. Following models might contribute to the cell cycle regulation via Hdp1.

After pheromone stimulation, the cAMP and MAPK pathways are activated, leading to transcriptional and posttranscriptional activation of Prf1. Rop1 is required for *prf1* expression in axenic culture, but is dispensable on the plant surface. Prf1 induces the expression of *rbf1*, a major regulator within the b-regulatory cascade, directly via PRE elements in the *rbf1* promoter. Since the b-pathway is not activated, *b*-dependent genes are not induced. Rbf1 further induces *hdp1* expression. Hdp1 induces *pcl12*

expression, leading to a cell cycle arrest; however, additional uncharacterized mechanisms have to be assumed. Strains deleted for *rbf1* still respond to pheromone, i.e. they are able to form conjugation hyphae containing one nucleus. Thus, contrary to the requirement of Rbf1 for the b-mediated cell cycle arrest, additional unknown pathways have to be present (Figure 32).

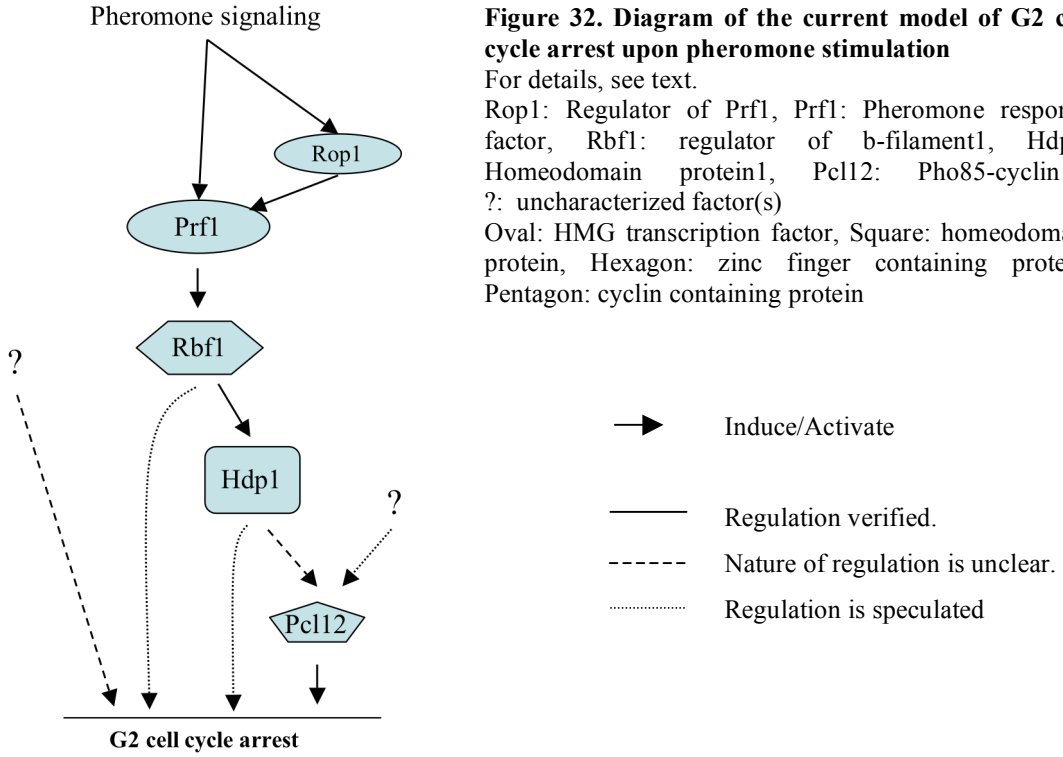

Figure 32. Diagram of the current model of G2 cell cycle arrest upon pheromone stimulation
For details, see text.
Rop1: Regulator of Prf1, Prf1: Pheromone response factor, Rbf1: regulator of b-filament1, Hdp1: Homeodomain protein1, Pcl12: Pho85-cyclin12, ?: uncharacterized factor(s)
Oval: HMG transcription factor, Square: homeodomain protein, Hexagon: zinc finger containing protein, Pentagon: cyclin containing protein

The active b-heterodimer leads to an induction of *rbf1* expression. Rbf1 induces the expression of both *biz1* and *hdp1*. Biz1 has been shown to directly down-regulate *clb1* expression, leading to filamentation and cell cycle arrest (Flor-Parra *et al.*, 2006). In addition, Hdp1 induces the *pcl12* expression, also leading to filamentation and cell cycle arrest. Since *rbf1* induction in a strain deleted for both *biz1* and *hdp1* still leads to cell cycle arrest (Figure 16D), additional uncharacterized mechanisms have to be present. Alternatively, Rbf1 itself could directly induce the cell cycle arrest (see 2.4) (Figure 33).

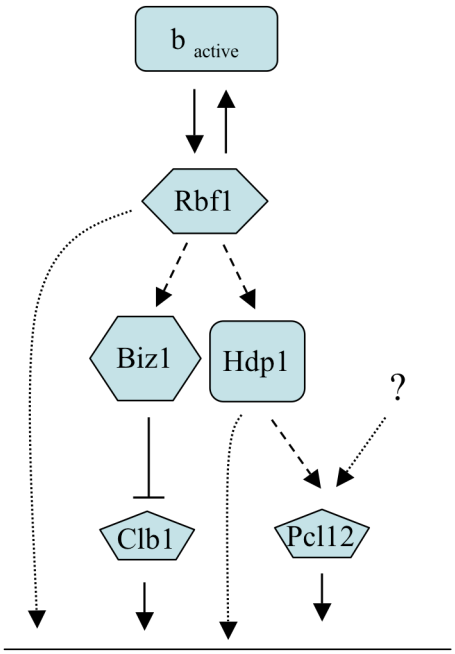

Figure 33. Diagram of the current model of filamentation and G2 cell cycle arrest within b-regulatory cascade
For details, see text.
b_{active}: active b-heterodimer, Rbf1: regulator of b-filament1, Biz1: b-induced zinc-finger1, Hdp1: Homeodomain protein1, Clb1: B-type cyclin 1, Pcl12: Pho85-cyclin12, ?: uncharacterized factor(s)

Square: homeodomain protein, Hexagon: zinc finger containing protein, Pentagon: cyclin containing protein

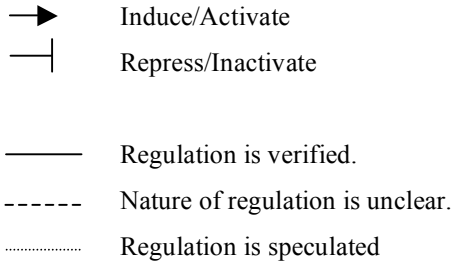

Integrating environmental cues is likely to be the main biological function of Hdp1 in cell cycle regulation. We favor the possibility that *hdp1* is required under nutrient limited conditions to fine-tune the cell cycle to enable the fungus to complete the mating and infection processes. Furthermore, albeit *hdp1* is dispensable for mating and pathogenicity under laboratory or greenhouse conditions, the protein may be important for the fitness of the fungal cells in their natural environment.

4 Materials and methods

4.1 Materials and source of supplies

4.1.1 Chemicals, buffers and solutions, media, enzymes, and kits

Chemicals

All chemicals used in this study were obtained from Ambion, Sigma-Aldrich, Merck, Seakem, Difco, BD Biosciences, BioRad, Amersham, Pharmacia, Fluka, Invitrogen, Carl-Roth, Sigma and Vector Laboratories.

Buffers and solutions

All standard buffers and solutions used in this study were prepared as previously described in Ausubel *et al.* and Sambrook *et al.*, (1989). Additional specific buffers and solutions are listed at corresponding method parts.

Media

Except, specifically mentioned, all media were sterilized by autoclaving at 121°C for 5 min.

For *E. coli* culture, dYT liquid medium and YT solid medium were used (Ausubel *et al.* and Sambrook *et al.*, 1989). Ampicillin was added at a final concentration of 100 µg/ml.

dYT liquid medium

1.6 % (w/v) Trypton-Pepton (Difco)
1.0 % (w/v) Yeast-Extract (Difco)
0.5 % (w/v) NaCl

YT solid medium

0.8 % (w/v) Trypton-Pepton (Difco)
0.5 % (w/v) Yeast-Extract (Difco)
0.5 % (w/v) NaCl
1.3 % (w/v) Agar (Roth)

Plates were left at room temperature for at least 12 hours prior usage.

dYT-glycerol medium

1.6 % (w/v) Trypton-Pepton (Difco)
1.0 % (w/v) Yeast-Extract (Difco)
0.5 % (w/v) NaCl
80.0 % (v/v) 87% Glycerine (f.c. 69,6%)

For *U. maydis*, media used in this study are described in the following part.

CM-medium

0.25% (w/v) Casaminoacids (Difco)
0.1% (w/v) Yeast-Extract (Difco)
1.0% (v/v) Vitamin solution (Holliday, 1974)
6.25% (v/v) Salt solution (Holliday, 1974)
0.05% (w/v) DNA degr. Free Acid (Sigma, D-3159)
0.15% (w/v) NH_4NO_3

Before autoclaving, pH was adjusted to 7.0 with 5M NaOH.

For CM-solid medium, Agar (Difco) was added to a final concentration of 2%.

$YEPS_{light}$-medium (Tsukuda *et al.*, 1988)

1.0% (w/v) Yeast-Extract (Difco)
0.4% (w/v) Bacto™-Pepton (Difco)
0.4% (w/v) Sucrose

NM-medium

0.3% (w/v) KNO_3

6.25% (v/v) Salt solution (Holliday, 1974)

Sterile filtrated 50% (w/v) glucose or 25% (w/v) arabinose solution was added to a final concentration of 1%. pH was adjusted to 7.0 with 5M NaOH and sterile filtered.

Array-minimal medium

6.25% (v/v) Salt solution (Holliday, 1974)

30 mM L-Glutamine

Sterile filtrated 50% (w/v) glucose or 25% (w/v) arabinose solution was added to a final concentration of 1%. pH was adjusted to 7.0 with 5M NaOH and sterile filtered.

NSY-glycerol medium

0.8% (w/v) Nutrient Broth (Difco)

0.1% (w/v) Yeast-Extract (Difco)

0.5% (w/v) Sucrose (Roth)

80.0% (v/v) 87% Glycerol (f.c. 69.6%)

PD-solid medium

2.4% (w/v) Potato Dextrose Broth (Difco)

2.0% (w/v) Agar (Difco)

Charcoal CM-solid medium

1.0% (w/v) Casaminoacids (Difco)

0.2% (w/v) Yeast-Extract (Difco)

2.0% (v/v) Vitamin solution (Holliday, 1974)

25.0% (v/v) Salt solution from Holliday

0.1% (w/v) DNA degr. Free Acid (Sigma, D-3159)

0.6% (w/v) NH_4NO_3

1.0% (w/v) Charcoal (Sigma C-9157)

2.0% (w/v) Agar (Difco)

Before autoclaving, pH was adjusted to 7.0 with 5M NaOH.

Charcoal PD-solid medium

2.4% (w/v) Potato Dextrose Broth (Difco)

1.0% (w/v) Charcoal (Sigma C-9157)

2.0% (w/v) Agar (Difco)

Regeneration Agar

1.0% (w/v) Yeast-Extract (Difco)

2.0% (w/v) Bacto™-Pepton (Difco)

2.0% (w/v) Sucrose (Roth)

18.22% (w/v) Sorbitol (Sigma S-1876) (f.c. 1 M)

1.5 % (w/v) Agar (Difco)

See how to use under "*U. maydis* protoplast preparation and transformation"

Vitamin solution (Holliday, 1974)

0.1‰ (w/v) Thiamin (Hydrochlorid, Sigma T-4625)

0.05‰ (w/v) Riboflavin (Sigma R-4500)

0.05‰ (w/v) Pyridoxine (Monohydr.chl., Sigma p-9755)

0.2‰ (w/v) Calcium pantothenate (Hemi-Ca.Salz, Sigma P-2250)

0.05‰ (w/v) p-Aminobenzoic-acid (Free Acid, Sigma A-9878)

0.2‰ (w/v) Nicotinic acid (Free Acid, Sigma N-4126)

0.2‰ (w/v) Choline chloride (Sigma C-1879)

1.0‰ (w/v) myo-Inositol (Sigma I-5125)

Sterile filtered and stored at -20 °C

Salt solution (Holliday, 1974)

16.0‰ (w/v) KH_2PO_4

4.0‰ (w/v) Na_2SO_4

8.0‰ (w/v) KCl

2.0‰ (w/v) $MgSO_4$

1.32‰ (w/v) $CaCl_2{*}2H_2O$

8.0‰ (v/v) Traceelements

Sterile filtered

Trace element solution (Holliday, 1974)

0.06‰ (w/v) H_3BO_3

0.14‰ (w/v) $MnCl*4H_2O$

0.4‰ (w/v) $ZnCl_2$

0.4‰ (w/v) $Na_2MoO_4*2H_2O$

0.1‰ (w/v) $FeCl_3*6H_2O$

0.03‰ (w/v) $CuSO_4$

Sterile filtered

If arabinose or glucose was required as sole carbon source, sterile filtrated 50% (w/v) glucose or 25% (w/v) arabinose solution was added to a final concentration of 1%, for charcoal solid media, the final concentration is 2%. Additives to the medium were used in the following concentrations: carboxine (2 µg/ml), ClonNAT (150 µg/ml), hygromycin (200 µg/ml).

Enzymes

Restriction enzymes, Phusion™ High-Fidelity DNA polymerase, Quick T4 DNA ligase, Antarctic Phosphatase, Klenow Fragment and Labeling buffer were obtained from NEB. *Taq* DNA polymerase was obtained from Roche, NEB or laboratory made.

Used kits and miscellaneous materials

The following kits were used regularly and as recommended by the supplier: QiaQuick PCR purification Kit (Qiagen) was used to purify PCR products. QiaQuick Gel Extraction Kit (Qiagen) was used to extract DNA fragments from agarose gel. TOPO TA Cloning Kit (Invitrogen) was used to directly clone PCR products. QIAprep Spin MiniPrep Kit (Qiagen) was used to isolate and purify plasmid DNA before sequencing. GeneRacer Kit (Invitrogen) was used to perform 5'-3' Rapid Amplification of cDNA Ends (5'-3' RACE). RNeasy Kit (Qiagen) was used to purify total RNA before 5'-3' RACE, real-time RT-PCR and Microarray. DNA-freeTM (Ambion) was used for DNA removal before first strand cDNA synthesis. SuperScript® III First-Strand Synthesis SuperMix (Invitrogen) was used for first strand cDNA synthesis. Platinum® SYBR® Green qPCR SuperMix-UDG (invitrogen) was used for real-time PCR. BioArray-HighYield-RNA Transcript Labelling Kit (Enzo) was used for cRNA synthesis. BigDye-Kit (ABI) was used for DNA sequencing. MicroSpin™ S-300 HR Columns were used for purification of P^{32} labelled probes.

4.1.2 Oligonucleotide list

Table 5 Sequences of oligonucleotides used in this study

Names of primers		Sequences (5'→3')	References
***hdp1* deletion and GFP-fusion constructions**			
OCP1		GTGGCCGCGTTGGCCTCTAGCTCGGTTTTAGTTTTGGT	
OCP2		AAGCTTCAGCCTTCCCGCTCTTCA	
OCP3		GCGGCCTGAGTGGCCTCACTCTGCCGTGTTGGCAACGC	
OCP4		CGACAAGCCTATTCCGGTTGATCG	
OCP5		GCGGCCGCGTTGGCCTGGTTGAGCAACGAGCATCGGTGG	
OCP6		TTGGCGGCTCTAGCGTGCGGTAAC	
***hdp1* deletion with Clonnat resistance cassette construction**			
OCP5e		GTTGGCCATCTAGGCCTGGTTGAGCAACGAGCATCG	
***pcl12* deletion construction**			
w35um030-lb1		CACGAACGCCAAAGATGC	
w35um030-lb1-nested		GCAGTAATTCACGCCGTAG	
w35um030-lb2		GTTGGCCATCTAGGCCCTCGTTCTCGCATATCTC	
w35um030-rb1		GTTGGCCTGAGTGGCCCGAGAGGAGTTGATTTG	
w35um030-rb2-nested		GACAAGTCCGCTTTCCTG	
w35um030-rb2		GAGATGGACCTCGTTTACAG	
***hdp1* overexpression plasmid construction**			
F-OvG211-120		TGCCATGGTCGTTGCTCAACCACCGTT	
R-OVG211-120		GTCTGTTTTGGGCCGCGACCTGTGC	
O-hdp1WF-AAr		GTCTGTTTTGGGCCGCGACCTGTGC	
O-hdp1WF-AAf		TGCCATGGTCGTTGCTCAACCACCGTT	
5'-3' RACE: *hdp1* gene specific primers			
F-E1		CGGCTCAGCCACAAACTCTCC	
R-E3		GAAGCGGTGTCGAGGGCGAAC	
N-R-E2		ACCAAGTTGGGAAGCGGCAG	
***hdp1* probe**			
Hdp1-cDNA-2198F		CGAGCATGTCGCCTCAAAG	
Hdp1-cDNA-2485R		CTGGACGAAGCTCTGTTG	
Real-time RT-PCR: gene specific primers			
hdp1	hdp1-F	CCGAAAGCGTCTGGGATGAG	
	hdp1-R	GTCGTGCGTACATCGTACGG	
bE	bE-F	GCACAACACCTTCCATTGAC	(Scherer et al, 2006)
	bE-R	ACTGCTCCCGAATGTACT	
rbf1	RT_rbf1_F	AGTACGAGCTACGACGGATTC	(Scherer et al, 2006)
	RT_rbf1_R	GGGTAGGTGTTGGACACATTC	
clb1	clb1RT-a	CAGCATCAGGTATCCCATCAG	(I. Flor-Parra, unpublished data)
	clb1RT-b	GACGCACGGACCATTGAAG	
pcl12	pcl12-F	GGCGACTGTAGCATACAAG	
	pcl12-R	GCGAGAACGAGAACAAGAC	
rop1	Rop1-F	TACACCACAATCGCCAACTC	
	Rop1-R	AAGGTGTTGGGAAGGAATCG	
prf1	SL-57	TCGGTAGAACGAGCTGTGATG	(K. Zarnack and M. Feldbrügge , unpublished data)
	SL-58	CTGTTGGACGATGTTGGAGTTG	
elf2B	rt-elF-2B-F	ATCCCGAACAGCCCAAAC	(M. Vranes, unpublished data)
	rt-elF-2B-R	ATCGTCAACCGCAACCAC	

4.1.3 Strains

***Escherichia coli* strains**

E. coli TOP10 (Invitrogen) (F^- *mcr*A Δ(*mrr-hsd*RMS-*mcr*BC) φ80*lac*ZΔM15 Δ*lac*X74 *deo*R nupG *rec*A1 *ara*D139 Δ(*ara-leu*)7697 *gal*U *gal*K *rps*L(Str^R) *end*A1 λ^-) that is a derivative of *E. coli* K12 or *E. coli* Mach1 (Invirogen) (Δ*rec*A1398 *end*A1 *ton*A Φ80Δ*lac*M15 Δ*lac*X74 *hsd*R(r_K^- m_K^+)) that is a derivative of *E. coli* W strains (ATCC 9637, S. A. Waksman) were used for cloning purposes.

Corn variety (*Zea mays* spec.)

For all pathogenicity tests, the corn variety Early Golden Bantam (Olds Seed Company, Madison Wisconsin, USA) was used.

***Ustilago maydis* strains**

U. maydis strains used in this study are listed in table 6 and 7. Table 6 shows progenitor strains that were already available. Table 7 shows the strains generated in this study. All strains in table 7 were analyzed by southern analysis.

Table 6 *Ustilago maydis* progenitor strains

Strain	Relevant genotype	Resistances	Reference
AB31	*a2 bW2*^{crg1P},*bE1*^{crg1P}	$Phleo^R$	(Brachmann *et al.*, 2001)
AB32	*a2 bW2*^{crg1P},*bE2*^{crg1P}	$Phleo^R$	(Brachmann *et al.*, 2001)
AB33	*a2 bW2*^{nar1P},*bE1*^{nar1P}	$Phleo^R$	(Brachmann *et al.*, 2001)
AB34	*a2 bW2*^{nar1P},*bE2*^{nar1P}	$Phleo^R$	(Brachmann *et al.*, 2001)
FB1	*a1 b1*	-	(Banuett and Herskowitz, 1989)
FB2	*a2 b2*	-	(Banuett and Herskowitz, 1989)
FBD11	*a1a2 b1b2*	-	(Banuett and Herskowitz, 1989)
SG200	*a1mfa2 bW2bE1*	$Phleo^R$	(Bölker *et al.*, 1995)
SG200*Δrbf1*	*a1mfa2 bW2bE1 Δrbf1*	$Phleo^R$, Hyg^R	(M. Scherer unpublished)
AB31*Δbiz1*	*a2 bW2*^{crg1P},*bE1*^{crg1P}*Δbiz1*	$Phleo^R$, Hyg^R	(M. Vranes unpublished)
TAU41	*a1 b1, clb1*^{nar1P}	Cbx^R	(Garcia-Muse *et al.*, 2004)
FB1P_{crg1}:fuz7DD	*a1 b1 ip*^{r}*[*P_{crg1}*:fuz7DD]ip*^{s}	Cbx^R	(Müller *et al.*, 2003)

Table 7 *Ustilago maydis* strains generated during this study

Strain	Relevant genotype	Resistances	Progenitor
FB1*Δhdp1*	*a1 b1 Δhdp1*	Hyg^R	FB1
FB2*Δhdp1*	*a2 b2 Δhdp1*	Hyg^R	FB2
SG200*Δhdp1*	*a1mfa2 bW2bE1 Δhdp1*	$Phleo^R$, Hyg^R	SG200
UECP98	*a2 bW2^{crg1P},bE1^{crg1P} hdp1:eGFP*	$Phleo^R$, Hyg^R	AB31
UECP19	*a1 b1 ip^r[P$_{crg1}$:hdp1$_{wt}$]ip^s*	Cbx^R	FB1
UECP106	*a1 b1 ip^r[P$_{crg1}$:hdp1$_{AA}$]ip^s*	Cbx^R	FB1
FB1hdp1*Δhum2*	*a1 b1 ip^r[P$_{crg1}$:hdp1$_{wt}$]ip^{s}Δhum2*	Cbx^R, Hyg^R	UECP19
AB31*Δhdp1*	*a2 bW2^{crg1P},bE1^{crg1P} Δhdp1*	$Phleo^R$, Hyg^R	AB31
AB31*Δhdp1Δbiz1*	*a2 bW2^{crg1P},bE1^{crg1P} Δhdp1Δbiz1*	$Phleo^R$, Hyg^R, Nat^R	AB31*Δbiz1*
AB32Pcrg1:hdp1	*a2 bW2^{crg1P},bE2^{crg1P} ip^r[Pcrg:hdp1$_{wt}$]ip^s*	$Phleo^R$, Cbx^R	AB32
FB1Pcrg1Fuz7DD Δhdp1	*a1 b1 ip^r[P$_{crg}$:fuz7DD]ip^s Δhdp1*	Cbx^R, Hyg^R	FB1P$_{crg1}$:fuz7DD
UECP107	*a1 b1 ip^r[P$_{crg}$:hdp1$_{wt}$]ip^s Δrop1*	Cbx^R, Hyg^R	UECP19
SG200*Δpcl12*	*a1mfa2 bW2bE1 Δpcl12*	$Phleo^R$, Hyg^R	SG200
UECP77	*a1 b1 ip^r[P$_{crg}$:hdp1$_{wt}$]ip^s Δpcl12*	Cbx^R, Hyg^R	UECP19
UECP101	*a1 b1, clb1^{nar1P}, ip^r[P$_{crg}$:hdp1,hph]ip^s*	Cbx^R, Hyg^R	TAU41
UECP113	*a1 b1, clb1^{nar1P}, ip^r[P$_{crg}$:hdp1,hph]ip^s Δpcl12*	Cbx^R, Hyg^R, Nat^R	UECP101

4.1.4 Plasmids and Plasmid constructs

pCR2.1-TOPO (invitrogen): Used for direct cloning of PCR products.

p238 (M. Treutlein, unpublished): Used for *rep1* probe preparation

pBS-hhn (Kämper, 2004): Used for *pcl12* gene deletion.
Contains a 1,884 bp-*Sfi*I-fragments harboring hygromycin resistant cassette (Hyg^R). The *hph* gene is franked by the *hsp70*-promoter and T*nos*-terminator.

pUMa317 (pMF5-1h) (M. Feldbrügge, unpublished) : Used for *hdp1* gene deletion and Hdp1:egfp fusion.
Contains a 3,730 bp-*Sfi*I-fragment harboring the *egfp* gene and hygromycin resistance cassette. The *egfp* gene is followed by the T*nos*-Terminator. This *Sfi*I Fragment is used for C-terminal GFP fusion. The *hph* gene is flanked by the *hsp70*-promoter and the *hsp70* terminator.

pUMa262 (pMF1n) (Brachmann *et al.*, 2004): Used for *hdp1* gene deletion in AB31*Δhdp1Δbiz1 and pcl12* deletion in UECP113.
Contains a 1,390 bp-*Sfi*I-fragments harboring the nourseothricine resistance cassette (Nat^R). The *Nat^R* gene is flanked by the *hsp70*-promoter and *hsp70* -terminator.

4.1.5 Plasmids and Plasmid constructions during this work

pKO1 was used for the amplification of the *hdp1* deletion construct. In general, the pCR2.1 TOPO vector containing the 5' border and the 3' border of the *hdp1* gene was ligated to the eGFP-*hph* cassette of pUMa317. The 5' border was PCR amplified with the primers OCP5 and OCP6. The 3' border was PCR amplified with the primers OCP3 and OCP4 using genomic DNA of *U. maydis* 521 as template.

pFus1 was used for the amplification of Hdp1:egfp fusion construct, similarly as described in **"pKO1"**. The primers OCP1 and OCP2 were used for PCR amplification of the 3' region without stop codon of the *hdp1* gene instead of the 5' border.

pPcrg1-gORF-*hdp1*$_{wt}$ was used for the integration of the *hdp1* ORF under the control of the arabinose inducible *crg1* Promoter (Brachmann *et al.*, 2001) into the *ip* locus of FB1, generating UECP19. A genomic DNA fragment of the *hdp1*$_{wt}$ ORF was PCR amplified as a 3084 bp *Nco*I/*Not*I fragment with the primers F-OvG211-120 and R-OVG211-120 primers from *U. maydis* 521 genomic DNA. Transcription initiation and termination are mediated by the *crg1* promoter and the T*nos* terminator, respectively. Besides, **pPcrg1-gORF-*hdp1*$_{wt}$** harbors the *ip*^{r} locus used for homologous integration and selection.

pPcrg1-gORF-*hdp1*$_{AA}$ was used for the integration of a mutated version of *hdp1* into the *ip* locus of FB1, generating UECP106. The wildtype *hdp1* ORF of **pPcrg1-gORF-*hdp1*$_{wt}$** was replaced with the mutated allele of which amino acids $W_{230}F_{231}$ were mutated to alanines as described in 4.3.4.

pPcrg1-gORF-*hdp1*$_{wt}$-*hph* was used for the integration of the genomic ORF of *hdp1* into the *ip* locus of TAU41, generating UECP101. Plasmid Pcrg-gORF-*hdp1*$_{wt}$ was digested with *Hpa*I and blunt end ligated to a blunted NotI/NotI *hph* fragment from pSL-hyg.

For the integration into the *ip* locus, the plasmids were linearized with *Ssp*I before transformation of *U. maydis*.
All plasmids constructed in this thesis were analyzed by restriction digestion and DNA sequencing.

4.2 Genetic, microbiology and cell biology methods

4.2.1 Escherichia coli

Cultivation and media of *E. coli*

E. coli was grown in dYT liquid medium or on YT solid medium. Liquid cultures were incubated at 37°C at 200 rpm. Solid media were incubated under aerobic condition at 37°C. Glycerol stocks were made from exponentially growing cultures

containing the appropriate antibiotic by mixing with dYT-glycerin at a 1:1 ratio and stored at -80°C.

Determination of cell density in *E. coli*

E. coli liquid cultures were measured photometrically with a NovospecII photometer (Phamacia Biotech) at 600 nm. In order to obtain the measurement in linear reference, the *E. coli* cultures were diluted to a value of OD_{600} below 0.8. A corresponding culture medium was used as a reference. A culture density of $OD_{600} = 1$ correlates to about 1.0×10^9 cells/ml

Competent cell preparation and transformation of *E. coli* (Cohen et al., 1972)

Competent cell preparation ($RbCl/CaCl_2$) and chemical transformation of *E. coli* were modified from Cohen *et al.* (1972). *E. coli* TOP10 or Mach1 cells were pregrown in 20 ml dYT medium overnight at 37ºC at 200 rpm and diluted 1:200 in 1000 ml dYT medium and continually grown to a cell density of $OD_{600} \sim 0.6$. The culture was transferred to a centrifuge tube, incubated on ice for 30 min and centrifuged for 8 min at 3000 rpm at 4ºC. The supernatant was discarded and the cells were resuspended in 1/3 culture volume (330 ml) of pre-chilled RF1-solution and incubated for 30 min at 4ºC. The suspension was centrifuged for 8 min at 3000 rpm at 4ºC and the supernatant was discarded. *E. coli* cells were resuspended in 1/20 culture volume (50 ml) of pre-chilled RF2-solution and incubated for 30 min on ice. Finally, 100 µl aliquots of competent cell suspension in 1.5-ml Eppendorf tubes were kept on ice for usage or stored at - 80°C.

RF1 solution

100 mM RbCl
50 mM $MnCl_2 \times 4\ H_2O$
30 mM K-acetate
10 mM $CaCl_2 \times 2\ H_2O$
15% (v/v) glycerol
in H_2Obid.
pH was adjusted to 5.8 with HCl and sterile filtered.

RF2 solution

10 mM MOPS
10 mMRbCl
75 mM $CaCl_2 \times 2\ H_2O$
15% (v/v) glycerol
in H_2Obid.
pH was adjusted to 5.8 with NaOH and sterile filtered.

In order to transform *E. coli* by chemical transformation, aliquots of 100 µl competent cells were thawed on ice for 5 min. Then, 1-5 ng of plasmid DNA was added, gently mixed and incubated on ice for 20-30 min. The *E. coli* cells were heat shocked at 42°C for 30 s and cooled on ice for 5 min. For the recovery of the cells, 500 µl dYT medium was added and incubated at 200 rpm for 30 min at 37°C. Finally, 200 µl of *E.coli* cell suspension was plated on YT-agar containing the appropriated antibiotic (100 µg/ml of amplicilin) and incubated at 37°C overnight.

4.2.2 Ustilago maydis

Cultivation and media of *U. maydis*

Liquid cultures were incubated at 28°C with shaking at 200 rpm. On solid media, *U. maydis* plates were incubated under aerobic condition at 28°C (or 22°C for charcoal containing solid media). Glycerol stocks were made from exponentially growing cultures by mixing with NSY-glycerol media at 1:1 ratio and stored at -80°C.

Determination of cell density in *U. maydis*

U. maydis liquid cultures were photometrically measured by NovospecII photometer (Phamacia Biotech) at 600 nm. In order to obtain the measurement in linear reference, the *U. maydis* cultures were diluted to a value of OD_{600} below 0.8. A corresponding culture medium was used as a reference. A culture density of OD_{600}= 1 correlates to about 1-5 x 10^7 cells/ml.

Induction of *U. maydis*

The use of inducible promoters enables the control of gene induction or repression by switching the cultivation media. The inducible promoter used in this study is the arabinose inducible *crg1* promoter (Brachmann *et al.*, 2001) that is repressed in media containing glucose.

The induction strains were grown in CM, NM or array-minimal media containing glucose as a sole carbon source. The cultures were grown at 28ºC at 200 rpm until a cell density of OD_{600} ~ 0.5. Then, cells were harvested by centrifugation for 5 min at 3500 rpm. Cells were washed once in the corresponding arabinose containing media. After that, the cells were continually grown in media containing arabinose as a sole carbon source at a final concentraion of 1% at 28ºC at 200 rpm.

Protoplast preparation and transformation of *U. maydis* (Schulz *et al.*, 1990)

Protoplast preparation and transformation of *U. maydis* strains was performed as described previously in Schulz *et al.* (1990).

Briefly, *U. maydis* cells were grown overnight in $YEPS_{light}$ medium at 28°C to a cell density of OD_{600} 0.8 – 1. The cells were harvested by centrifugation for 10 min at 3000 rpm at room temperature and washed in 25 ml SCS and resuspended in 2 ml SCS containing 3.5 mg/ml Novozyme. Cells were incubated for ~ 10 min at room temperature to digest the cell wall material. This process was followed under the microscope. After rounding up the elongated *U. maydis* cells were washed three times with ice-cold SCS and centrifuged at 2400 rpm for 8 min at 4°C. This was followed with an additional wash with ice-cold STC. Finally, the protoplast pellet was resuspended in 0.5 ml STC and aliquots of 50 µl were used immediately or stored at -80°C.

For transformation of Protoplasts, linearised DNA (3-5 µg) and 1 µl Heparin (1 mg/ml) was added to the protoplast aliquot and incubated for 10 min on ice. Subsequently, 500 µl STC/PEG were added and the protoplast mix was incubated for another 15 min on ice. The transformation mix was plated on Regeneration-agar. Transformed colonies appeared after 3-7 days and were singled-out and grown on CM-agar plates containing the appropriate antibiotic. Single colonies were picked and saved on CM-plates.

The regeneration-agar plate was prepared by first making a bottom phase with 10 ml Regeneration agar containing the appropriate concentration of antibiotics (hygromycin, carboxin and clonnat = 400µg/ml, 4µg/ml and 300 µg/ml, respectively) was plated into a round plate and waited till it was completely solidified. Then, another 10 ml regeneration agar without antibiotics was plated on the top of it. The regeneration-agar plates can be used after complete solidification.

SCS
20 mM Na-citrate, pH 5,8
1 M Sorbitol
in distilled water, sterile filtered

STC
10 mM Tris-Cl, pH 7,5
100 mM CaCl2
1 M Sorbitol
in distilled water, sterile filtered

STC/PEG
15 ml STC
10 g PEG 4000

Stereomicroscopy and microscopy

Stereomicroscopy analysis was performed using a Zeiss Stemi SV11 and photographs were taken with a (Sony DSC-S75) digital camera and processed by PHOTOSHOP 6.0 (Adobe).

Microscopic analysis was performed using a Zeiss Axioplan 2 microscope with Nomarski optics. Excitation and emission spectra of the filters used for fluorescence microscopy: DAPI, 365nm and >397 nm; GFP, 470±20 nm and 505-530 nm; and YFP, 500±20 nm and 535±30 nm. Photomicrographs were obtained with an Axiocam HrM or Photometrics CoolSNAP HQ and the images were processed with Axiovision (Zeiss) or Metamorph (Universal Imaging Corp.) and PHOTOSHOP 6.0 (Adobe). For staining of nuclei with DAPI, Vectashield H-1200 (Vector Laboratories) was used.

***U. maydis* cell fixation**

U. maydis cells were fixed in 1% formaldehyde, CH_3OH free (Polysciences Inc.) for 30 min at room temperature. After washing with PBS buffer twice, cells were resuspended in PBS buffer and stored at 4ºC.

Nuclear intensity measurement (Snetselaar and McCann, 1997)

In order to specifically measure the nuclear DNA content of cells forming conjugation hyphae in *U. maydis*, the microdensitometry technique (Snetselaar and McCann, 1997) has been modified. The nuclei of tested cells were stained with DAPI, Vectashield H-1200 (Vector Laboratories). Stained cells were visualized by a Zeiss Axioplan 2 microscope and images were captured in the range of linear exposure and further analyzed by Metamorph (Universal Imaging Corp.). The intensities of whole nuclei of the tested cells after substraction of background cytoplasm were calculated. A FB1P_{otef}:*yfp* cell forming a small bud, grown in CM-glucose media, was used as a reference for a nucleus in the G2 phase cells as described in Snetselaar and McCann, 1997. In order to interpret the nuclear stage of the tested cells, the nuclear intensity of the tested cell was divided with that of the reference cell, obtaining the relative nuclear intensity to a nucleus in the G2 phase. Theoretically, nuclei in the G1 and G2 phase give values of approximately 0.5 and 1.0, respectively. This method was tested with the nuclei that are in G1 (two cells completing in karyokinesis but not in cytokinesis) or G2 phase. (See additional detail in Appendix 6.4).

Pheromone treatment, mating and filamentation assays.

For **pheromone treatment**, FB1 cells were grown in CM or NM media containing glucose to an OD_{600} of 0.4 -0.5 at 28°C, harvested by centrifugation at 3500 rpm for 5 min, resuspended in corresponding media containing the synthetic Mfa2 pheromone (2.5 μg/ml in DMSO) and continually rotated at 28°C for 6 or 8 hours as indicated. Cells grown in media containing identical amounts of DMSO were used as control. Conjugation hyphae forming cells were observed under the microscope.

For **charcoal mating assays** compatible strains were incubated until a density of OD_{600} approximately 0.8-1 was reached, washed once with sterile water and concentrated to an OD_{600} of approximately 3. Compatible strains were equally mixed. 5 μl of the mixture were spotted on charcoal containing CM-glucose or PD solid media plates and incubated at 22°C for 2 days.

For **filamentation assays** mutants of solopathogenic strains (SG200) were used instead of compatible strains. UECP19 and its *hum2* deletion derivative (FB1hdp1*Δhum2*) were spotted on CM-arabinose solid media containing charcoal.

Surface hydrophobicity measurement

Surface hydrophobicity was determined as contact angle based as previously described (Doehlemann *et al.* 2006). 5 μl of water containing 0.4% Evan blue dye were spotted on a 3-day old colony surface. The droplet was air-dried overnight and the diameter of the dye was measured by vernier to obtain the diameter of the contact area. The volume of the droplet and the diameter of contact area was used to calculate the contact angle.

Plant infection assay

Pathogenic development of tested strains was assayed by infection of the corn variety Early Golden Bantam (Olds Seeds, Madison, Wins.). Tested strains and their respective progenitors were cultured to an OD_{600} of 0.8-1, washed once with distilled water and concentrated in distilled water to an OD_{600} of 3. Compatible haploid strains were equally mixed prior to infection and 0.5 ml of the cell suspension were syringe-injected at the basal stem of 6-day old seedlings. The infected plants were incubated in the green house at 28°C with 14-hour light per day. Tumor formation was investigated 7 days after infection.

Flow cytometry

Flow cytometry was performed in cooperation with Ignacio Flor-Parra, Spain. *U. maydis* cells (10^5) were pelleted, washed twice with distilled water and fixed in 1 ml 70% ethanol overnight at -20ºC. After fixation, cells were washed once in 50 mM sodium citrate (pH 7.5, adjusted with acid) by centrifugation for 5 min at 4000 rpm, at 4ºC, and then resuspended in 1 ml of 50 mM sodium citrate. 25 µl RNase A (10 mg/ml) was added to obtain a final concentration of 0.25 mg/ml and incubated at 50ºC for 1 hour. Next 50 µl proteinase K (20 mg/ml) was added to obtain a final concentration of 1 mg/ml and incubated at 50ºC for another hour. Cells were stained with propidium iodide (16 µg/ml) at 4ºC for 4 hours, and then analyzed with a Coulter Epics XL-MLC.

4.3 Molecular biology standard methods

Standard molecular biology methods, such as purification, precipitation, electrophoresis of DNA or molecular cloning technique, are followed protocols described in Ausubel *et al*. and Sambrook *et al.*, (1989). The concentration of nucleic acids was determined by photometry. Photometric measurements were performed using Ultrospec 3000 pro UV/Visible Spectrophotometer or NanoDrop ND-1000 Spectrophotometer. The puritiy of nucleic acids was determined by the ratio of A_{260} to A_{280}. For the pure DNA and RNA, the ratio of A_{260} to A_{280} should be ~1.8.

4.3.1 Isolation of nucleic acids

***E. coli* plasmid minipreparation**

E. coli plasmid minipreparation was perfomed by "LYSIS BY BOILING" as previously described in Sambrook *et al.* (1989). 1.5 ml *E. coli* overnight culture was centrifuged in a 1.5- ml Eppendorf tube for 1 min at 13000 rpm. The supernatant was discarded and the cell pellet was resuspended in 350 µl of STET, then 25 µl of Lysozyme solution (10 mg/ml in 10 mM Tris-Cl, pH 8.0) was added and shaken for 5 min on a Vibrax-VXR shaker (IKA) followed by an incubation for 1 min at 95 °C. To pellet the cell debris, the *E. coli* lysate was centrifuged for 10 min at 13000 rpm, next, cell debris was removed by a sterile toothpick. To precipitate plasmid DNA, 40 µl of 3 M sodium acetate (pH 5.2) and 420 µl isopropanol were added. The mixture was incubated at room temperature for 5 min followed by centrifugation for 5 min at 13000 rpm. The supernatant was discarded and the DNA pellet was washed with 70%

ethanol and air-dried for 5 min. The DNA pellet was dissolved in 50-100 µl TE buffer with 20 µg/ml RNase A. This technique can yield 15 µg plasmid DNA per 1.5 ml overnight culture.

STET:
50 mM Tris-Cl, pH 8.0
50 mM Na_2-EDTA
8% (w/v) Saccharose
5% (v/v) Triton X-100
in $H_2O_{bid.}$

Isolation of genomic DNA from *Ustilago maydis* (Hoffman and Winston, 1987)

2 ml of *Ustilago* culture grown overnight in $YEPS_{Light}$ were centrifuged in Eppendorf tubes containing 300 mg glass beads for 2 min at 13000 rpm. The supernatant was discarded and 400 µl Ustilago lysis buffer and 500 µl phenol/chloroform (1:1) was added and shaken for 6-10 min on a Vibrax-VXR shaker (IKA). After centrifugation for 15 min at 13000 rpm 400 µl of the aqueous phase were transferred to new 1.5-ml Eppendorf tubes. After addition of 1 ml ethanol the mixture was inverted 2-3 times and incubated at room temperature for 5 min. Subsequently the mixtures were centrifuged for 15 min at 13000 rpm. The DNA pellets were washed once with 70% Ethanol and briefly air-dried. Finally, DNA pellets were dissolved in 50 µl TE/RNAse A and incubated at 55°C for 10 min. Genomic DNA was stored at - 20°C

Ustilago lysis buffer
50 mM Tris-Cl, pH 7.5
50 mM Na_2-EDTA
1% (v/v) SDS
in $H_2O_{bid.}$

***U. maydis* total RNA isolation** (Invitrogen)

Trizol reagent was used according to the manufacturer's protocol. For liquid culture, *U. maydis cells* were harvested from 10 to 50 ml of culture having a cell density of OD_{600} ~ 0.5-1. The pellet was resuspended in 1.0 ml trizol and transferred to 2-ml Eppendorf tube containing 300 mg glass beads and homogenized with a cell mill (Retsch MM200) for 5 min at 30 s^{-1}. After a 5-min incubation at room temperature, 200 µl chloroform were added, shaken for 15 s and incubated for another 2 to 3 min. The sample was centrifuged for 15 min at 11500 rpm at 4°C. The upper aqueous phase (~500 µl) was transferred to a 1.5-ml RNase-free Eppendorf tube, and RNA was precipitated by addition of 500 µl isopropanol and incubated for 10 min at room temperature. After centrifugation for 10 min at 11500 rpm at 4°C, The pellet was

washed once with 70% ethanol by centrifugation at 7500g for 5 min and air-dried. Finally, the RNA pellet was dissolved in 50-100 µl RNase-free water and incubated for 10 min at 55°C.

Total RNA isolation of *U. maydis* growing on CM solid media containing charcoal

In order to grow *U. maydis* on CM solid media containing charcoal, the culture was grown at 28°C at 200 rpm until an OD_{600} of 0.8 -1 and cells were washed once with distilled water and resuspended in 1 ml of distilled water. 400 µl of the cell suspension, or 200 µl of each compatible strain for crossing, was plated on charcoal-CM solid media and incubated for 48 hours at 22°C. *U. maydis* mycelia or cells were harvested with a sterile glass pipette and frozen in liquid nitrogen. The frozen sample was ground with a mortar and pestle prechilled in liquid nitrogen followed by homogenization with a prechilled metal bead-beater for 5 min at 30 s^{-1}. The frozen powder was transferred to 50 ml tube with Trizol reagent (10 ml per 1 gram of sample). 1 ml glass beads were added and vortexed for 20 s 10 times and stored on ice in between. Then, the sample was treated as described in "***U. maydis* total RNA isolation** (Invitrogen)"

4.3.2 Nucleic acid blotting and hybridization

DNA blotting and hybridization.

This method is modified from Southern (1975). 15 µg of genomic DNA were digested using 5U of the respective restriction enzyme in a total volume of 20 µl overnight and separated on a 1X TAE 1% agarose gel for 2 hours at 100V.

The nucleic acid fragments were transferred to a nylon membrane (Hybond-XL, Amersham Pharmacia Biotech) by capillary blotting in 0.4 M NaOH. Prior to the capillary transfer, the gel was incubated in 0.25 M HCl for DNA depurination for 15 min and neutralized in 0.4 M NaOH for another 15 min. The capillary transfer was performed overnight and DNA was cross-linked by an UV Stratalinker 1800 (Stratagene).

The membranes were hybridized with P^{32}-labelled probes. To block non-specific binding of probe, the membranes were pre-hybridized in Southern-hybridization buffer for 1 hour at 65°C. In parallel, the DNA probe fragment was labeled by

random priming with $P^{32}\alpha$-dCTP (Hartmann analytic). The DNA probe was denatured at 95°C for 5 min and quickly chilled on ice. After addition of 5 µl labeling buffer (NEB), 6 µl dNTP(-dCTP), 5 µl $P^{32}\alpha$-dCTP and 1 µl (5U) klenow fragment, the mixture was incubated at 37°C for 1 hour. Finally, the labeled probe was purified with a S-300 HR Column and denatured at 95°C for 5 min in 10 ml Southern hybridization buffer. Hybridization was performed overnight at 65°C. After two washing steps with Southern-wash buffer at 65°C for 15 min each, the membrane was wrapped in a plastic bag and exposed to a phosphor screen (Molecular dynamics) for 12-24 hours. The Analysis of the screen was performed using a Storm 840 scanner (Molecular dynamics) and processed with IMAGEQUANT (Molecular dynamics).

Southern-hybridization buffer	**Southern-wash buffer**
50.0% (v/v) 1 M Na-phosphate buffer, pH 7.0 (f.c. 0.5 M)	10.0% (v/v) 1 M Na-phosphate buffer, pH 7.0 (f.c. 0.1 M)
35.0% (v/v) 20% SDS	5.0% (v/v) 20% SDS

RNA blotting and hybridization.

In order to determine the expression level of genes, RNA blotting and hybridization was performed. Total RNA was denaturated in 1X MOPS, 0.8 M glyoxial and 50% (v/v) DMSO, incubated at 50°C for 1 hour, then separated by 1x MOPS 1% agarose gel electrophoresis for 2 hours at 80V with circulated buffer reservoir and transferred to a nylon membrane by capillary transfer.

The capillary transfer of total RNA is similar to genomic DNA. The RNA gel was saturated in 20X SSC buffer for 1 hour and blotted to a Hybond-NX membrane (Amersham Biosciences). The hybridization was similarly performed as described in "**DNA blotting and hybridization**". The Southern-hybridization and wash buffers were replaced with Northern-hybridization and wash buffers. The *hdp1* probe was generated by PCR amplification of genomic DNA of *U. maydis* 521 using primers Hdp1-cDNA-2198F and Hdp1-cDNA-2485R and *rep1* probe was ~ 500 bp *EcoR*I/*EcoR*I fragment of p238.

10X MOPS buffer

200.0 mM MOPS

80.0 mM Sodium acetate

10.0 mM Na_2-EDTA*$2H_2O$

pH was adjusted to 7.0 with 5 M NaOH

20X SSC buffer

3.0 M NaCl

0.3 M Sodium acetate *$2H_2O$

pH was adjusted to 7.0 with HCl

Northern-hybridization buffer

5.0% (v/v) 1 M Na-phosphate buffer, pH 7.0 (f.c. 50 mM)

5.0% (v/v) 1 M PIPES (f.c. 50 mM)

2.0% (v/v) 5 M NaCl (f.c. 100 mM)

25.0% (v/v) 20% SDS (f.c.5%)

0.2% (v/v) 0.5 M EDTA pH 8.0 (f.c. 1 mM)

Northern-wash buffer

5.0% (v/v) 20xSSC (f.c. 1X)

25% (v/v) 20% SDS (f.c. 5%)

4.3.3 Sequence and structure analysis

DNA sequencing technique

DNA was sequenced by an ABI 377 Automated DNA Sequencer (Perkin Elmar). DNA was purified with the QiaQuick PCR purification Kit (Qiagen). The principle of this sequencing technique is based on "DNA sequencing with chain-terminating inhibitors" (Sanger *et al.*, 1992) by use of BigDye-Kits (ABI).

The sequencing reaction was performed as follows:

BigDye Terminator v3.1 Cycle Mix	2 µl	Sequencing cycling condition
5X dilution buffer	3 µl	
sequencing primer (5 pmol/ µl)	1 µl	96 °C for 1 min
DNA (3-8 kb plasmid)	400 ng	30 cycles of 10 s at 96 °C
H_20 add to a final volume of	20 µl	4 min at 60°C

Sequencing reaction was precipitated using 10 µl 125 mM EDTA, 9 µl 3M sodium acetate (pH 4.6-4.8), 80 µl HPLC graded H_2O and 400 µl 96% ethanol per 20 µl reaction, by centrifugation for 20-30 min at 13000 rpm at room temperature followed by two wash steps with 70% ethanol. The pellet was air-dried and resuspended in 20 µl formamide with 25 mM Na_2-EDTA (pH 8.0).

Sequence and structure analysis

SEQUENCENAVIGATOR 1.0.1 (ABI): working with sequence raw data

SEQUENCHER 4.1 (Genecodes): working with sequence raw data

DNA-STRIDER 1.4 (Douglas, 1995): construction and working with plasmid or genomic DNA sequences for cloning and restriction analysis

BLAST2 (Altschul *et al.*, 1990; Altschul *et al.*, 1997; Gish and States, 1993): searching sequence similarity of interested DNA or protein sequences on Genbank database.

PFAM (Sonnhammer *et al.*, 1997): prediction of conserved domains or motifs of given protein sequences.

PSORT2 (Nakai and Horton, 1999): prediction of subcellular localizations of given protein sequences.

CLONEMANAGER (Version 7 and 8; Sci Ed Central): construction and working with plasmid or genomic DNA sequences for cloning, restriction analysis, and mainly primer design.

4.3.4 PCR techniques

Standard PCR reaction

This method is modified from Innis *et al.* (1990). A typical PCR reaction is composed of 10 ng template DNA, 1 μM of a pair of primers, 200 μM dNTPs, 1-2 U *Taq* DNA polymerase and 1 x PCR buffer (10 mM Tris-HCl, 1.5 mM $MgCl_2$, 50 mM KCl, pH 8.3) in a 50-100 μl reaction and pipette tips with filter were used to prevent cross-contaminations. The used cycling conditions typically were as follows: initial denaturation at 94 ^oC for 2 min, 30 cycles of 1) denaturation for 30 s at 94^oC, 2) annealing for 30 s at 3 to 5^oC lower than melting temperature (Tm) of the primers, and 3) elongation for 30 seconds for 1 kb of product at 72^oC, and final elongation for 7 min at 72^oC. The PCR reaction was performed using a Thermocycler PTC-100 or PTC-200 (MJ Research). PCR reactions with Phusion™ High-Fidelity DNA Polymerase were performed according to the manufacturer's protocol.

PCR generation of gene deletion constructs and eGFP fusion of *U. maydis*

The *hdp1* and *pcl12* gene deletions and the *Hdp1:eGFP*-gene fusion were performed by a PCR-based approach (Kämper, 2004). In principle, the 5' and 3' borders of the target sequence were amplified by PCR and a distinct *Sfi*I site for each fragment was incorporated via primer. The size of amplified 5' and 3' regions are approximately 1 kb for efficient recombination. The Phusion™ High-Fidelity DNA Polymerase was used to minimize the mutation rate. Optionally, amplified 5' and 3' regions were

cloned to pCR2.1-TOPO. PCR products and the resistance cassette with compatible *Sfi*I sites were digested with *Sfi*I and subsequently ligated directionally via two distinct *Sfi*I sites, providing gene deletion or GFP-gene fusion constructs. Finally, the ligated product was PCR amplified. In case of gene fusion, plasmid clones were sequenced to verify the in-frame fusion.

***hdp1* deletion (*egfp* gene and hygromycin resistance cassette)** was performed by the amplification of *hdp1*-deletion construct using primers OCP4 and OCP6 and pKO1 as a template.

***hdp1:GFP* gene fusion (*egfp* gene and hygromycin resistance cassette)** was performed by the amplification of Hdp1:egfp fusion construct using primers OCP2 and OCP4 and pFUS1 as a template.

***hdp1* deletion (clonnat resistance cassette)**

5' and 3' borders were amplified from pKO1 as described in plasmid construction, except for 5' border using primers OCP5e and OCP6, and digested with *Sfi*I and ligated to 1.4 kb clonnat resistance cassette from pUMa262. Finally the deletion construct was PCR amplified.

***pcl12* deletion (hygromycin resistance cassette)** of the primers w35um030-lb1 and w35um030-lb2 primers and the primers w35um030-rb1 and w35um030-rb2 primers were used to PCR amplify the 5' and 3' borders of the *pcl12* gene from genomic DNA of *U. maydis* 521, respectively. PCR fragments were purified, digested with *Sfi*I, gel purified and subsequently ligated to a 1.9 kb *Sfi*I fragment of pBS-hhn that harbors the hygromycin resistant cassette. The 4 kb ligation product was used as a template for amplification of the *pcl12* deletion construct with the primers w35um030-lb1-nested and w35um030-rb2-nested.

***pcl12* deletion (clonnat resistance cassette)** was performed as described in "*pcl12* deletion (hygromycin resistant cassette)", except that 5' and 3' borders were ligated to 1.4 kb clonnat resistance cassette from pUMa262.

$hdp1_{AA}$ construction

***hdp1*$_{AA}$ construction** was performed by two separated PCR amplifications of the plasmid Pcrg-gORF-*hdp1*$_{wt}$ using two pairs of primers; first F-OvG211-120 and O-hdp1WF-AAr and; second O-hdp1WF-AAf and R-OVG211-120. Both PCR products were gel purified with a gel purification kit (QIAGEN) in order to prevent the contamination of template plasmid. Then, the two PCR products were used as template for PCR amplification of full-length gORF-*hdp1*$_{AA}$ using pairs of F-OvG211-120 and R-OVG211-120 primers.

Full-length, RNA ligase-mediated Rapid Amplification of 5' and 3' cDNA Ends (RLM-RACE)

In order to clone 5' and 3' fragments of *hdp1* cDNA, total RNA of AB31 grown in array medium containing arabinose for 5 hours was isolated and purified with the RNeasy Kit (QIAGEN). To amplify 5' and 3' end of *hdp1* cDNA via RLM-RACE, the GeneRACER Kit (Invitrogen) was used according to the manufacturer's protocol. In case of 5' RACE, reverse GSP and reverse GSP nested primer are R-E3 and N-R-E2, respectively. In case of 3' RACE, forward GSP primer is F-E1 primer. The PCR products were purified by QiaQuick PCR purification Kit and subsequently cloned into pCR2.1-TOPO. The respective clones were subjected to DNA sequencing.

Real-time Reverse Transcription -PCR

Total RNA was purified using the RNeasy Kit (QIAGEN) and treated with DNA-freeTM (Ambion) according to the manufacturer's protocol in order to remove genomic DNA contamination. First strand synthesis was performed using the SuperScript III first strand synthesis SuperMix (Invitrogen) according to the manufacturer's protocol. 300 to 500 ng of purified total RNA were used as a template. Oligo-dT oligos were used as a primer and the reaction was incubated at 50^{o}C for 50 minutes.

Real-time PCR was performed on a Bio-Rad iCycler system using the Platinum SYBR Green qPCR SuperMix-UDG (Invitrogen) according to the manufacturer's protocol. For the PCR reaction, 1-3 µl of the first strand reaction was used as template. Fluorescein (1 µl of 1 µM stock solution in 50 µl PCR reaction) from Biorad was used as a calibration dye. Cycling conditions were as follows: 95^{o}C for 30 s, 45 cycles of 15 s at 95^{o}C, 30 s at 62^{o}C, and 30 s at 72^{o}C followed by, in order to calculate the melting curve, 100 cycles of 7 seconds starting at 70^{o}C with 0.2^{o}C increasing per cycle. The threshold cycle above background was calculated using Bio-Rad iCycler software. The relative expression values were calculated by the Bio-Rad Gene Expression Macro program from Biorad. Forward (F) and reverse (R) primers used for detection and for internal control were described in 4.1.2.

4.4 DNA microarray analyses

U. maydis DNA Microarray analyses were used to compare the expression profile of AB31 and AB31*Δhdp1* 12-hour post induction and those of AB32 and AB32*Pcrg1:hdp1* 5-and 12-hours post induction.

Growth conditions

AB31 and AB31*Δhdp1* were grown in duplicate of 50 ml of glucose containing array-minimal media at 28°C at 200 rpm to a density of OD_{600} ~ 0.5 and harvested by centrifugation for 5 min at 3500 rpm at room temperature. Cells were washed once with arabinose containing array-minimal media and continually grown for 12 hours, harvested by centrifugation for 5 min at 3500 rpm and quick frozen in liquid nitrogen. Samples were stored at -80°C or used for RNA isolation. In case of AB32 and AB32*Pcrg1:hdp1*, the experiment was performed as described previously. The samples were harvested 5 and 12 hours after shifting to arabinose containing array-minimal media.

RNA isolation and purification

RNA isolation was performed as described in **"*U. maydis* total RNA isolation"** and purified using the RNeasy Kit (Qiagen) according to the manufacturer's protocol. Prior to first and second strand cDNA synthesis, the quality of total RNA was examined the Bioanalyzer 2100 and RNA 6000Nano reagent (Agilent).

cDNA synthesis via affymetrix

First and second strand cDNA synthesis was performed as described in "GeneChip® Expression Analysis Technical Mannual"

For **first strand cDNA synthesis**, 5 μg of total RNA and 2 μl T7-oligo(dT) primer, 50 μM in 12 μl reaction were incubated at 70°C for 10 min, then quick spun down and stored on ice. 4 μl 5X First-strand cDNA buffer, 2 μl 0.1 M DTT and 1 μl 10 mM dNTP mix were added and incubated at 42°C for 2 min. 1 μl of SuperScript II RT (Gibco) was added into the reaction, mixed and incubated at 42°C for 1 hour.

For **the second strand cDNA synthesis**, 91 μl RNase free H_2O, 30μl 5X Second-Strand Reaction buffer, 3 μl 10 mM dNTP mix, 1 μl 10U/μl *E. coli* DNA Ligase, 4 μl 10U/μl *E. coli* DNA PolymeraseI and 1 μl 2U/μl *E. coli* RNase H were added into the first strand cDNA reaction, briefly spun down and incubated at 16°C for 2 hours. After that, the T4 DNA Polymerase was added and continually incubated at 16°C for 5 min. Finally 10 μl of 0.5M EDTA was added in order to stop reaction.

Cleanup of double strand cDNA

All components in this step were supplied with the GeneChip® Sample Cleanup Module (Qiagen). 600 µl cDNA Binding buffer was added to the 162 µl cDNA reaction, mixed, applied to a cDNA Cleanup Spin Column and centrifuged for 1 min at 10000 rpm at room temperature. The flow-through was discarded and 750 µl cDNA Wash Buffer was added and centrifuged for 1 min at 10000 rpm at room temperature. The flow-through was discarded and centrifuged again for 5 min at 13000 rpm at room temperature with opened cap. The column was transferred to 1.5-ml collecting tube and 14 µl Elution Buffer was added into the column, incubated for 1 min and centrifuged for 1 min at 13000 rpm at room temperature. The quality of the cDNA was examined using the Bioanalyzer 2100 and the RNA 6000Nano reagent (Agilent).

cRNA Synthesis- in vitro transcription

The cRNA Synthesis- *in vitro* transcription was perormed using Enzo® BioArray™ HighYield™ RNA Transcript labelling Kit. The 12 µl double strand cDNA , 4 µl 10X HY Reaction Buffer, 4 µl 10X Biotin-Labeled Ribonucleotides ,4 µl DTT ,4 µl 10X RNase Inhibitor Mix and 2 µl 20X T7 RNA Polymerase were filled with RNase-free H_2O to 40 µl final volume. The reaction was gently mixed, spun down briefly and incubated in a Thermomixer at 37^{o}C for 16 hours, with 750 rpm shaking for 30 s for every 30 min.

Cleanup of cRNA

All components in this step were supplied with the GeneChip® Sample Cleanup Module (Qiagen). 60 µl RNase-free H_2O was added to the in vitro transcription reaction and mixed by vortexing for 3 s 350µl IVT cRNA Binding Buffer was added and mixed by vortexing for 3 s 250 µl absolute ethanol was added into the mixture, mixed by pipetting, applied to the IVT cRNA Cleanup Spin Column and centrifuged for 15 s at 10000 rpm at room temperature. 500 µl of 80% ethanol was added into the column and centrifuged for 15 s at 10000 rpm at room temperature.

The flow-through was discarded and centrifuged again for 5 min at 13000 rpm at room temperature with opened cap. The column was transferred to a 1.5-ml collecting tube and 11 µl RNase-free H_2O was added into the column and centrifuged for 1 min at 13000 rpm at room temperature. Again, 10 µl RNase-free H_2O was added into the column and centrifuged for 1 min at 13000 rpm at room temperature. The quality of

the cRNA was examined using a Bioanalyzer 2100 and RNA 6000Nano reagent (Agilent).

cRNA Fragmentation for target preparation.

5X Fragmentation buffer was supplied with the GeneChip® Sample Cleanup Module (Qiagen). This step is critical in obtaining optimal assay sensitivity. Up to 21 µl of 20 µg cRNA and 8 µl 5X Fragmentation buffer were filled with RNase-free H2O to 40 µl final volume. The reaction was incubated at 94°C for 35 min followed by stored on ice. The quality of fragmented-cRNA was examined by 2100 Bioanalyzer and RNA 6000 Nano reagent (Agilent).

Microarray hybridization

The Array used in this study is a custom Affymetrix array that covers approximately 90% of the predicted 7050 *U. maydis* genes. First, 15 µg fragmented cRNA were mixed with 15 µl 3 nM Control Oligonucleotide B2, 15 µl 20X Eukaryotic Hybridization Control, 3 µl Herring Sperm DNA (10 mg/ml), 3 µl acetylated BSA and 150 µl 2X Hybridization buffer and filled with RNase-free H_2O to 300 µl final volume. The hybridization cocktail was heated at 99°C for 5 min, and then shifted to 45°C for 5 min. Next, the cocktail was centrifuged for 5 min at 13000 rpm at room temperature. To equilibrate an array, 200 µl 1X hybridization buffer was filled into the DNA chip and incubated at 45°C for 10 min with rotation. After equilibration, the solution was removed and refilled with 250 µl of the hybridization cocktail. The array was placed into the hybridization oven and hybridized at 45°C with 60 rpm for 16 hours. The hybridization oven used during this study is the GeneChip® Hybridization Oven 640.

Microarray detection reaction

After 16 hours of hybridization, the hybridization cocktail was removed from the hybridized array and refilled with 300 µl wash buffer (Wash A). The detection reaction was followed by the washing and staining procedure 2: antibody amplification stain for eukaryotic target of the protocol from Affymetrix. The staining reagents used were SAPE stain solution composed of 300 µl 2x MES stain buffer, 24 µl BSA (50 mg/ml), 6 µl Streptavidin Phycoerythrin (1 mg/ml) in a final volume of 600 µl and antibody solution composed of 300 µl 2x MES stain buffer, 24 µl BSA (50 mg/ml), 6 µl normal Goat IgG (10 mg/ml) and biotinylated antibody (0.5 mg/ml). The

Fluidics station 400 and EuGE-WS2v4-Program were used for sample washing and staining.

Microarray analysis

After washing and staining, the array was scanned by the Affymetrix GeneChip® Scanner. The data were processed, normalized and calculated expression values were acquired using AFFYMETRIX MICROARRAY SUITE 5.0 (Affymetrix). The array comparisons were calculated by dChip 2004 (Li and Hung Wong, 2001). Further data analysis was performed using the Biconductor R package (http://www.bioconductor.org/). Expression values were converted to $\log_2$ (value + 1). Limma (Smyth, 2004) was used for the expression analysis of differentially regulated genes.

Using lmFit (Linear Model for Series of Arrays), a linear model was fitted to the $\log_2$ (value + 1) expression data for each probe, and contrasts.fit (Compute Contrasts from Linear Model Fit) was used to obtain coefficients and standard errors for contrasts of the coefficients of the original model. An empirical Bayes method, ebayes (Empirical Bayes Statistics for Differential Expression), was used to rank genes in order of evidence for differential expression. A table of the top-ranked genes from the linear model fit was extracted by topTable (Table of Top Genes from Linear Model Fit). The P-values for the coefficients/contrasts of interest were adjusted for multiple testing by the Benjamini and Hochberg (1995) method fdr.

5 References

ALTSCHUL, S. F., GISH, W., MILLER, W., MYERS, E. W., and LIPMAN, D. J. (1990). Basic local alignment search tool. *J Mol Biol* **215**, 403-410.

ALTSCHUL, S. F., MADDEN, T. L., SCHAFFER, A. A., ZHANG, J., ZHANG, Z., MILLER, W., and LIPMAN, D. J. (1997). Gapped BLAST and PSI-BLAST: a new generation of protein database search programs. *Nucleic Acids Res* **25**, 3389-3402.

ANDREWS, D. L., EGAN, J. D., MAYORGA, M. E., and GOLD, S. E. (2000). The *Ustilago maydis ubc4* and *ubc5* genes encode members of a MAP kinase cascade required for filamentous growth. *Mol Plant Microbe Interact* **13**, 781-786.

ARNAISE, S., ZICKLER, D., POISIER, C., and DEBUCHY, R. (2001). pah1: a homeobox gene involved in hyphal morphology and microconidiogenesis in the filamentous ascomycete *Podospora anserina*. *Mol Microbiol* **39**, 54-64.

AUSUBEL, M. A., AUSUBEL, M. A., BRENT, R., KINGSTON, R. E., MOORE, D. D., SEIDMANN, J. G., and SMITH, J. A., eds.*Current protocols in molecular biology* (John Wiley & Sons, Inc.).

BANUETT, F., and HERSKOWITZ, I. (1989). Different *a* alleles of *Ustilago maydis* are necessary for maintenance of filamentous growth but not for meiosis. *Proc Natl Acad Sci USA* **86**, 5878-5882.

BANUETT, F., and HERSKOWITZ, I. (1994a). Identification of fuz7, a *Ustilago maydis* MEK/MAPKK homolog required for a-locus-dependent and -independent steps in the fungal life cycle. *Genes Dev* **8**, 1367-1378.

BANUETT, F., and HERSKOWITZ, I. (1994b). Morphological transitions in the life cycle of *Ustilago maydis* and their genetic control by the *a* and *b* loci. *Exp Mycology* **18**, 247-266.

BANUETT, F., and HERSKOWITZ, I. (1996). Discrete developmental stages during teliospore formation in the corn smut fungus, *Ustilago maydis*. *Development* **122**, 2965-2976.

BANUETT, F., and HERSKOWITZ, I. (2002). Bud morphogenesis and the actin and microtubule cytoskeletons during budding in the corn smut fungus, *Ustilago maydis*. *Fungal Genet Biol* **37**, 149-170.

BÖLKER, M. (2001). *Ustilago maydis*--a valuable model system for the study of fungal dimorphism and virulence. *Microbiology* **147**, 1395-1401.

BÖLKER, M., GENIN, S., LEHMLER, C., and KAHMANN, R. (1995). Genetic regulation of mating, and dimorphism in *Ustilago maydis*. *Can J Bot* **73**, 320-325.

BÖLKER, M., URBAN, M., and KAHMANN, R. (1992). The *a* mating type locus of *U. maydis* specifies cell signaling components. *Cell* **68**, 441-450.

BORTFELD, M., AUFFARTH, K., KAHMANN, R., and BASSE, C. W. (2004). The Ustilago maydis a2 mating-type locus genes lga2 and rga2 compromise pathogenicity in the absence of the mitochondrial p32 family protein Mrb1. *Plant Cell* **16**, 2233-2248.

BRACHMANN, A. (2001) Die frühe Infektionsphase von *Ustilago maydis*: Genregulation durch das bE/bW-Heterodimer, Ludwig-Maximilian-University, Munich.

BRACHMANN, A., KÖNIG, J., JULIUS, C., and FELDBRÜGGE, M. (2004). A reverse genetic approach for generating gene replacement mutants in *Ustilago maydis*. *Mol Genet Genomics* **272**, 216-226.

BRACHMANN, A., SCHIRAWSKI, J., MÜLLER, P., and KAHMANN, R. (2003). An unusual MAP kinase is required for efficient penetration of the plant surface by *Ustilago maydis*. *EMBO J* **22**, 2199-2210.

BRACHMANN, A., WEINZIERL, G., KÄMPER, J., and KAHMANN, R. (2001). Identification of genes in the bW/bE regulatory cascade in *Ustilago maydis*. *Mol Microbiol* **42**, 1047-1063.

BREFORT, T., MULLER, P., and KAHMANN, R. (2005). The high-mobility-group domain transcription factor Rop1 is a direct regulator of prf1 in *Ustilago maydis*. *Eukaryot Cell* **4**, 379-391.

BUSSINK, H. J., and OSMANI, S. A. (1998). A cyclin-dependent kinase family member (PHOA) is required to link developmental fate to environmental conditions in Aspergillus nidulans. *EMBO J* **17**, 3990-4003.

CARROLL, A. S., and O'SHEA, E. K. (2002). Pho85 and signaling environmental conditions. *Trends Biochem Sci* **27**, 87-93.

CASSELTON, L. A., and OLESNICKY, N. S. (1998). Molecular genetics of mating recognition in basidiomycete fungi. *Microbiol Mol Biol Rev* **62**, 55-70.

CASTILLO-LLUVA, S., ALVAREZ-TABARES, I., WEBER, I., STEINBERG, G., and PEREZ-MARTIN, J. (2007). Sustained cell polarity and virulence in the phytopathogenic fungus *Ustilago maydis* depends on an essential cyclin-dependent kinase from the Cdk5/Pho85 family. *J Cell Sci* **120**, 1584-1595.

CASTILLO-LLUVA, S., GARCIA-MUSE, T., and PEREZ-MARTIN, J. (2004). A member of the Fizzy-related family of APC activators is regulated by cAMP and is required at different stages of plant infection by *Ustilago maydis*. *J Cell Sci* **117**, 4143-4156.

CASTILLO-LLUVA, S., and PEREZ-MARTIN, J. (2005). The induction of the mating program in the phytopathogen Ustilago maydis is controlled by a G1 cyclin. *Plant Cell* **17**, 3544-3560.

CHRISTENSEN, J. J. (1963). Corn smut induced by *Ustilago maydis*. *Amer Phytopathol Soc Monogr* **2**.

COHEN, S. N., CHANG, A. C., and HSU, L. (1972). Nonchromosomal antibiotic resistance in bacteria: genetic transformation of *Escherichia coli* by R-factor DNA. *Proc Natl Acad Sci U S A* **69**, 2110-2114.

DHAVAN, R., and TSAI, L. H. (2001). A decade of CDK5. *Nat Rev Mol Cell Biol* **2**, 749-759.

DOEHLEMANN, G., BERNDT, P., and HAHN, M. (2006). Different signalling pathways involving a Galpha protein, cAMP and a MAP kinase control germination of *Botrytis cinerea* conidia. *Mol Microbiol* **59**, 821-835.

DOU, X., WU, D., AN, W., DAVIES, J., HASHMI, S. B., UKIL, L., and OSMANI, S. A. (2003). The PHOA and PHOB cyclin-dependent kinases perform an essential function in *Aspergillus nidulans*. *Genetics* **165**, 1105-1115.

DOUGLAS, S. E. (1995). DNA Strider. An inexpensive sequence analysis package for the Macintosh. *Mol Biotechnol* **3**, 37-45.

DÜRRENBERGER, F., WONG, K., and KRONSTAD, J. W. (1998). Identification of a cAMP-dependent protein kinase catalytic subunit required for virulence and morphogenesis in *Ustilago maydis*. *Proc Natl Acad Sci U S A* **95**, 5684-5689.

ESPINOZA, F. H., OGAS, J., HERSKOWITZ, I., and MORGAN, D. O. (1994). Cell cycle control by a complex of the cyclin HCS26 (PCL1) and the kinase PHO85. *Science* **266**, 1388-1391.

FINKERNAGEL, F. (2007) *in silico*-DNA. Bindemotivsuche in *Ustilago maydis*: DNA-Bindemotiv des b-induzierten Transkriptionsfaktors Biz1, Philipps-Universität, Marburg/Lahn.

FLOR-PARRA, I., CASTILLO-LLUVA, S., and PEREZ-MARTIN, J. (2007). Polar Growth in the Infectious Hyphae of the Phytopathogen *Ustilago maydis* Depends on a Virulence-Specific Cyclin. *Plant Cell*.

FLOR-PARRA, I., VRANES, M., KAMPER, J., and PEREZ-MARTIN, J. (2006). Biz1, a zinc finger protein required for plant invasion by *Ustilago maydis*, regulates the levels of a mitotic cyclin. *Plant Cell* **18**, 2369-2387.

GARCIA-MUSE, T., STEINBERG, G., and PEREZ-MARTIN, J. (2003). Pheromone-induced G2 arrest in the phytopathogenic fungus *Ustilago maydis*. *Eukaryot Cell* **2**, 494-500.

GARCIA-MUSE, T., STEINBERG, G., and PEREZ-MARTIN, J. (2004). Characterization of B-type cyclins in the smut fungus *Ustilago maydis*: roles in morphogenesis and pathogenicity. *J Cell Sci* **117**, 487-506.

GARRIDO, E., and PEREZ-MARTIN, J. (2003). The crk1 gene encodes an Ime2-related protein that is required for morphogenesis in the plant pathogen *Ustilago maydis*. *Mol Microbiol* **47**, 729-743.

GARRIDO, E., VOSS, U., MULLER, P., CASTILLO-LLUVA, S., KAHMANN, R., and PEREZ-MARTIN, J. (2004). The induction of sexual development and virulence in the smut fungus *Ustilago maydis* depends on Crk1, a novel MAPK protein. *Genes Dev* **18**, 3117-3130.

GILLISSEN, B., BERGEMANN, J., SANDMANN, C., SCHRÖER, B., BÖLKER, M., and KAHMANN, R. (1992). A two-component regulatory system for self/non-self recognition in *Ustilago maydis*. *Cell* **68**, 647-657.

GISH, W., and STATES, D. J. (1993). Identification of protein coding regions by database similarity search. *Nat Genet* **3**, 266-272.

GOLD, S., DUNCAN, G., BARRETT, K., and KRONSTAD, J. (1994). cAMP regulates morphogenesis in the fungal pathogen *Ustilago maydis*. *Genes-Dev* **8**, 2805-2816.

GOLD, S. E., BROGDON, S. M., MAYORGA, M. E., and KRONSTAD, J. W. (1997). The *Ustilago maydis* regulatory subunit of a cAMP-dependent protein kinase is required for gall formation in maize. *Plant-Cell* **9**, 1585-1594.

HARTMANN, H. A., KAHMANN, R., and BÖLKER, M. (1996). The pheromone response factor coordinates filamentous growth and pathogenicity in *Ustilago maydis*. *EMBO J* **15**, 1632-1641.

HARTMANN, H. A., KRUGER, J., LOTTSPEICH, F., and KAHMANN, R. (1999). Environmental signals controlling sexual development of the corn smut fungus *Ustilago maydis* through the transcriptional regulator prf1. *Plant Cell* **11**, 1293-1306.

HEIMAN, M. G., and WALTER, P. (2000). Prm1p, a pheromone-regulated multispanning membrane protein, facilitates plasma membrane fusion during yeast mating. *J Cell Biol* **151**, 719-730.

HERSKOWITZ, I., PARK, H. O., SANDERS, S., VALTZ, N., and PETER, M. (1995). Programming of cell polarity in budding yeast by endogenous and exogenous signals. *Cold Spring Harb Symp Quant Biol* **60**, 717-727.

HEWALD, S., LINNE, U., SCHERER, M., MARAHIEL, M. A., KAMPER, J., and BOLKER, M. (2006). Identification of a gene cluster for biosynthesis of mannosylerythritol lipids in the basidiomycetous fungus *Ustilago maydis*. *Appl Environ Microbiol* **72**, 5469-5477.

HIRST, K., FISHER, F., MCANDREW, P. C., and GODING, C. R. (1994). The transcription factor, the Cdk, its cyclin and their regulator: directing the transcriptional response to a nutritional signal. *EMBO J* **13**, 5410-5420.

HOFFMAN, C. S., and WINSTON, F. (1987). A ten-minute DNA preparation from yeast efficiently releases autonomous plasmids for transformation of *E. coli*. *Gene* **57**, 267-272.

HOLLIDAY, R. (1974). *Ustilago maydis*. In Handbook of Genetics, R. C. King, ed. (New York, USA, Plenum Press), pp. 575-595.

HUYER, G., KISTLER, A., NOUVET, F. J., GEORGE, C. M., BOYLE, M. L., and MICHAELIS, S. (2006). *Saccharomyces cerevisiae* a-factor mutants reveal residues critical for processing, activity, and export. *Eukaryot Cell* **5**, 1560-1570.

IMAI, Y., and YAMAMOTO, M. (1994). The fission yeast mating pheromone P-factor: its molecular structure, gene structure, and ability to induce gene expression and G1 arrest in the mating partner. *Genes Dev* **8**, 328-338.

INNIS, M. A., GELFAND, D. H., SNINSKY, J. J., and WHITE, T. J., eds. (1990). *PCR Protocols: a guide to methods and applications.* (San Diego, USA, Academic Press).

JACOBS, C. W., MATTICHAK, S. J., and KNOWLES, J. F. (1994). Budding patterns during the cell cycle of the maize smut pathogen *Ustilago maydis*. *Can J Bot* **72**, 1675-1680.

KAFFARNIK, F., MÜLLER, P., LEIBUNDGUT, M., KAHMANN, R., and FELDBRÜGGE, M. (2003). PKA and MAPK phosphorylation of Prf1 allows promoter discrimination in *Ustilago maydis*. *Embo J* **22**, 5817-5826.

KAFFMAN, A., HERSKOWITZ, I., TJIAN, R., and O'SHEA, E. K. (1994). Phosphorylation of the transcription factor PHO4 by a cyclin-CDK complex, PHO80-PHO85. *Science* **263**, 1153-1156.

KAHMANN, R., and KÄMPER, J. (2004). *Ustilago maydis*: how its biology relates to pathogenic development. *New Phytologist* **164**, 31-42.

KÄMPER, J. (2004). A PCR-based system for highly efficient generation of gene replacement mutants in *Ustilago maydis*. *Mol Genet Genomics* **271**, 103-110.

KÄMPER, J., REICHMANN, M., ROMEIS, T., BÖLKER, M., and KAHMANN, R. (1995). Multiallelic recognition: nonself-dependent dimerization of the bE and bW homeodomain proteins in *Ustilago maydis*. *Cell* **81**, 73-83.

KETCHUM, C. J., SCHMIDT, W. K., RAJENDRAKUMAR, G. V., MICHAELIS, S., and MALONEY, P. C. (2001). The yeast a-factor transporter Ste6p, a member of the ABC superfamily, couples ATP hydrolysis to pheromone export. *J Biol Chem* **276**, 29007-29011.

KOTHE, E. (1996). Tetrapolar fungal mating types: sexes by the thousands. *FEMS Microbiol Rev* **18**, 65-87.

LI, C., and HUNG WONG, W. (2001). Model-based analysis of oligonucleotide arrays: model validation, design issues and standard error application. *Genome Biol* **2**, RESEARCH0032.

MARTINEZ-ESPINOZA, A. D., RUIZ-HERRERA, J., LEON-RAMIREZ, C. G., and GOLD, S. E. (2004). MAP kinase and cAMP signaling pathways modulate the pH-induced yeast-to-mycelium dimorphic transition in the corn smut fungus *Ustilago maydis*. *Curr Microbiol* **49**, 274-281.

MAYORGA, M. E., and GOLD, S. E. (1999). A MAP kinase encoded by the *ubc3* gene of *Ustilago maydis* is required for filamentous growth and full virulence. *Mol Microbiol* **34**, 485-497.

MAYORGA, M. E., and GOLD, S. E. (2001). The ubc2 gene of *Ustilago maydis* encodes a putative novel adaptor protein required for filamentous growth, pheromone response and virulence. *Mol Microbiol* **41**, 1365-1379.

MEASDAY, V., MOORE, L., OGAS, J., TYERS, M., and ANDREWS, B. (1994). The PCL2 (ORFD)-PHO85 cyclin-dependent kinase complex: a cell cycle regulator in yeast. *Science* **266**, 1391-1395.

MEASDAY, V., MOORE, L., RETNAKARAN, R., LEE, J., DONOVIEL, M., NEIMAN, A. M., and ANDREWS, B. (1997). A family of cyclin-like proteins that interact with the Pho85 cyclin-dependent kinase. *Mol Cell Biol* **17**, 1212-1223.

MÜLLER, P., AICHINGER, C., FELDBRÜGGE, M., and KAHMANN, R. (1999). The MAP kinase kpp2 regulates mating and pathogenic development in *Ustilago maydis*. *Mol Microbiol* **34**, 1007-1017.

MÜLLER, P., WEINZIERL, G., BRACHMANN, A., FELDBRÜGGE, M., and KAHMANN, R. (2003). Mating and pathogenic development of the Smut fungus *Ustilago maydis* are regulated by one mitogen-activated protein kinase cascade. *Eukaryot Cell* **2**, 1187-1199.

NAKAI, K., and HORTON, P. (1999). PSORT: a program for detecting sorting signals in proteins and predicting their subcellular localization. *Trends Biochem Sci* **24**, 34-36.

OH, C. S., TOKE, D. A., MANDALA, S., and MARTIN, C. E. (1997). ELO2 and ELO3, homologues of the *Saccharomyces cerevisiae* ELO1 gene, function in fatty acid elongation and are required for sphingolipid formation. *J Biol Chem* **272**, 17376-17384.

PEREZ-MARTIN, J., CASTILLO-LLUVA, S., SGARLATA, C., FLOR-PARRA, I., MIELNICHUK, N., TORREBLANCA, J., and CARBO, N. (2006). Pathocycles: *Ustilago maydis* as a model to study the relationships between cell cycle and virulence in pathogenic fungi. *Mol Genet Genomics* **276**, 211-229.

REGENFELDER, E., SPELLIG, T., HARTMANN, A., LAUENSTEIN, S., BÖLKER, M., and KAHMANN, R. (1997). G proteins in *Ustilago maydis*: Transmission of multiple signals? *Embo Journal* **16**, 1934-1942.

ROMEIS, T., BRACHMANN, A., KAHMANN, R., and KÄMPER, J. (2000). Identification of a target gene for the bE/bW homeodomain protein complex in *Ustilago maydis*. *Mol Microbiol* **37**, 54-66.

RUIZ-HERRERA, J., and MARTINEZ-ESPINOZA, A. D. (1998). The fungus *Ustilago maydis*, from the aztec cuisine to the research laboratory. *Int Microbiol* **1**, 149-158.

SAMBROOK, J., FRISCH, E. F., and MANIATIS, T. (1989). *Molecular Cloning: A Laboratory Manual* (Cold Spring Harbour, New York, Cold Spring Harbour Laboratory Press).

SANGER, F., NICKLEN, S., and COULSON, A. R. (1992). DNA sequencing with chain-terminating inhibitors. 1977. *Biotechnology* **24**, 104-108.

SCHERER, M., HEIMEL, K., STARKE, V., and KÄMPER, J. (2006). The Clp1 protein is required for clamp formation and pathogenic development of *Ustilago maydis*. *Plant Cell* **18**, 2388-2401.

SCHLESINGER, R., KAHMANN, R., and KÄMPER, J. (1997). The homeodomains of the heterodimeric bE and bW proteins of *Ustilago maydis* are both critical for function. *Mol Gen Genet* **254**, 514-519.

SCHNEIDER, K. R., SMITH, R. L., and O'SHEA, E. K. (1994). Phosphate-regulated inactivation of the kinase PHO80-PHO85 by the CDK inhibitor PHO81. *Science* **266**, 122-126.

SCHULZ, B., BANUETT, F., DAHL, M., SCHLESINGER, R., SCHÄFER, W., MARTIN, T., HERSKOWITZ, I., and KAHMANN, R. (1990). The *b* alleles of *U. maydis*, whose combinations program pathogenic development, code for polypeptides containing a homeodomain-related motif. *Cell* **60**, 295-306.

SGARLATA, C., and PEREZ-MARTIN, J. (2005a). Inhibitory phosphorylation of a mitotic cyclin-dependent kinase regulates the morphogenesis, cell size and virulence of the smut fungus *Ustilago maydis*. *J Cell Sci* **118**, 3607-3622.

SGARLATA, C., and PEREZ-MARTIN, J. (2005b). The cdc25 phosphatase is essential for the G2/M phase transition in the basidiomycete yeast *Ustilago maydis*. *Mol Microbiol* **58**, 1482-1496.

SMYTH, G.K. (2004). Linear models and empirical Bayes methods for assessing differential expression in microarray experiments. *Stat. Appl. Genet. Mol. Biol.* **3,** Article 3.

SNETSELAAR, K. M., and MCCANN, M. P. (1997). Using Microdensitometry to Correlate Cell Morphology with the Nuclear Cycle in *Ustilago maydis*. *Mycologia* **89**, 689-697.

SNETSELAAR, K. M., and MIMS, C. W. (1992). Sporidial fusion and infection of maize seedlings by the smut fungus *Ustilago maydis*. *Mycologia* **84**, 193-203.

SNETSELAAR, K. M., and MIMS, C. W. (1993). Infection of maize stigmas by *Ustilago maydis*: Light and electron microscopy. *Phytopathology* **83**, 843.

SNETSELAAR, K. M., and MIMS, C. W. (1994). Light and electron microscopy of *Ustilago maydis* hyphae in maize. *Mycol Res* **98**, 347-355.

SONNHAMMER, E. L., EDDY, S. R., and DURBIN, R. (1997). Pfam: a comprehensive database of protein domain families based on seed alignments. *Proteins* **28**, 405-420.

SOUTHERN, E. M. (1975). Detection of specific sequences among DNA fragments separated by gel electrophoresis. *J Mol Biol* **98**, 503-517.

STEINBERG, G., WEDLICH-SOLDNER, R., BRILL, M., and SCHULZ, I. (2001). Microtubules in the fungal pathogen *Ustilago maydis* are highly dynamic and determine cell polarity. *J Cell Sci* **114**, 609-622.

TANAKA, K., and OKAYAMA, H. (2000). A pcl-like cyclin activates the Res2p-Cdc10p cell cycle "start" transcriptional factor complex in fission yeast. *Mol Biol Cell* **11**, 2845-2862.

TEERTSTRA, W. R., DEELSTRA, H. J., VRANES, M., BOHLMANN, R., KAHMANN, R., KÄMPER, J., and WÖSTEN, H. A. (2006). Repellents have functionally replaced hydrophobins in mediating attachment to a hydrophobic surface and in formation of hydrophobic aerial hyphae in *Ustilago maydis*. *Microbiology* **152**, 3607-3612.

TOH-E, A., TANAKA, K., UESONO, Y., and WICKNER, R. B. (1988). PHO85, a negative regulator of the PHO system, is a homolog of the protein kinase gene, CDC28, of *Saccharomyces cerevisiae*. *Mol Gen Genet* **214**, 162-164.

TORRES-GUZMAN, J. C., and DOMINGUEZ, A. (1997). HOY1, a homeo gene required for hyphal formation in *Yarrowia lipolytica*. *Mol Cell Biol* **17**, 6283-6293.

TSUKUDA, T., CARLETON, S., FOTHERINGHAM, S., and HOLLOMAN, W. K. (1988). Isolation and characterization of an autonomously replicating sequence from *Ustilago maydis*. *Mol Cell Biol* **8**, 3703-3709.

URBAN, M., KAHMANN, R., and BÖLKER, M. (1996a). Identification of the pheromone response element in *Ustilago maydis*. *Mol Gen Genet* **251**, 31-37.

URBAN, M., KAHMANN, R., and BÖLKER, M. (1996b). The biallelic *a* mating type locus of *Ustilago maydis*: remnants of an additional pheromone gene indicate evolution from a multiallelic ancestor. *Mol Gen Genet* **250**, 414-420.

VRANES, M. (2006) Transkriptom-Analyse der frühen Infektionsphase von *Ustilago maydis*: Identifikation neuer pathogenitätsrelevanter Gene, Philipps-Universität, Marburg/Lahn.

WEINZIERL, G. (2001) Isolierung und Charakterisierung von Komponenten der b-vermittelten Regulationskaskade in *Ustilago maydis*, Philipps-Universität marburg, Marburg.

WÖSTEN, H. A., BOHLMANN, R., ECKERSKORN, C., LOTTSPEICH, F., BÖLKER, M., and KAHMANN, R. (1996). A novel class of small amphipathic peptides affect aerial hyphal growth and surface hydrophobicity in *Ustilago maydis*. *EMBO J* **15**, 4274-4281.

YUAN, W. M., GENTIL, G. D., BUDDE, A. D., and LEONG, S. A. (2001). Characterization of the *Ustilago maydis sid2* gene, encoding a multidomain peptide synthetase in the ferrichrome biosynthetic gene cluster. *J Bacteriol* **183**, 4040-4051.

ZARNACK, K. (2006) Die Auswirkung der posttranslationellen Aktivierung des Transkriptionsfaktors Prf1 auf die Pheromonantwort in *Ustilago maydis*, Philipps-Universität, Marburg/Lahn.

6 Appendixes

Appendix 6.1 cDNA sequence of *hdp1*

cDNA sequence of *hdp1* is derived from 5' and 3' Rapid amplification of cDNA end (5'-3' RACE). The length of 5' and 3' untranslated regions are 648 and 69 nucleotides, respectively. The open reading frame of *hdp1* encodes an 856 amino acid protein containing one homeodomain; a putative homeodomin ranging from amino acid position 184 to 240 is indicated by bold letters. Arrows indicate the positions of introns within cDNA.

```
                                                        -648 CGCGGCGCTTGGATCGCTTCACGTCGCCATCTGGAGCCACTCGAATTT -601
-600 CCCACGCCCCTGCCAAGGCCATCATCAACTCGCTCTCCATCCTGCTTGCTACCGGTGAAGCCGCTCAAGCGTGGTTGTCACTCGTTGCGTTTTCGCCGTT -501
-500 TCATTCACGATTCGCGCACAGGCGTCCGTTTGCAGCTGCAAATCTACACAATCCGATTGCGTGGCTCGCACCGCTCACTTGGGTCTCGTACTTGGCTTCT -401
-400 TGACGAAAACAGCGCGACGCCGTGCTTGCATCCGTGCACATTAGCTGTTGCTCTGATCGTCGCTAGTTGCTTCATCGCCAAGCCGAAAAGTGTTATTCGC -301
-300 GCCGCCTACTTGCCCCAATCGGCGCTCTCAACACTTTGGTGTGGCGCTCAAGCCGTCGAGAACAATCTCCAGACACTCCATACGCAGCATTAAGAGGGAC -201
-200 TAAACTCGAGCCTCGTAACAGCACAGCTTTCGGGCCTATTCGTTCTGTGCTAAGAGCTTGCCTTGGGTGTACAAGTCTTTGTACAACCCTCCTGGAATCT -101
-100 ATATAGAGAACAGGCCCCATCATCCGTCACACATTTTCATTGGATCCTCTTTCTCTCCACAAGTGAAAAGAGAACTGGAGGAGGAAGAAACCCGCCACCG -1

   1 ATG CTC GTT GCT CAA CCA CCG TTG CTG CGA TCA AGC GAG TTG AAA ATG GCG CAC TCT CCG CGA ACC GCA GCT TGC  75
   1 M   L   V   A   Q   P   P   L   L   R   S   S   E   L   K   M   A   H   S   P   R   T   A   A   C   25

  76 TCT TCA AGA AGC CGA AGA AGC GTC GAT CCG ATG CAA CAT CGC GCC TCA TCT CCA TCA TCT CTA GCT CTC TCC CAC  150
  26 S   S   R   S   R   R   S   V   D   P   M   Q   H   R   A   S   S   P   S   S   L   A   L   S   H   50

 151 CCT TCT CGC TTC CAC GCA ACC TCT GAT CCA ACT CAT GCT TAC CGT CCT CGA TCT CAC CAT TTC CCC CAC CAG CCT  225
  51 P   S   R   F   H   A   T   S   D   P   T   H   A   Y   R   P   R   S   H   H   F   P   H   Q   P   75

 226 CAT CCA CCT GTC TCA CCG GCG TTC CAG GCA ACA ACG CCC AAA CCG GGC CTC GCA GCA CCA CCA CTA GCA GTA TCT  300
  76 H   P   P   V   S   P   A   F   Q   A   T   T   P   K   P   G   L   A   A   P   P   L   A   V   S   100

 301 TCG TCG TCG TTT TCT TCT GGT GCG GCT GCT CTC GTA CTG GCT GCT TCG AGA CAG GAC GAC AAC GCC AGC CTC TCT  375
 101 S   S   S   F   S   S   G   A   A   A   L   V   L   A   A   S   R   Q   D   D   N   A   S   L   S   125

 376 CTC AGT GAC GAA GAT ATG CTG GTT TGC GAC GAA GCC GAC CAA GAC GAC GAC CGT TGG TCA GAT GCT GGT CTC TCT  450
 126 L   S   D   E   D   M   L   V   C   D   E   A   D   Q   D   D   D   R   W   S   D   A   G   L   S   150

 451 TCG ATC GAA GGC GCA GTA AGC AAC GCG GAA AGA CGC AGC AGA ACC GGC TCA GCC ACA AAC TCT CCT CCT GGA ACT  525
 151 S   I   E   G   A   V   S   N   A   E   R   R   S   R   T   G   S   A   T   N   S   P   P   G   T   175

 526 GGT AAT AGC AAA CGA AAC GTC AAT GGC AGG AGC AGG AGA TTG CTC TCT TTG GAA CAG TCG AAA GTG CTC TAC AAG  600
 176 G   N   S   K   R   N   V   N  G   R   S   R   R   L   L   S   L   E   Q   S   K   V   L   Y   K   200

 601 ATT CTA GAC AAG ACA CAC TTT CCA TCT ACA CAG TCG CGT GAG GCT GCC GCT TCC CAA CTT GGT GTT TCT CCG CGA  675
 201 I   L   D   K   T   H   F   P   S   T   Q   S   R   E   A   A   A   S   Q   L   G   V   S   P   R   225

 676 AAA GTC CAA GTC TGG TTC CAA AAC AGA CGT CAA GTG GGT AAG AAA AGA ATG ATG GAG GCG GTG CAA TCC TTG CTC  750
 226 K   V   Q   V   W   F   Q   N   R   R   Q   V   G   K   K   R   M   M   E   A   V   Q   S   L   L   250

 751 TCG GCG TAT CCA TGT TCG CCC TCG ACA CCG CTT CTC TCG TTC GAC ATT GTG CAG GAC CTG TTG CGA TCG ACG GGA  825
 251 S   A   Y   P   C   S   P   S   T   P   L   L   S   F   D   I   V   Q   D   L   L   R   S   T   G   275

 826 AAG ATG CGA TTT TCG TCC AAC GAG GAT GAA CGA ACA CGC GCG TGG CGT CAG CAC ACG ATG CGT CTT GCG CTC AAC  900
 276 K   M   R   F   S   S   N   E   D   E   R   T   R   A   W   R   Q   H   T   M   R   L   A   L   N   300

 901 CCT TCG GCG CAG GAG GAG GCG GAG AGC AAG GCT GCG ATT CGC GAG CTC GAG AGA ACA AGT GGG GGA TCG GCT CGA  975
 301 P   S   A   Q   E   E   A   E   S   K   A   A   I   R   E   L   E   R   T   S   G   G   S   A   R   325

 976 GAG ATT GGC TGT CGA GGT CCG CAC GAG CAG CGC TAC TAT TCG GCT CAA CGG CAT GAG CGT GAG CAG CAA GTG TAT 1050
 326 E   I   G   C   R   G   P   H   E   Q   R   Y   Y   S   A   Q   R   H   E   R   E   Q   Q   V   Y   350

1051 CGA CAG CGT TCG GCA ACG CAT TCG CAC GGT AGT GGT GGG TAT GCG CGT GGA CGT GAG CGC GAT GGT GCG ACA GAC 1125
 351 R   Q   R   S   A   T   H   S   H   G   S   G   G   Y   A   R   G   R   E   R   D   G   A   T   D   375

1126 TCG GTC GCT GCA ATC TCA GCT CAG GCT GCT CGC AAC TCA TAC GAG TGC GAG CTC ACC GAA AAC GAT CGA CGT CGA 1200
 376 S   V   A   A   I   S   A   Q   A   A   R   N   S   Y   E   C   E   L   T   E   N   D   R   R   R   400

1201 GGG CTC GCG AGA ATT CGA GCT TCC CGA TCT GCT GCT GCG CTT CGG ATC AAC GTC CCC CAC CTC GCG CCT CAT CCA 1275
 401 G   L   A   R   I   R   A   S   R   S   A   A   A   L   R   I   N   V   P   H   L   A   P   H   P   425

1276 GCC ACC AAC CAG CTC TTG CTG GAT GCA CAC ACT CCT GCT ACC GCT ACC ATT TCG ACT CCC ACC TAC ACC GGT CCG 1350
 426 A   T   N   Q   L   L   L   D   A   H   T   P   A   T   A   T   I   S   T   P   T   Y   T   G   P   450

1351 GGG AGT GCG ACA CAT CTC GAA ACG TTG TCG GCT CGC AGC AGT CAC GCT ACA TCG TTC CTT CCA CCT TGC ACT CTG 1425
 451 G   S   A   T   H   L   E   T   L   S   A   R   S   S   H   A   T   S   F   L   P   P   C   T   L   475

1426 ATG CCA CCG CTC ACA CCT GTA CGA TCT GGC GTG ATC GCA CCG GCT ATC GTG ACA AGT CAA AAG GAA AGC TTC AGC 1500
 476 M   P   P   L   T   P   V   R   S   G   V   I   A   P   A   I   V   T   S   Q   K   E   S   F   S   500

1501 CTT CCC GCT CTT CAC CAA CAC CAT CAC GCT CTG TAT CCT CCT CCC TTC TTG CAG CAA GAG TAC TCG CAC CGG CAT 1575
 501 L   P   A   L   H   Q   H   H   H   A   L   Y   P   P   P   F   L   Q   Q   E   Y   S   H   R   H   525
```

```
1576 TAC TCT GCG ACA GCT ACC GCA CAG CCG CAG CTT GCG GCT CAA CCG CAT GCG CGA CGC GCC ACT CCA CCC GAA CAT  1650
 526 Y   S   A   T   A   T   A   Q   P   Q   L   A   A   Q   P   H   A   R   R   A   T   P   P   E   H    550

1651 CAG CTA CGC ACC AGT GCG CAA GTA GGC GAG ATG AGC TTG GTT CGA CGC GAT CGA CGC GAT CGA AGC GCC ACA TTT  1725
 551 Q   L   R   T   S   A   Q   V   G   E   M   S   L   V   R   R   D   R   R   D   R   S   A   T   F    575

1726 ACC AGT GCG CGC TCG CTA GCA TCG TGG CCA GAT AAC GGA GCG GGG ATC AAG CAA GTG CGC ACC ACG TTG ACT GCT  1800
 576 T   S   A   R   S   L   A   S   W   P   D   N   G   A   G   I   K   Q   V   R   T   T   L   T   A    600

1801 GAA TGG CAC GCG CAG CAG CGA ATG CTC CAC CAT GAA CTC AAG AAG CAT ACC ACC AGT CGG AGC ACA TCG CCG CCT  1875
 601 E   W   H   A   Q   Q   R   M   L   H   H   E   L   K   K   H   T   T   S   R   S   T   S   P   P    625

1876 CAC AAT GCT GAT ACG CAA ACG CAG AGT GCA GCA CCG AAA GCG TCT GGG ATG AGG TAC CGT TCG TCG ACG GAT GCC  1950
 626 H   N   A   D   T   Q   T   Q   S   A   A   P   K   A   S   G   M   R   Y   R   S   S   T   D   A    650

1951 GTG TCG CGG CTG CCG GTG CTG GTG TCG AGT AGG AGA GCG CAC CAG AGG TAC GCG CCG TAC GAT GTA CGC ACG ACC  2025
 651 V   S   R   L   P   V   L   V   S   S   R   R   A   H   Q   R   Y   A   P   Y   D   V   R   T   T    675

2026 AAT ATG CAG TCG CAG ACA CTG CCA CCG ATG CGT ACA GGA GAC GCG CGT CGA GAT GAC ATG CAA GCT CAG AGT GGC  2100
 676 N   M   Q   S   Q   T   L   P   P   M   R   T   G   D   A   R   R   D   D   M   Q   A   Q   S   G    700

2101 ACG CAA AAA AGC GGT ACG AGC CAC TCG ATC TGT GCT CAT CCG GCG AGC ATG TCG CCT CAA AGT AGT GAT TCG GTT  2175
 701 T   Q   K   S   G   T   S   H   S   I   C   A   H   P   A   S   M   S   P   Q   S   S   D   S   V    725

2176 TCC GAC GAT CAT GTT TCT CGT CAT GCT GAG CAG CCA AGC GAG TCG ACA GGC TGC AGC GCT TTG CGT GCT TGC TCT  2250
 726 S   D   D   H   V   S   R   H   A   E   Q   P   S   E   S   T   G   C   S   A   L   R   A   C   S    750

2251 CGC CGT ACC GCC AAC ACC GCC TCG CCC ATC CGT ACT GCC GCC GTC CAC GTC TGC GCA TCC TCG TCC CCG TGC CTA  2325
 751 R   R   T   A   N   T   A   S   P   I   R   T   A   A   V   H   V   C   A   S   S   S   P   C   L    775

2326 GGC CCC GAT GCA AGC CAA CCC ACA CGT CGT CGA TCC ATC GCA TAC GCT CCA GCC TCG CAC GTC TCG CGC ACG AAT  2400
 776 G   P   D   A   S   Q   P   T   R   R   R   S   I   A   Y   A   P   A   S   H   V   S   R   T   N    800

2401 CTG CAA GAT TCC TCA ACA GAG CTT CGT CCA GAA CAA ACG CAC TCG AGA TGT CAC AGA ATG GAC GTT CGC TCA CTC  2475
 801 L   Q   D   S   S   T   E   L   R   P   E   Q   T   H   S   R   C   H   R   M   D   V   R   S   L    825

2476 ACC AAC ATC GAC ATC AAC ATC GAC ATG GTC GGC GCC GGT GCA AAA GCT AAA GCT GAA ACT GAA ACC AAA ACC AAA  2550
 826 T   N   I   D   I   N   I   D   M   V   G   A   G   A   K   A   K   A   E   T   E   T   K   T   K    850

2551 ACT AAA ACC GAG CTA GAA TGA CTCACTCTGCCGTGTTGGCAACGCAGCGCTGCGCGTGTTGTGCATGGAATCGCGATTCGTCTTCACGCA    2640
 851 T   K   T   E   L   E                                                                                856
```

Appendix 6.2 131 *hdp1*-regulated genes

Table 8 List of 131 *hdp1*-regulated genes that shows a differential regulation of more than two fold (P < 0.01)

probe set	MUMDB	Annotation	Fold change		Number of
			5 hours	12 hours	PRE motif
W70um170	um11562	hydrophobin 2	71,37	22,69	-
C80um257	um12024	putative protein	29,36	19,68	-
C81um257	um12024	putative protein		16,88	-
W40um030	um10528	related to STE6 - ABC transporter	12,17		2
W15um049	um00082	putative protein		9,48	-
W40um261	um11935	conserved hypothetical Ustilago-specific protein		9,20	-
C112um175	um02713	pheromone response factor Prf1	8,21	6,05	2
W175um086	um06158	probable glutaminase A		7,31	-
C85um097	um11514	probable High-affinity glucose transporter	7,03	5,94	-
W40um248	um03034	conserved hypothetical protein	6,09	4,47	-
C158um132	um10189	ferrichrome siderophore peptide synthetase	5,08		-
W5um075	um11596	related to CSR1 - phosphatidylinositol transfer protein	3,88	2,29	-
W75um036	um02763	conserved hypothetical protein	3,76		-
W75um145	um04385	hypothetical protein	3,64		-
C105um075	um06063	related to GAD1 - glutamate decarboxylase	3,59		-
W20um109	um04347	probable isp4 - oligopeptide transporter		3,58	-
W30um135	um01663	conserved hypothetical protein	3,30		-
UG16-16l20-80e12	um10992	conserved hypothetical Ustilago-specific protein, pseudogene	3,30	3,90	-
C155um019	um06422	conserved hypothetical protein	3,26		-
C135um025	um04114	probable PHO8 - repressible alkaline phosphatase vacuolar	3,20		-
C140um075	um06071	related to Para-nitrobenzyl esterase	3,12		1
W20um280	um11605	related to THG1 - protein required for tRNA-His guanylylation at 5 prime end	3,06		-
W40um114	um10718	chitin synthase 1	3,05		-
W85um258	um04399	probable succinate-fumarate transporter (mitochondrial)	3,04		-
C90um112	um11544	putative protein	3,03		-
C10um163	um00695	putative exochitinase	2,87	3,33	-
W50um079	um15004	probable malate synthase, glyoxisomal	2,82		-
W110um228	um12175	conserved hypothetical protein	2,60		-
W115um155	um11556	probable enoyl-CoA hydratase precursor, mitochondrial	2,59		-
W125um144	um04064	related to Glucoamylase precursor	2,57		-
W10um134	um05114	related to multidrug resistance protein 4	2,54		-
W50um103	um01986	probable sterol carrier protein	2,53		-
W25um216	um12033	HMG-box transcription factor (C-terminal fragment)	2,51		-
C20um077	um12220	related to PRM1 - Pheromone-regulated multispanning membrane protein	2,47		2
W140um049	um00109	probable DAK2 - dihydroxyacetone kinase		2,45	-
W95um182	um05560	putative protein	2,31		-
C45um161	um02517	guanine nucleotide-binding protein alpha-2 subunit	2,29	3,87	-
W115um227	um11672	related to Protein farnesyltransferase alpha subunit	2,27		1
W150um281	um02224	conserved hypothetical protein	2,26	2,26	-
W95um249	um02990	conserved hypothetical protein	2,26		-
W85um098	um10038	probable multifunctional beta-oxidation protein	2,26		-
C13um226	um04324	probable POX1 - acyl-CoA oxidase	2,24		-
C60um177	um06495	putative protein		2,23	-
W75um209	um15048	related to 4-coumarate-CoA ligase 1		2,22	-
C155um005	um11191	related to phenylacetyl-CoA ligase	2,17		1

Table 8 (Cont.) List of 131 *hdp1*-regulated genes that shows a differential regulation of more than two fold (P < 0.01)

probe set	MUMDB	Annotation	Fold change		Number of
			5 hours	12 hours	PRE motif
W5um156	um04282	related to 3-phytase A precursor	2,15		-
UG14-15c10-91c8	um11682	related to STE14 - farnesyl cysteine carboxyl-methyltransferase	2,14		1
W110um005	um05827	conserved hypothetical protein	2,09		-
C135um096	um03958	probable FEN1 - fatty acid elongase	2,09		-
C40um172	um02900	conserved hypothetical protein	2,06		-
W35um277	um05290	putative protein	2,06		-
C45um071	um06374	related to GRE2 - methylglyoxal reductase (NADPH-dependent)	2,02		-
W5um052	um10537	protein kinase A, catalytic subunit	-2,00		-
C90um054	um00656	related to YSC84 - protein involved in the organization of the actin cytoskeleton	-2,02		-
C35um164	um00469	probable histone H2A F/Z family member HTZ1	-2,02		-
C81um183	um10356	probable 20S proteasome beta2 subunit		-2,05	-
C5um105	um11400	probable Thiamin biosynthetic enzyme		-2,06	-
W20um136	um02579	related to RFA2 - DNA replication factor A, 36 kDa subunit	-2,07	-2,61	-
C122um183	um05525	related to MRPL16 - mitochondrial ribosomal protein, large subunit	-2,08		-
C50um140	um03775	related to MCR1 - cytochrome-b5 reductase	-2,10	-2,22	-
C40um284	um10746	conserved hypothetical protein		-2,10	-
W80um175	um02718	related to PIF1 - DNA helicase involved in mitochondrial DNA repair and telomere length control	-2,12		-
C25um163	um11832	conserved hypothetical protein	-2,14		-
W5um185	um05502	related to MRPL17 - mitochondrial ribosomal protein, large subunit	-2,14		-
W10um154	um02557	related to DNA polymerase alpha 70 kDa subunit	-2,14		-
C10um226	um11750	probable RNR1 - ribonucleoside-diphosphate reductase large subunit	-2,18		-
W30um228	um01926	related to DAL2 - allantoinase	-2,19		-
C26um005	um05848	related to galactoside O-acetyltransferase	-2,20		-
C95um158	um01755	putative protein	-2,22		-
C15um235	um05153	related to MNT4 - putative alpha-1,3-mannosyltransferase	-2,22		-
C105um125	um05301	conserved hypothetical Ustilago-specific protein	-2,27		-
C61um184	um05505	related to mediator complex subunit soh1		-2,29	-
C75um213	um03649	hypothetical protein	-2,30		-
W55um184	um05507	conserved hypothetical protein	-2,33		-
W65um185	um10755	conserved hypothetical protein	-2,36		-
C115um099	um05899	conserved hypothetical protein	-2,36		-
W65um284	um11578	probable PRE6 - 20S proteasome subunit (alpha4)		-2,39	-
W40um256	um05786	related to UDP N-acetylglucosamine transporter	-2,40		-
C115um024	um01533	related to n-acetyltransferase	-2,41		-
C40um034	um05052	hypothetical protein	-2,41		-
W25um022	um00115	probable BAT2 - branched-chain-amino-acid transaminase (cytosolic)	-2,45		-
C10um081	um03234	related to CDC5 - Serine/threonine-protein kinase	-2,51		-
UG23-1i5-133h4_RC	um05421	related to Multidrug resistance protein	-2,51		-
W85um164	um00459	related to Condensin complex subunit 3	-2,52		-

Table 8 (Cont.) List of 131 *hdp1*-regulated genes that shows a differential regulation of more than two fold (P < 0.01)

probe set	MUMDB	Annotation	Fold change		Number of
			5 hours	12 hours	PRE motif
W55um146	um05951	conserved hypothetical protein	-2,53		-
W48um184	um10348	conserved hypothetical protein		-2,68	-
W15um082	um10394	related to Dihydrofolate reductase		-2,72	-
W70um114	um05644	related to alcohol dehydrogenase	-2,79		-
W45um256	um05787	conserved hypothetical protein	-2,79		-
W15um126	um02212	related to trehalase precursor	-2,85	-3,87	-
W55um065	um10885	hypothetical protein	-2,90		-
C10um102	um03611	related to LAG1 - longevity-assurance protein	-2,95		-
C85um054	um00657	related to RAD7 - nucleotide excision repair protein	-2,98		-
C145um074	um01804	related to kynurenine/alpha-aminoadipate aminotransferase mitochondrial precursor	-3,01		-
W35um189	um00712	probable YOR1 - ABC transporter	-3,01		-
C30um203	um12012	conserved hypothetical protein		-3,07	-
C30um256	um11585	related to capsular associated protein	-3,08		-
W105um153	um10306	conserved hypothetical protein	-3,11		-
C70um087	um11022	related to SRY1 - 3-hydroxyaspartate dehydratase	-3,14		-
W130um003	um01951	conserved hypothetical protein	-3,28		-
C25um282	um02683	conserved hypothetical protein	-3,28		-
CLUSTER2	um00262	conserved hypothetical protein	-3,51	-2,11	-
W35um256	um05785	acyl transferase-like protein	-3,68		-
C20um097	um03881	related to Heat shock protein Hsp20	-3,77		-
W125um228	um01900	conserved hypothetical protein	-3,86		-
W85um175	um11720	related to cystathionine beta-lyase (N-terminal fragment)	-4,04		-
W60um043	um02792	related to CYS4 - cystathionine beta-synthase	-4,25		-
W95um183	um05531	related to Phosphoserine aminotransferase	-4,29		-
C51um184	um12305	probable GTP-binding protein 1	-4,44		-
C230um012	um02062	related to multidrug resistance proteins	-4,45		-
W25um089	um10815	conserved hypothetical protein	-4,51		-
C25um144	um04044	related to Glucose oxidase	-4,57		-
W1um060	um02139	conserved hypothetical Ustilago-specific protein	-4,62	-3,26	-
W105um021	um03114	conserved hypothetical protein	-4,64	-6,21	-
W65um175	um02721	conserved hypothetical protein	-4,71		-
W4um060	um02137	conserved hypothetical Ustilago-specific protein	-4,93		-
C25um256	um05783	related to UDP-galactose transporter	-4,99		-
C117um228	um01902.2	conserved hypothetical protein	-5,30		-
C11um184	um05520	conserved hypothetical protein		-5,38	-
W40um273	um06266	putative protein	-5,87		-
W50um095	um01070	related to cyclopropane-fatty-acyl-phospholipid synthase	-6,01	-3,06	-
W7um082	um15095	HobS polyprotein, pseudogene	-6,24		-
C110um127	um12007	related to cellulase	-6,99	-4,43	-
W60um250	um10365	related to YBT1 - Vacuolar, ABC protein transporting bile acids	-7,44		-
C25um042	um05690	conserved hypothetical Ustilago-specific protein	-8,85		-
W10um164	um10120	chitin synthase 3	-8,92		-
C75um047	um03585	conserved hypothetical protein	-10,19		-
W35um258	um04410	probable siderophore iron transporter mirC	-13,50		-
C110um021	um03115	related to Sge1 - drug resistance protein	-14,19	-9,84	-
W15um008	um04364	probable EXG1 - Exo-1,3-beta-glucanase precursor	-14,57	-6,90	-

Table 8 (Cont.) List of 131 *hdp1*-regulated genes that shows a differential regulation of more than two fold (P < 0.01)

probe set	MUMDB	Annotation	Fold change		Number of
			5 hours	12 hours	PRE motif
C115um021	um03116	conserved hypothetical protein	-14,65	-10,22	-
W130um021	um10636	conserved hypothetical protein	-16,45	-10,50	-
ncp1	um04000	DNA binding protein Ncp1	-40,83	-3,82	-

Appendix 6.3 *hdp1*-regulated genes that are *a*-and/or *b*-dependent.

Table 9 List of 38 *hdp1*-regulated genes that are *a*-dependent.

probe set	MUMDB	Annotation	Fold change		Regulated by	Number	Overlapping
			5 hours	12 hours	*a**	of PRE	between *a* and *b*
W40um030	um10528	related to STE6 - ABC transporter	12,17		Up	2	No
C112um175	um02713	pheromone response factor Prf1	8,21	6,05	Up	2	Yes
C85um097	um11514	probable High-affinity glucose transporter	7,03	5,94	Down	-	Yes
W75um036	um02763	conserved hypothetical protein	3,76		Down	-	No
UG16-16l20-80e12	um10992	conserved hypothetical Ustilago-specific protein, pseudogene	3,30	3,90	Up	-	No
C140um075	um06071	related to Para-nitrobenzyl esterase	3,12		Up	1	No
W20um280	um11605	related to THG1 - protein required for tRNA-His guanylylation at 5 prime end	3,06		Up	-	Yes
W40um114	um10718	Chs1 Chitin Synthase 1	3,05		Up	-	Yes
C20um077	um12220	related to PRM1 - Pheromone-regulated multispanning membrane protein	2,47		Up	2	No
W140um049	um00109	probable DAK2 - dihydroxyacetone kinase (dak2)		2,45	Down	-	No
W115um227	um11672	related to Protein farnesyltransferase alpha subunit	2,27		Up	1	No
C13um226	um04324	probable POX1 - acyl-CoA oxidase	2,24		Up	-	No
C60um177	um06495	putative protein		2,23	Up	-	No
UG14-15c10-91c8	um11682	related to STE14 - farnesyl cysteine carboxyl-methyltransferase	2,14		Up	1	No
C5um105	um11400	probable Thiamin biosynthetic enzyme		-2,06	Down	-	No
C95um158	um01755	putative protein	-2,22		Down	-	No
C15um235	um05153	related to MNT4 - putative alpha-1,3-manNosyltransferase	-2,22		Down	-	Yes
W40um256	um05786	related to UDP N-acetylglucosamine transporter	-2,40		Down	-	Yes
W25um022	um00115	probable BAT2 - branched-chain-amiNo-acid transaminase (cytosolic)	-2,45		Down	-	No
C10um081	um03234	related to CDC5 - Serine/threonine-protein kinase	-2,51		Down	-	Yes
W85um164	um00459	related to Condensin complex subunit 3	-2,52		Down	-	No
W55um146	um05951	conserved hypothetical protein	-2,53		Down	-	No
W15um082	um10394	related to Dihydrofolate reductase		-2,72	Down	-	Yes
W45um256	um05787	hypothetical protein	-2,79		Down	-	Yes
C145um074	um01804	related to kynurenine/alpha-amiNoadipate amiNotransferase mitochondrial precursor	-3,01		Down	-	No
C30um256	um11585	related to capsular associated protein	-3,08		Down	-	No
W130um003	um01951	conserved hypothetical protein	-3,28		Down	-	No
CLUSTER2	um00262	conserved hypothetical protein	-3,51	-2,11	Down	-	No
W35um256	um05785	acyl transferase-like protein	-3,68		Down	-	Yes
W125um228	um01900	conserved hypothetical protein	-3,86		Up	-	No
C25um256	um05783	related to UDP-galactose transporter	-4,99		Down	-	Yes
C117um228	um01902.2	conserved hypothetical protein	-5,30		Up	-	No
W50um095	um01070	related to cyclopropane-fatty-acyl-phospholipid synthase	-6,01	-3,06	Down	-	Yes
W10um164	um10120	Chitin Synthase 3	-8,92		Down	-	No
W15um008	um04364	probable EXG1 - exo-beta-1,3-glucanase (I/II), major isoform	-14,57	-6,90	Down	-	Yes
C115um021	um03116	conserved hypothetical protein	-14,65	-10,22	Down	-	Yes
W130um021	um10636	conserved hypothetical protein	-16,45	-10,50	Down	-	Yes
ncp1	um04000	DNA binding protein Ncp1	-40,83	-3,82	Up	-	No

Table 10 List of 38 *hdp1*-regulated genes that are *b*-dependent.

probe set	MUMDB	Annotation	Fold change		Regulated by	Number	Overlapping
			5 hours	12 hours	*b***	of PRE	between *a* and *b*
W40um261	um11935	conserved hypothetical Ustilago-specific protein		9,20	Up	-	No
C112um175	um02713	pheromone response factor Prf1	8,21	6,05	Down	2	Yes
W175um086	um06158	probable glutaminase A		7,31	Up	-	No
C85um097	um11514	probable High-affinity glucose transporter	7,03	5,94	Up	-	Yes
W40um248	um03034	conserved hypothetical protein	6,09	4,47	Up	-	No
W5um075	um11596	related to CSR1 - phosphatidyliNositol transfer protein	3,88	2,29	Up	-	No
W75um145	um04385	hypothetical protein	3,64		Up	-	No
W20um280	um11605	related to THG1 - protein required for tRNA-His guanylylation at 5 prime end	3,06		Up	-	Yes
W40um114	um10718	Chs1 Chitin Synthase 1	3,05		Up	-	Yes
C10um163	um00695	putative exochitinase	2,87	3,33	Up	-	No
W125um144	um04064	related to Glucoamylase precursor	2,57		Up	-	No
W95um182	um05560	putative protein	2,31		Up	-	No
C45um161	um02517	guanine nucleotide-binding protein alpha-2 subunit (Gpa2)	2,29	3,87	Up	-	No
W95um249	um02990	conserved hypothetical protein	2,26		Up	-	No
C155um005	um11191	related to phenylacetyl-CoA ligase	2,17		Up	1	No
W110um005	um05827	hypothetical protein	2,09		Up	-	No
C10um226	um11750	probable RNR1 - ribonucleoside-diphosphate reductase large subunit	-2,18		Down	-	No
C15um235	um05153	related to MNT4 - putative alpha-1,3-manNosyltransferase	-2,22		Down	-	Yes
W40um256	um05786	related to UDP N-acetylglucosamine transporter	-2,40		Down	-	Yes
C40um034	um05052	hypothetical protein	-2,41		Down	-	No
C10um081	um03234	related to CDC5 - Serine/threonine-protein kinase	-2,51		Down	-	Yes
W15um082	um10394	related to Dihydrofolate reductase		-2,72	Down	-	Yes
W45um256	um05787	hypothetical protein	-2,79		Down	-	Yes
W15um126	um02212	related to trehalase precursor	-2,85	-3,87	Down	-	No
W55um065	um10885	hypothetical protein	-2,90		Down	-	No
C10um102	um03611	related to LAG1 - longevity-assurance protein	-2,95		Down	-	No
W35um256	um05785	acyl transferase-like protein	-3,68		Down	-	Yes
W95um183	um05531	related to Phosphoserine amiNotransferase	-4,29		Down	-	No
C25um144	um04044	related to Glucose oxidase	-4,57		Down	-	No
W105um021	um03114	conserved hypothetical protein	-4,64	-6,21	Down	-	No
W65um175	um02721	conserved hypothetical protein	-4,71		Down	-	No
C25um256	um05783	related to UDP-galactose transporter	-4,99		Down	-	Yes
W50um095	um01070	related to cyclopropane-fatty-acyl-phospholipid synthase	-6,01	-3,06	Down	-	Yes
C25um042	um05690	conserved hypothetical Ustilago-specific protein	-8,85		Down	-	No
C110um021	um03115	related to Sge1 - drug resistance protein	-14,19	-9,84	Down	-	No
W15um008	um04364	probable EXG1 - exo-beta-1,3-glucanase (I/II), major isoform	-14,57	-6,90	Down	-	Yes
C115um021	um03116	conserved hypothetical protein	-14,65	-10,22	Down	-	Yes
W130um021	um10636	conserved hypothetical protein	-16,45	-10,50	Down	-	Yes

Note: *hdp1* up-regulated genes are shown in red; *hdp1* down-regulated genes are shown in green.

* Zarnack (2006)

** J. Kämper and M. Scherer, unpublished data

Appendix 6.4 Testing of applicability of nuclear densitrometry for determination of the nuclear DNA content.

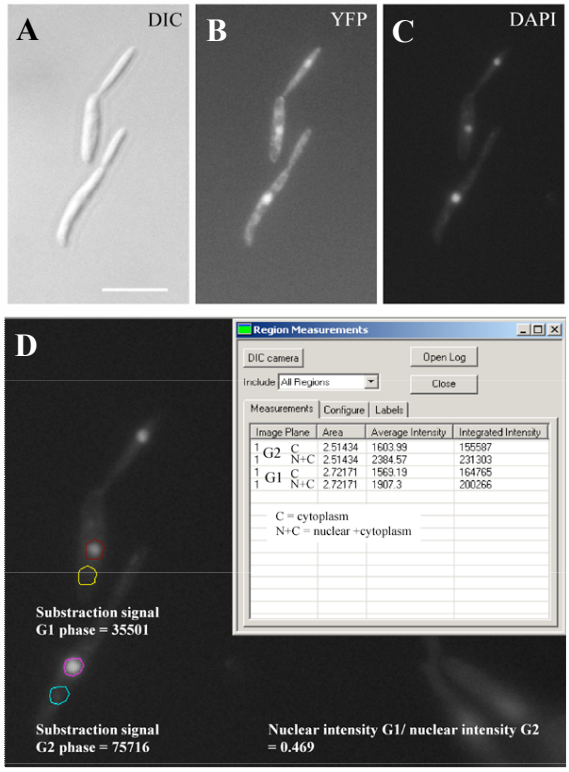

Figure 34. Determination of nuclear DNA content by means of nuclear densitrometry
Morphology of two budding cells (A) DIC image and (B) YFP filter, indicating that both cells are FB1*yfp*^{otefP}. (C) Nuclear staining with DAPI of both cells.
The lower cell is a bud-forming cell before nuclear division whereas the upper cell is a bud-forming cell after nuclear division. Thus, the nuclei of the upper cell are in G1 phase, 1C DNA content, and in the lower cell in G2 phase, 2C DNA content, respectively as previously described in Snetselaar and McCann (1997). Scale bar = 5 μm.

(D) Microdensitrometry measurement by Metamorph program (Universal Imaging Corp.) indicates that nuclear intensities of G1 and G2 phases are 35501 and 75716, respectively. These values are obtained by subtraction of background intensity (cytoplasmic region, C) from nuclear intensity (N+C). As a result, the relative nuclear intensity of G1 to G2 is 0.469 similar to the expected value 0.5, supporting the applicability of the technique for the investigation of the nuclear DNA content.

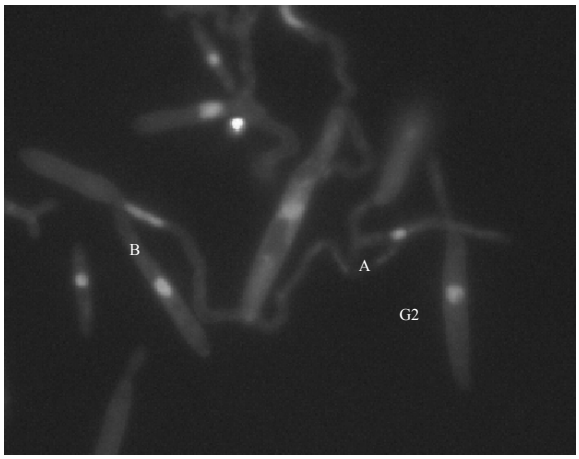

Figure 35. Example of a determination of nuclear DNA content in conjugation hyphae

Nuclear staining of FB1*Δhdp1* sporidia forming conjugation hyphae and control sporidia with a small bud. G2 indicates the control FB1 having nuclear phase in G2 harboring 2C DNA content (Snetselaar and McCann, 1997). Two tested cells forming conjugation hyphae are indicated by A and B. Their relative nuclear intensities to the nuclear intensity of G2 control cells are shown here.

Cell A = 0.498 ~ 1C DNA content
Cell B = 1.115 ~ 2C DNA content

Appendix 6.5 Microarray analysis of *hdp1* deletion

To investigate the role of *hdp1* within b-regulatory cascade, *hdp1* was deleted by replacement with the hygromycin resistance cassette in AB31 (*a2 bW2*^{crg1P}/*bE1*^{crg1P}), resulting in AB31*Δhdp1*. The expression profiles of AB31 and AB31*Δhdp1* were compared after 12 hours of b-induction. Genes showing a differential regulation of more than two fold ($P < 0.01$) were considered as *hdp1*-regulated genes. After 12-hours of *b*-induction, excluding *hdp1*, *gfp*, and the hygromycin phosphotransferase gene, 16 genes were identified as induced and 29 genes were identified as repressed. Up to 55.6% (25/45) of *hdp1*-required genes cannot be annotated yet.

Interestingly, Five *hdp1* down-regulated genes (um05782, um05783, um11585, um05785, and um05787) are located in a cluster that has been previously identified as the *cab* locus. Genes within the *cab* locus show both *a*- and *b*-dependent repression (Brachmann, 2001).

Thirteen of twenty annotated genes are involved in metabolism and energy production, for examples, um05170; the most up-regulated gene encoding for probable formate dehydrogenase, ferrichrome siderophore peptide synthetase *sid2*; one of genes involved in siderophore synthesis (Yuan *et al*., 2001). There is no gene putatively involved in cell cycle regulation or progression identified here, consistent with an unaltered observed cell cycle arrest.

Table 11 List of the up and down *hdp1*-required genes after 12 hours of *b*-induction (AB31/AB31*Δhdp1*)

* 5 *hdp1* down-regulated genes belonging to the *cab* locus are marked in grey.

probe set	MUMDB	MUMDB Annotation	Fold Change (AB31/AB31*Δhdp1*)
W140um132	um05170	probable formate dehydrogenase	16,229
W40um261	um11935	conserved hypothetical Ustilago-specific protein	8,555
C30um080	um03246	related to versicolorin b synthase	8,305
W50um159	um11886	conserved hypothetical protein	8,104
C25um195	um01850	conserved hypothetical protein	5,880
C10um043	um02804	conserved hypothetical protein	4,799
W25um285	um11434	hypothetical protein	4,545
C158um132	um10189	ferrichrome siderophore peptide synthetase (*sid2*)	3,218
C85um097	um11514	probable High-affinity glucose transporter	3,188
UG13-15p13-73e11	um11427	conserved hypothetical protein	3,141
W111um003	um01958.2	putative protein	3,013
W113um122	um11895	putative protein	2,900
W60um134	um05104	putative protein	2,769
C15um138	um02642	conserved hypothetical protein	2,565
W156um005	um11190	putative protein	2,364
C50um078	um03304	conserved hypothetical protein	2,150
W50um010	um01269	conserved hypothetical protein	-2,166
C80um220	um06302	putative protein	-2,522
W2um007	um10207	related to AMD2 - acetamidase	-2,683
W55um073	um05731	conserved hypothetical protein	-2,706
C40um126	um02206	conserved hypothetical protein	-2,752
W135um068	um04915	probable Major allergen Mal f 1 precursor	-2,787
C60um007	um05347	conserved hypothetical protein	-2,942
C30um036	um02774	related to alternative oxidase precursor, mitochondrial	-3,125
W60um152	um05272	conserved hypothetical protein	-3,418
W75um008	um04353	related to glycosyl transferase, group 2 family protein	-3,513
W15um126	um02212	related to trehalase precursor	-3,991
W50um012	um02095	putative protein	-4,862
C26um006	um02298	hypothetical protein	-5,114
W21um256	um05782	capsule-associated protein-like protein	-5,159
W105um153	um10306	conserved hypothetical protein	-5,219
C35um250	um10364	related to KRE6 - glucan synthase subunit	-5,479
C20um006	um02300	probable alpha-amylase	-5,494
W40um165	um00441	hypothetical protein	-5,880
W45um256	um05787	conserved hypothetical protein	-5,982
UG14-15g12-91e11	um04106	related to O-methyltransferase B	-7,546
C10um102	um03611	related to LAG1 - longevity-assurance protein	-7,720
W5um229	um01897	conserved hypothetical protein	-7,897
W85um194	um01508	related to Aquaporin 3	-8,766
C200um074	um01793	probable AAD14 - Putative aryl-alcohol reductase	-10,449
W35um074	um01829	related to alpha-L-arabinofuranosidase I precursor	-10,573
C30um256	um11585	related to capsular associated protein	-11,171
W35um256	um05785	acyl transferase-like protein	-15,886
W65um066	um04185	conserved hypothetical protein	-21,877
C25um256	um05783	related to UDP-galactose transporter	-25,690

Appendix 6.6 Data CD: Microarray data and thesis in PDF format

The CD content is composed of two main folders:

1. Microarray folder containing microarray data of *hdp1* induction and deletion.

It is composed of two subfolders:

1.1 dChip folder containing the raw expression data processed by dChip 2004

The folder contains 2 files:

Dhdp1_expression12h.xls: Data of *hdp1*-deleted strain and its control after 12-hour induction (see detail in Appendix 6.5)

hdp1_crg5-12h.xls: Data of *hdp1*-induced strain and its control after 5- and 12-hour induction (see detail in 2.5)

1.2 R_Program folder containing the raw (_result) and filtered (_filtered) data of fold-change in $\log_2$ and adjusted P-value calculated by Bioconductor.

The folder contains 6 files:

hdp1_del_12_result.xls
hdp1_del_12_filtered.xls — Data of *hdp1*-deleted strain and its control after 12-hour induction

hdp1_5h_result.xls
hdp1_5h_filtered.xls — Data of *hdp1*-induced strain and its control after 5-hour induction

hdp1_12h_result.xls
hdp1_12h_filtered.xls — Data of *hdp1*-induced strain and its control after 12-hour induction

2) Thesis PDF folder containing one file of thesis in PDF format:

Chetsada_Pothiratana_Thesis.pdf

Acknowledgements

I would like to express my deepest gratitude and appreciation to my supervisor, Prof. Dr. Jörg Kämper for his valuable guidance, advices, discussion and supporting throughout the work on this thesis. I am also really grateful thank to Prof Dr. Michael Bölker, Prof Dr. Uwe Maier and Prof. Dr. Lotte Søgaard-Andersen for their helpful advice and comment.

I would like to thank Dr. Mario Scherer and Dr. Miroslav Vranes for helping me in microarray anlysis of *hdp1* deletion and induction. I also would like to thank Dr. Ignacio Flor-Parra for FACS analysis, Volker Vincon for his excellent technical support, especially for FB1Pcrg1:hdp1,Δhum2, Florian Finkernagel and Kathi Zarnack for the array data of pheromone induction and PRE motif analysis, and Patrick Berndt for his advice for a contact angle measurement. Additionally, I would like to thank Dr. Miroslav Vranes, Ramon Wahl and Kai Heimel for their supporting during my thesis writing. Moreover, I thank for Alexander Zahiri, former lab members, and the members of organismic interactions department for their warm friendship.

I would like to thank Prof. Dr. Regine Kahmann for providing me an opportunity to work in her department. I extremely thank to the Development and Promotion of Science and Technology Talent Project (DPST) and International Max Planck Research School (IMPRS) for the scholarship and excellent course works and workshops along my study. I would like to thank Dr. Juliane Dörr and Susanne Rommel for useful living guidance during I was staying in Marburg.

Finally, I would like to express my deepest appreciation and thankfulness to my parents, my brother and all members of my family for their care, concern, love and encouragement throughout my study.

CURRICULUM VITAE

Personal information

	Chetsada Pothiratana
Date of Birth	26.04.1977
Birth place	Bangkok, Thailand

Background

1983-1988	Udomsuksa School, Bangkok, Thailand
1989-1994	Bodindecha (Sing Singhaseni) School, Bangkok, Thailand
1995-1998	Faculty of Science, Chulalongkorn University, Bangkok, Thailand Bachelor of Science (Gentics)
2000-2002	Institute of Molecular Biology and Genetics, Mahidol University, Nakhonpathom, Thailand Master of Science (Molecular genetics and Genetic Engineering) Thesis title: "Molecular cloning of a putative octopamine/tyramine receptor from *Penaeus monodon*"
April 2004-December 2007	Dissertation at the Max-Planck-Institute for terrestrial Microbiology, Karl-von-Frisch-Strasse, D-35043 Marburg, Germany; Supervisor: Prof. Dr. Jörg Kämper Thesis title: "Functional characterization of the homeodomain transcription factor Hdp1 in *Ustilago maydis*"